UNIVERSITÀ DEGLI STUDI DI CAGLIARI

Department of Biomedical Science and Technology
Section of General Microbiology and Virology
& Microbial Biotechnologies

BIO/19

Research Doctorate in:
Development and Experimentation of Antiviral Drugs
XXIII Cycle – A.A. 2007-2010
Coordinator of the Doctorate:
Prof. Alessandra Pani

STUDIES ON THE ROLE OF CHOLESTEROL IN THE PATHOGENESIS OF PRION DISORDERS

Supervisor:
Prof. Pani Alessandra

Candidate:
Dott. Sarah Vascellari

TABLE OF CONTENTS

1 INTRODUCTION

1.1 Protein Misfolding Diseases

The biological function of cells depends on the correct folding of a network of thousands protein. The information required to fold a protein into a functional, specific three-dimensional structure is contained in its amino-acid sequence. In general proteins fold properly into their native conformation. However, it's possible that the protein adopts a wrong conformation, which keeps it from carrying out its function. This process is termed "Protein Misfolding". Misfolding diseases comprise a group of disorders with dissimilar symptoms which can affect various organs and tissues. Nevertheless, they have the same underlying pathogenetic mechanism, namely an altered protein conformer with high β-sheet structure content. These conformational diseases include Alzheimer's (AD), Huntington's and Parkinson's disorders, Prion-related Disorders (PrD), Systemic Amyloidosis, and Amyotrophic Lateral Sclerosis (Soto C., 2003) (Figure 1).

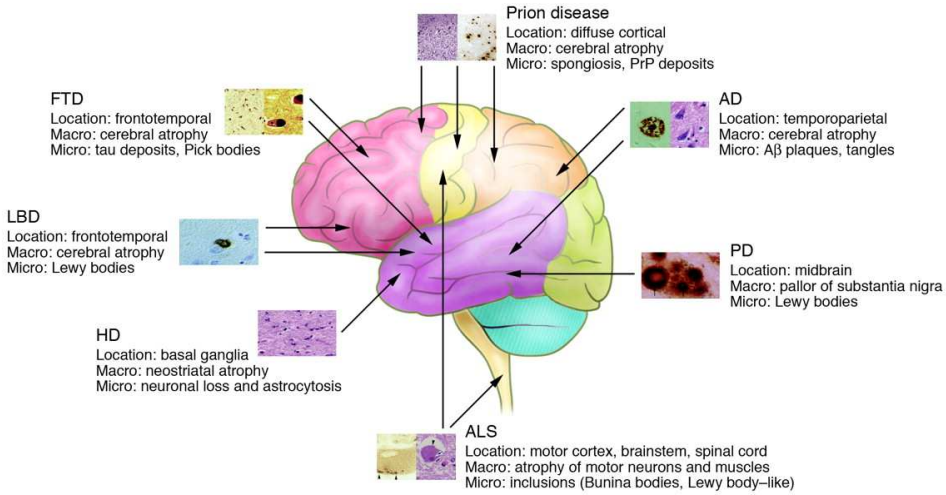

Fig. 1 Overview of the anatomical location of and macroscopic and microscopic changes characteristic of the neurodegenerative disorders. Note that the full neuropathological spectrum of these disorders is much more complex than depicted here. When there is more than one characteristic histopathological feature, these are depicted from left to right, as indicated in the labels listing microscopic changes (e.g., the 2 panels for AD depict an Aβ plaque [left] and neurofibrillary tangles [right]; Bertram, L. et al. J. Clin. Invest. 2005;115:1449-1457.

Normally, the cell has a number of defense mechanisms to contrast the formation of misfolded proteins, as the system of chaperones, which induces re-folding, or the ubiquitin-proteasome system and the phagosome-lysosome system that limit the accumulation of misfolded proteins (Forman *et al*., 2004) (Figure 2). However, these control systems may well little against the pathological accumulation.

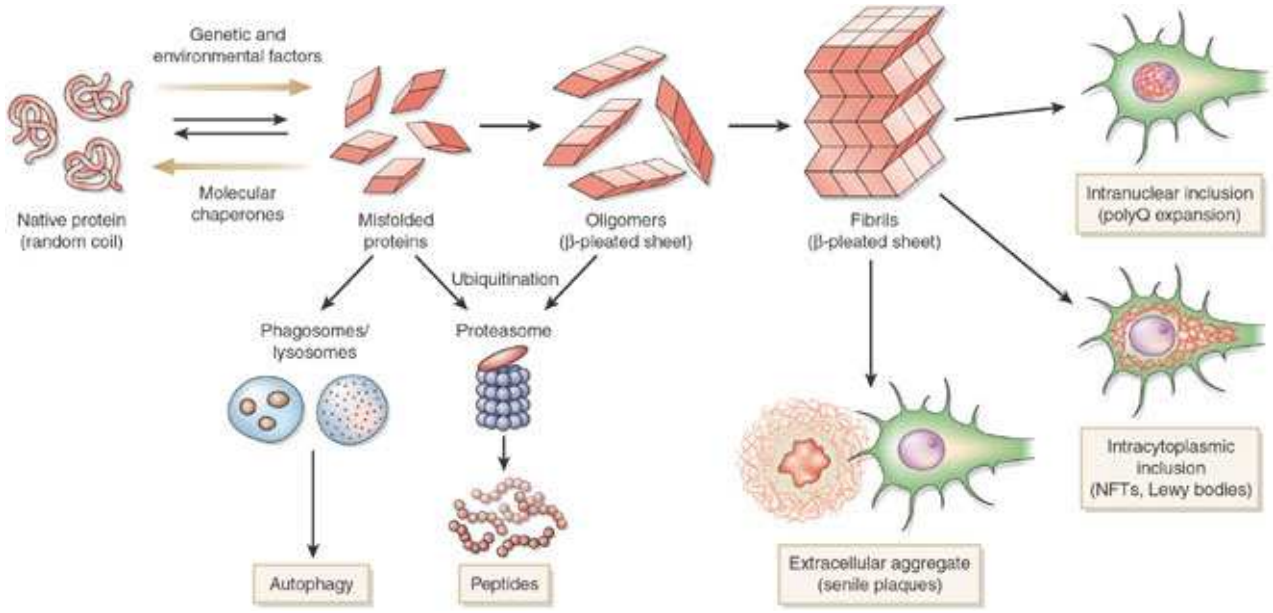

Fig. 2 Model of protein misfolding and fibrilization, leading to the deposition of aggregated protein in the nucleus, cytoplasm and extrecellular space. Genetic and environmental factors may accelerate this process, whereas cellular quality-control systems including molecular chaperones, the ubiquitin-proteasome system and the phagosome-lysosome system limit the accumulation of misfolded proteins.

The key event is a change in the secondary and tertiary structure of a normal protein without alteration in the primary structure. The unstable structural isoforms thus generated, in an attempt to seek lower energy levels and more stability, have a tendency to aggregate in ordered fibrils that are called amyloid. These fibrils, other than sharing cross β-structure, exhibit specific tinctorial properties such as iodine, Congo red and thioflavin-T have been used extensively for characterising the presence of amyloid fibrils and their rates of formation, both in tissue samples and, in an adapted method, *in vitro* (Klunk *et al*., 1989). Currently, there is no effective therapy for inhibiting or reversing protein aggregation and deposition in patients with protein misfolding diseases. However, the progress made in understanding the molecular basis of abnormal conformation has opened new perspectives for designing medications for these highly devastating disorders. In this context, growing evidence supports the notion that alterations in cholesterol homeostasis represent an additional feature shared by misfolding diseases, and that cholesterol may have a role in the formation of misfolded proteins (Mattson *et al*., 1999; Stefani *et al*., 2007).This is particularly apparent for AD and PrD in which abnormal cholesterol metabolism is frequently observed (Sjögren *et al.*, 2006; Stefani *et al.*, 2009).

Although the precise nature of how cholesterol influences conformational transition has not yet been identified, studies exploring the effects of drugs interfering with cholesterol synthesis,

processing, and trafficking could be an evolving strategy for the identification of novel targets for the diagnosis, prevention and treatment of amyloidogenic disorders.

1.2 Alzheimer's Disease

Alzheimer's disease (AD) is the most common progressive neurodegenerative disease affecting millions of people worldwide. Multiple pathways have been implicated in AD pathogenesis, including neuronal cell death, oxidative damage, chronic inflammation, and protein aggregation (Govaerts *et al*., 2007; Giannakopoulos *et al*., 2009). Many years ago, silver and Congo-red stains have evidenced in the cortical regions of the brains of patients affected by AD, the presence of characteristic dark, irregular, thread-like structures often with a brownish material in the centre, which was called neuritic plaque. The central core was represented by amyloid substance, while the irregular, beaded linear structures by small dendrites and axons with degenerative changes (dystrophic neuritis). Around the plaque, various cell types including astrocytes and microglia/macrophages were found. Afterwards, it was discovered that the amyloid deposit consisted of a peptide of 4 kDa in a β-sheet conformation that was called β-amyloid (Aβ) (Selkoe *et al*., 2001), and that it was part of a 79 kDa transmembrane protein, the amyloid precursor protein (APP). It is now well known that APP is processed by three enzymes α, β and γ secretases (Nunan *et al*., 2000). These secretases cut APP in different sites, resulting in distinct peptide fragments that, depending on the involved secretases, may have physiological or pathological functions. α-secretase, a member of the ADAM family of metalloproteases (ADAM10), cleaves APP generating a secreted ectodomain (sAPPα) and a shorter membrane- fragment (C83). After this initial cleavage, γ secretase, a multi-protein complex (i.e. PSEN-1, APH-1, PEN-2), cleaves C83 domain releasing a small fragment called AICAD. Since the AICAD fragment dissolves easily within the cells without producing plaques, the APP processing *via* α-secretase was called "non-amyloidogenic pathway". β-secretase, a membrane bound aspartyl protease, also called BACE1, cleaves APP in its luminal domain to generate a β-secreted ectodomain (sAPP β). The remaining 10-kD β-cleaved carboxy-terminal fragment of APP (C99) is subsequently substrate for γ-secretase, which cleaves C99 to release fragments with 40 or 42 aa residues known as Aβ1-40 or Aβ1-42. These fragments do not dissolve in the cells, but move to the extracellular side of the neural membrane where they aggregate generating the senile plaques (Figure. 3). This is known as the amyloidogenic way of APP metabolism (Ehehalt *et al*., 2003). Generally Alzheimer disease and Prion diseases are included among rafts neurodegenerative diseases, since the aberrant proteolytic processing of PrP and A-Beta occur in these lipidic membrane domains. Therefore, it is most likely that alterations in the composition of lipid rafts can lead to a variety of disease of lipid metabolism.

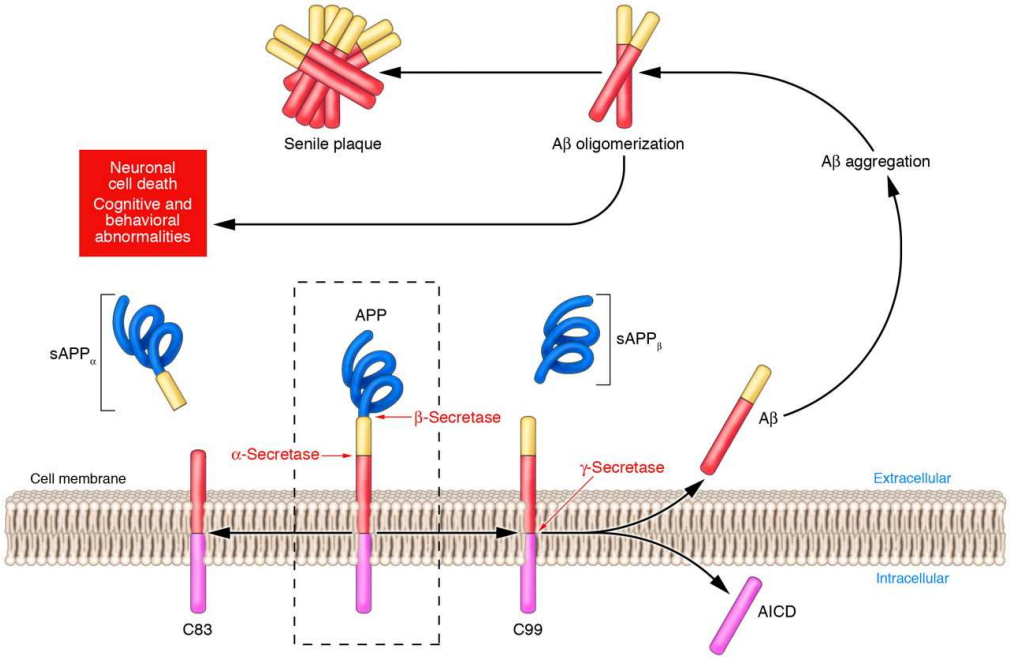

Figura 3. Processing of the APP and Aß store. The mature garage APP is tried along two metabolic streets in competition between them: The street of α-secretasy pathway that produces APP_{α} and C83 (left), and the street of the ß-secretasy pathway that produces $sAPP_{\beta}$ and C99 (right).

1.3 Prion Disorders

Prion Disease (PrD) are invariably fatal neurodegenerative disordes that. include Kuru, Creutzfeldt-Jakob disease (CJD), Gerstman-Straussler-Scheinker syndrome (GSS) and fatal familial insomnia in humans (Bate et al., 2004), scrapie in sheep and goats, bovine spongiform encephalopathy (BSE) in cattle, and encephalopathies in mink, cats, mule deer, elk and several exotic ungulates (Harris, 1999). In human beings a sporadic (~85% of cases), genetic (~15%) or acquired through dietary or medical exposure to infected tissues (<1%), while in animals only the infectious origin has been identified. (Novakofshi *et al.*, 2005). Nevertheless, the expression Transmissible Spongiform Encephalopathies (TSE) is now commonly used to indicate all prion diseases, both in humans and animals, regardless of their origin. The first description of a Transmissible spongiform encephalopathies (TSE), ovine scrapie, was published in the middle of the 18th century (Koster *et al.*; 2003). These diseases are rapidly progressive, fatal and untreatable neurodegenerative syndromes that are neuropathologically characterized by spongiform change (microcavitation of the brain), neuronal loss, glial activation and accumulation of an abnormal amyloidogenic protein. The clinical features of TSEs which consist of mental changes, ataxia, and loss of fine control of body homeostasis are due to massive loss of neuron function in the brain and are characteristic of many other fatal neurodegenerative diseases. A human TSE, Creutzfeldt-Jakob disease (CJD), was first described in older humans by Creutzfeldt (1920). In the early 1950s a group of scientists led by

Gadjusek recognised a disease, Kuru, in the fore tribe of New Guinea, which showed great similarities with scrapie and CJD. Other human transmissible spongiform encephalopathies occurring after the age of 40 are Gerstmann-Straüssler-Scheinker syndrome (GSS) and fatal familiar insomnia (FFI), which are associated with a ataxia and progressive dementia, as also Kuru and CJD. Since 1996, a new variant CJD (vCJD), which probably derives from the consumption of cattle neural tissues contaminated with the Bovine spongiform encephalopathy (BSE), has been identified in the United Kingdom, France, the Republic of Ireland, Hong Kong, Italy, the United States and Canada and is characterized by young age of onset, a stereotypical pattern of illness progression and distinctive neuropathological features (Forman *et al*.; 2004) (Table 1).

Disease	**Host**	**Mechanism of pathogenesis**
Kuru	Fore people	Infection through ritualistic cannibalism
iCJD	Humans	Infection from prion-contaminated HGH, dura mater grafts, etc.
vCJD	Humans	Infection from bovine prions?
FCJD	Humans	Germ-line mutations in PrP gene
GSS	Humans	Germ-line mutations in PrP gene
FFI	Humans	Germ-line mutation in PrP gene (D178N, M129)
SCJD	Humans	Somatic mutation or spontaneous conversion of PrPC into PrPSc?
FSI	Humans	Somatic mutation or spontaneous conversion of PrPC into PrPSc?
Scrapie	Sheep	Infection in genetically susceptible sheep
BSE	Cattle	Infection with prion-contaminated MBM
TME	Mink	Infection with prions from sheep or cattle
CWD	Mule deer, elk	Unknown
FSE	Cats	Infection with prion-contaminated bovine tissues or MBM
Exotic ungulate encephalopathy	Greater kudu, nyala, oryx	Infection with prion-contaminated MBM

Table 1. **The prion diseases.** iCJD, iatrogenic CJD; vCJD, variant CJD; fCJD, familial CJD; sCJD, sporadic CJD; GSS, Gerstmann–Straussler–Sheinker disease; FFI, fatal familial insomnia; FSI, fatal sporadic insomnia; BSE, bovine spongiform encephalopathy; TME, transmissible mink encephalopathy; CWD, chronic wasting disease; FSE, feline spongiform encephalopathy; HGH, human growth hormone; MBM, meat and bone meal (Aguzzi et al., 2000).

For a long time it was believed that the source of infection of the TSEs was a virus of a viroid. However, purification and characterization studies showed the possibility of a proteinaceous nature of the TSE agent. These results were consolidated by further studies, which showed that the scrapie agent is resistant to procedures that destroy nucleic acids such as treatment with nucleases and UV radiation (Koster *et al*.; 2003). In 1982 Prusiner isolated a protease and heat-resistant protein from the brain of scrapie-infected hamsters. He termed it PrPsc (scrapie-associated prion protein) and proposed that PrPsc is identical with the infectious agent. Although the exact physical nature of the transmissible agent is still controversial, a very large body of experimental data supports the `protein only' hypothesis, first outlined in general terms by Griffith in 1967 and enunciated in its updated and detailed form by Prusiner. This theory proposes that the agent is devoid of nucleic acid and consists solely of an abnormal conformer of the cellular prion protein, PrPc. The exact mechanism of the conversion from the cellular PrPc to the infectious form PrPsc is still unknown. The "normal", cellular isoform of the prion protein has exactly the same amino acid sequence as the scrapie isoform, but it does have different characteristics: PrPc is a monomeric protein predominantly α-helical (42%) with little β-sheet structure (3%), which is soluble in so-called "soft" detergents and is sensitive to digestion with proteinase K (PK). In contrast, PrPsc is mostly β-sheet (43%) with less α-helical structure (30%), which is insoluble, and the N-terminus (aa 90-231) is unusually resistant to PK digestion (Harris *et al.,* 1999; Caughey *et al.,* 1991) (Figure. 4).

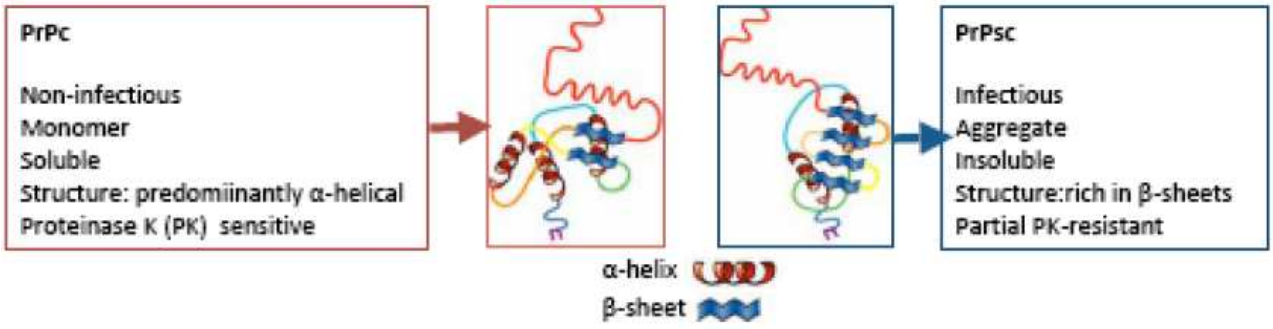

Figure.4. Features of PrPc and PrPsc.

It has been proposed that a direct interaction between the correctly folded PrPc form and the infectious misfolded isoform (PrPsc) is required for the abnormal conformational transition (Campana *et al.,* 2005; Prusiner *et al.,* 1998). According to this theory (Figure 5), PrPsc would act as a template upon which molecules of PrPc refold into exogenous PrPsc molecules through a process facilitated by another, thus far unidentified, protein termed "protein X". During prion

propagation, protein X appears to bind to the terminus of the normal protein structure, which acquires substantial β-sheet structure post-translationally (Legname *et al*., 2007).

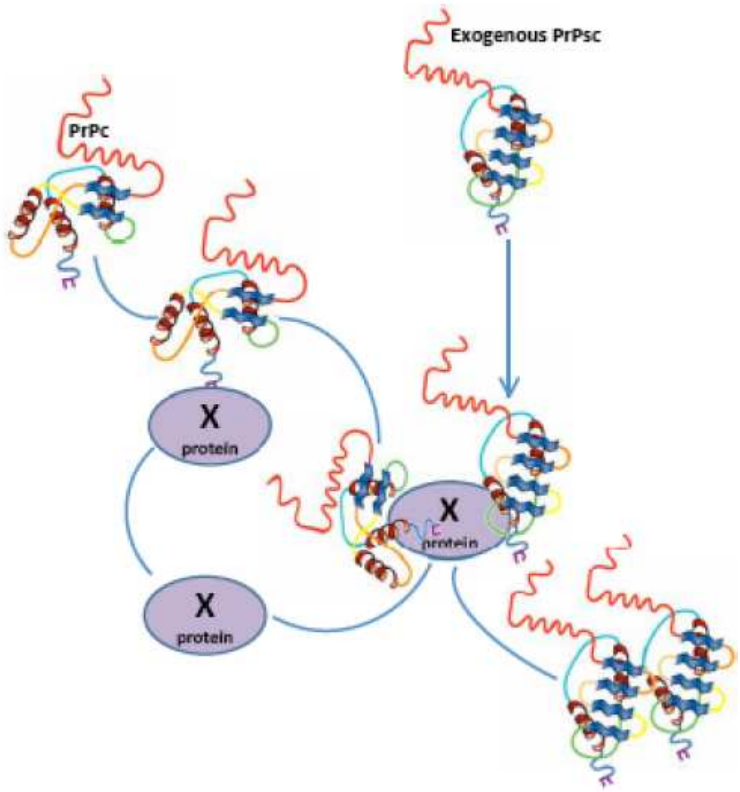

Figure. 5. Conversion of PrPc into PrPsc.

PrPc is formed by a C-terminal half compact domain structure consisting of three α-helices and a two stranded anti-parallel β-sheet, and by less structured N terminal half (Donne *et al*., 1997). Within this N-terminal domain there are four copies of an octapeptide repeat sequence that bind copper ions. Within the centre, there is a highly conserved hydrophobic region (aa residues 106–126) that, at least as an isolated peptide, has neurotoxic properties (Chiesa *et al*., 2001) (Figura 6)**.**

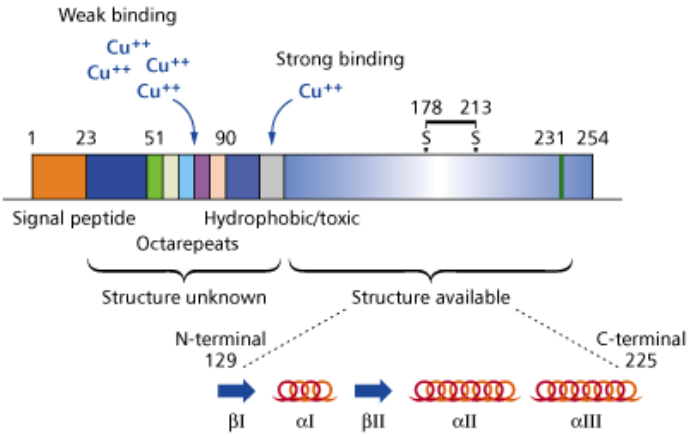

Figure 6. PrP^{C} schematic rappresentation: In this scheme protein's functional domines and the portion of the protein with a well known secondary structure are indicated.

So far, PrPsc represent the unique marker for the diagnosis (post-mortem) as well as the only known component of the infectious agent, being able of self-propagation by inducing structural conversion of the normal PrPc into a likeness of itself. No effective means for ante-mortem diagnosis or therapeutic interventions are presently available for TSEs. Besides other reasons, the development of efficacious prevention/therapeutic strategies are also hampered by the knowledge that the pathogenesis of the prion diseases is the result of a fine and complex interaction between the infectious agent and one or more genetic factors (Hsiao *et al*., 1989; Gabizon, *et al*., 1993). The complexity of this interaction is well documented in the ovine scrapie (Pocchiari, 1994), in which many polymorphic codons have been described to date in the PrP open-reading frame. However, only the mutations at codons at 136 (A→V), 154 (R→H) e 171 (Q→R o H) are associated with susceptibility/resistence to the disease. These mutations originate different alleles: VRQ, ARQ, AHQ, ARH, ARR and 15 different genotypes. Of these, VRQ and ARQ allele are associated with high scrapie susceptibility, while ARR allele is associated with resistance (Goldmann *et al*., 1994). Given that ovine scrapie is the most studied prion diseases that displays pathogenetic similarities with the human CJD, it represents an ideal experimental model to gain more information on the prion biology and its correlation with cholesterol metabolism.

It was previously reported that. the formation of PrPsc is dependent upon the interaction of PrPc with specific, cholesterol-rich membrane microdomains, commonly called lipid rafts (Vey *et al.*, 1996; Naslavsky *et al.*, 1997). Over the last few years a significant amount of genetic, biochemical, and pharmacological data highlighted cholesterol modifications associated with PrPsc biogenesis. (Bach *et al*., 2009; Sorensen *et al*., 2009; Hwang *et al*., 2009). Cholesterol, a well known critical regulator of membrane structure and raft function, was demonstrated to be essential for the cell-surface localization of PrPc (Bate et al., 2004; Gilch et al., 2006) and now emerges as the most important factor involved in the formation of misfolded proteins.

1.4 The Crucial Role of Cholesterol in Cell Physiology

The cholesterol is a vital biological molecule in mammals. It is the starting material or an intermediate compound from which the body synthesizes bile acids, steroid hormones, and vitamin D, as well as a the major component of plasma membranes (PM). Except for specialized cells (i.e.hepatocytes and enterocytes etc.) all other mammalian cells generally require cholesterol for the proper functioning of their membranes. In PM, rather than diffusing freely within the phospholipid bilayer, cholesterol mainly interacts, through its hydroxyl group, with the amide group of saturated phospholipids (sphingomyelin and glycosphingolipids). These cholesterol-sphingolipid complexes occur in high concentration in the outer bilayer leaflet, forming tightly packed domains called lipid

rafts (London *et al*., 2002). Lipid rafts are dynamic highly ordered membrane microdomains enriched in cholesterol, sphingolipids and saturated phospholipids. Conversely, the PM areas rich in phosphatidylcholine, and other unsaturated glycerol-based phospholipids having lower cholesterol affinity, are considered cholesterol-poor regions; these tend to be less densely packed and form liquid-disordered regions outside the rafts (non-raft regions) (Ohvo-Rekila *et al*., 2002; Clejan *et al*., 1998). In the lipid rafts, longer and saturated fatty acid phospholipids move in synchrony with the phospholipids on the inner side of the membrane, while in the non-raft regions the unsaturated phospholipids on one side of the membrane move independently of those on the other (Schmitz *et al*., 1990; Ridgway *et al*., 1999). The high concentrations of cholesterol-bound longer and saturated fatty acid sphingolipid tails make rafts ideal for holding a number of non-transmembrane proteins (Lucero *et al*., 2004), which include i) glycosyl phosphatidyl inositol (GPI)- anchored proteins, such as PrPc, which is involved in PrD, ii) proteolytic enzymes, such as β and γ secretases, which are involved in AD, and iii) acylated proteins, such as tyrosine kinases of the Src family, which are involved in signal transduction (in the cytoplasmic side). Transmembrane integral proteins are generally excluded from rafts, and are principally found in the non-raft regions (Rouvinski *et al*., 2003). Once the cell is activated, membrane rafts are believed to function as a concentrating platform for a variety of signal transduction molecules (Esler *et al*., 2001). During activation, many rafts would cluster, forming a larger platform, thus allowing functional proteins to concentrate and interact, likely with cytoplasmic signalling factors, such as small G proteins, that are recruited to the cytoplasmic face of rafts in response to clustering, thereby facilitating the initiation of signaling events. Importantly, this clustering is believed to be cholesterol dependent (Selkoe *et al*., 2001; De Strooper *et al*., 2000). Cholesterol is thought to serve as a spacer between the saturated fatty acid chains of the sphingolipids and to function as a glue keeping raft proteins assembled together (Simons *et al*., 2004). It seems that cholesterol acts as a molecular sorting machine capable of the space-temporal coordination of the segregation, processing, trafficking, and functioning of raft-resident proteins. Given this, even minor changes in raft cholesterol may lead to dissociation of resident proteins, rendering them non-functional and thus contributing to a variety of diseases, including misfolding disorders. Fortunately, cells and organisms have developed extraordinarily sophisticated mechanisms for controlling lipid composition, and hence the properties of biological membranes. This control mainly consists in aligning cholesterol content with the demands imposed by cell metabolic requirements.

1.5 Metabolism and Intracellular Trafficking of Cholesterol

Commonly cited that in non-specialized cells 75-85% of total cellular cholesterol is mainly in rafts, in the form of free cholesterol (FC), while 10-15% is in cytoplas-mic lipid droplets (LDs), in the form of cholesterol esters (CEs), and only 0.1-2% is in ER membranes (Figure. 7). In these cells, FC derives either from the internalization of low-density lipoprotein (LDL) *via* LDL receptors (LDL–R) localized in clathrin-coated pits of non-raft PM, or from endogenous biosynthesis in the ER via 3-hydroxy-3-methy-lglutaryl coenzyme reductase A (HMGCoA-R)., or both CEs are formed by the action of an ER resident enzyme, acyl-CoA: cholesterol acyltransferase (ACAT1), also known as sterol O-acyltransferase (SOAT1), encoded by the SOAT1 gene. It catalyzes the bond between the hydroxyl FC group and the long-chain fatty-acyl-coenzyme A carboxylic group (Dessi *et al*., 2004). A tightly controlled network of cellular signalling and lipid transfer systems orchestrates the functional compartmentalization of cholesterol within and between organellar membranes. Despite the fact that, under normal conditions, ER cholesterol levels are very low, it appears that ER membrane FC is essential for the correct regulation of cholesterol homeostatic machinery (Prinz W *et al*., 2002). When ER-FC increases, a cellular sensor, SCAP, a sterol-regulatory-element-binding protein (SREBP)-cleavage-activating-protein is blocked. SCAP is necessary for the proteolytic activation of SREBP-2, a transcription factor that promotes the expression of genes involved in cholesterol synthesis (HMGCoA-R) and uptake (LDL-R). Thus, high ER-FC represses cholesterol synthesis and uptake, while allosterically activating ACAT1, which is responsible for cholesterol esterification. The resulting CEs are stored, along with triglycerides (TG), in LD cores, which serve as transient neutral lipid depots (Maxfield *et al*., 2005). Since an excess of CEs in LDs leads to foam-cell-like formation, the excess must be removed. The only way for LDs to get rid of CE excess is to re-hydrolyze them to FC through nCEH activation. FC is then recycled to the membranes by cholesterol-binding proteins (cav1 and cav2), where it can be delivered to extracellular high-density lipoproteins (HDL), via the ATP binding- cassette-sub-family A-member 1 (ABCA-1) transporter (Albrecht *et al*., 2007), for efflux. On the other hand, when FC-ER decreases, the SREBP–SCAP complex exits the ER, and SREBP2 undergoes two proteolytic cleavages. These cleavages release the SREBP2 cytosolic domain, which moves into the nucleus, where it induces LDL-R and HMG-CoA-R transcription, thus activating cholesterol synthesis and uptake. Concurrently, ACAT1 activity is inhibited and that of nCEH is induced. By hydrolyzing CE back to FC and fatty acids, nCEH allows cholesterol to leave the LDs, providing a prompt source of FC to replenish raft domains (Figure. 7).

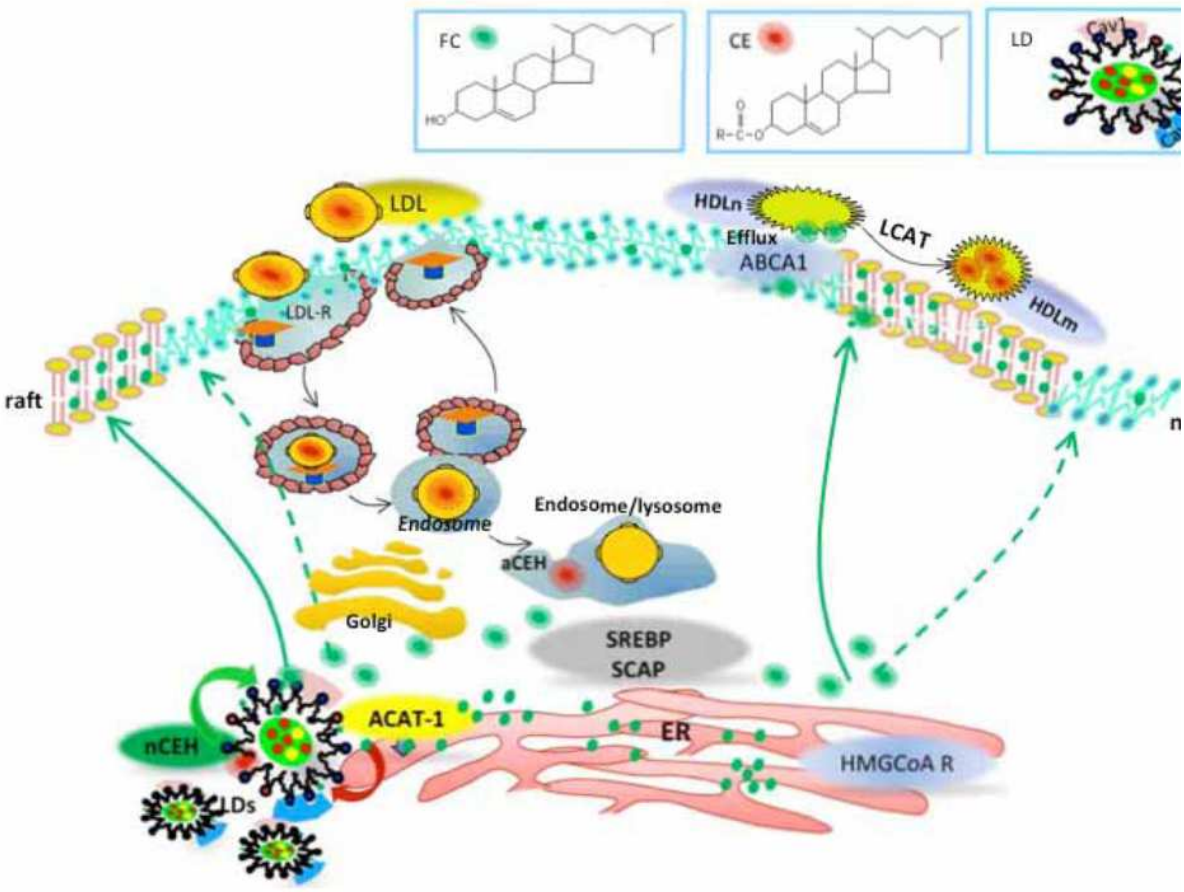

Figure 7. Compartmentalization and key homeostatic molecules of cellular cholesterol.

In this scenario the cholesterol ester cycle emerges as the principal short-term protection to keep PM cholesterol within a range in harmony with cell metabolic needs.

1.6 Cholesterol Homeostasis in the brain

The mammalian nervous system contains a disproportionate amount of cholesterol. In the brain the cholesterol content is about 10-fold greater than in any other organ (Dietschy *et al*., 2004) indicating that cholesterol plays a central role in the development and maintenance of the brain and nervous system. Within the brain some 70% of cholesterol is present in myelin, where it fulfils a critical insulating role. It is likely that the requirement for efficient signalling despite a small transverse diameter of axons was a key selective pressure driving the accretion of cholesterol in the mammalian brain (Snipe *et al*., 1997). At a cellular level the myelin sheath consists of sections of plasma membrane repeatedly wrapped around an axon, with the extrusion of virtually all of the cytoplasm. Myelin is formed by two very specialized cells: the oligodendrocyte in CNS and the Schwann cell in the peripheral nervous system.

The remaining 30% of brain cholesterol is divided between glial cells (20%) and neurons (10%). According to various *in vitro* studies with cultured cells, astrocytes synthesize at least 2-3 fold more cholesterol than neurons, while oligodendrocytes have an even higher capacity for cholesterol synthesis, at least during periods of active myelination. (Bjorkhem *et al*., 2004). It is noteworthy that even minor changes in the structure of the constituent sterols of the nervous system, e.g. the presence of one additional double bond, leads to a change in the biophysical properties of the cell membrane with profound clinical effects. The strategy used by nature for cholesterol homeostasis in the brain and spinal cord is different from that in other parts of the body. Due to the efficient blood-brain barrier there is no passage of lipoprotein-bound cholesterol from the circulation to the brain (Dietschy *et al*., 2004). The blood-brain barrier thus prevents diffusion of large molecules at the level of tight junctional attachments between adjacent capillary endothelial cells. In addition to this, there is also no trans vesicular movement of solution across the capillaries. It is possible that one or more members of the ATP binding cassette transporter superfamily may be involved in the exclusion of circulating cholesterol from the brain, but conclusive evidence is lacking for this. Thus all the cholesterol present in the brain is formed by *de novo* synthesis and the same is true also for the cholesterol in the peripheral nervous system. Except for the active phase of specific pathological conditions, almost all (at least 99%) cholesterol in the nervous system is unesterified. In the adult brain most of its synthesis is balanced by formation of a hydroxylated metabolite, 24S-hydroxycholesterol (24S-OHC), which is able to pass across the blood-brain barrier and enter the circulation and it represents one of the most important mechanism for the elimination of brain-derived cholesterol (Bjorkhem *et al.,* 2001; Russell *et al.,* 2009). In addition to this there is a small efflux of cholesterol from the brain in the form of apolipoprotein E (APOE) containing lipoproteins via the cerebrospinal fluid (Pitas *et al*., 1987). The turnover of the cholesterol present in membranes of the neuronal cells and in astrocytes may however change in response to different factors. Under normal conditions cholesterol 24-hydroxylase (CYP46A1), the enzyme system responsible for formation of 24S-OHC is only present in neuronal cells, with particularly high levels in the pyramidal neurons in various layers of the cortex, in the hippocampus and in Purkinje cells in the cerebellum (Russell *et al.,* 2009).

The uptake of cholesterol by these cells may thus be balanced by the secretion of 24S-OHC. The 24S-OHC secreted from the neuronal cells may be of importance for regulation of cholesterol synthesis and secretion of this cholesterol in APOE-bound form astroglia. In contrast, cholesterol synthesis appears to be regulated by similar mechanisms both outside and inside the brain with hydroxy-methylglutaryl CoenzymeA reductase (HMGCR) being the most important regulatory enzyme (Dietschy *et al*., 2004).

Although formation of 24S-OHC is responsible for the removal of about two-thirds of cholesterol from the brain, under normal conditions APOE seems to be the most important carrier of cholesterol in the brain extracellular fluid. Therefore, in the brain, where the turnover of cholesterol is much slower than in other tissues, neuronal cells, in contrast to other cell types, require a constant supply of lipid molecules. The mammals have developed complex and sophisticated homeostatic mechanisms that function to maintain cellular cholesterol levels in membranes within a narrow range. Alterations and/or disturbances in these homeostatic mechanisms, either by genetic, environmental, diet-induced or natural aging can lead to altered cell function that probably result in greater susceptibility to aberrant processes and /or lower responsiveness to repair mechanisms.

1.7 Cholesterol and Protein Misfolding

Growing evidence indicates that rafts are involved in amyloid generation from APP and PrPc, possibly through the creation of a favourable lipid environment. It has been reported that, when APP and PrPc molecules occupy a lipid raft region of the membrane, they are more accessible to and, thus, preferentially cleaved by, amyloidogenic enzymes (i.e. raft resident β-secretase). On the other hand, when APP and PrPc molecules are outside rafts, they appear to be preferentially cleaved by non-amyloidogenic non-raft resident α-secretase (ADAM 10) (Allinson *et al*., 2003).

The most straightforward interpretation of this information is that APP and PrPc are present in two cellular pools: one, outside rafts, where these two proteins are processed in a normal way; the other, inside the rafts, where abnormal cleavage takes place [(Ehehalt *et al*., 2003; Harris *et al*., 1999).

Interestingly, very recent results (Sarnataro *et al*., 2009) include evidence that PrPc is found in non-raft regions, besides being present, as GPI-anchored protein, in rafts. These authors also reported that, in neuronal cells, PrPc translocates out of rafts, upon copper binding to the N-terminal octapeptide repeats, prior to being endocytosized through clathrin-coated pits. This membrane compartmen-talization model would explain how the same protein may be processed in two different and mutually exclusive ways. Interestingly, the amount of cholesterol associated with these domains exerts profound effects on the functions of the raft-resident proteins. It has been claimed that two alternative and opposite scenarios involving disturbance of the cholesterol-rich raft domains describe the role of cholesterol in PrPsc generation. The high membrane cholesterol model implies that cholesterol enrichment would favor contact between PrP and misfolded PrPsc isoforms, by triggering the raft-clustering process. The low membrane cholesterol model claims, instead, that undesired amyloidogenic protein-protein interactions are favoured by raft disassembly caused by cholesterol depletion (Simons et al 2002).

Constant low levels of cholesterol in lipid rafts could lead to a continuous stimulus of cell growth promotion (Wang et al., 2005), or induce cellular prion protein PrPc to undergo pathologic processes (Figure 10) leading to the generation of their corresponding pathogenic forms (Simons *et al*., 2001; Diomede *et al*., 2002).

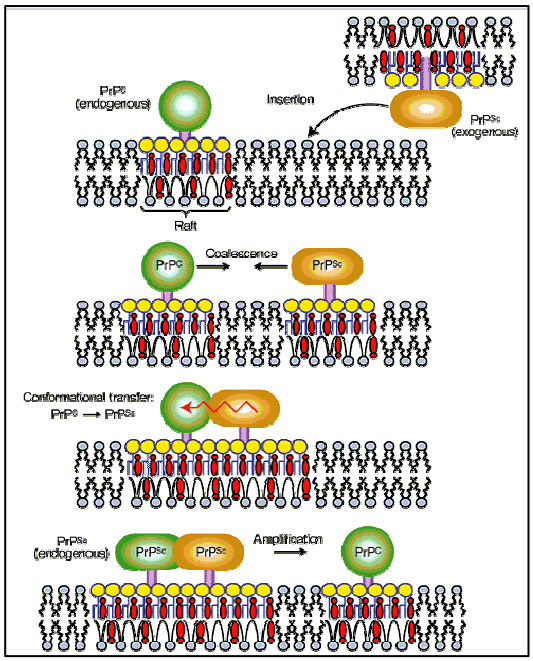

Figure10. The PrP^{C} to PrP^{Sc} conversion in membrane rafts ("Raft clustering").

2. THE PRESENT INVESTIGATION:

It is now well established that cellular cholesterol metabolism plays an important role in PrPsc generation. In the last decade, several lines of evidence indicated that prion disorders are likely associated with lipid metabolic alterations that involve an increase in the cellular cholesterol pool. In this respect, in our laboratory, during the period of my internship for Degree in Biology and the post-lauream training period, we investigated the role of cholesterol in the pathogenesis of prion diseases, and obtained evidences of an abnormal accumulation of CE in brains, as well as in *ex vivo* peripheral blood mononuclear cells (PBMCs) and skin fibroblast cultures, from scrapie-affected with respect to healthy sheep. Compared to sheep carrying a scrapie-resistant genotype, increased CE pool was also found in tissue and cell samples from sheep carrying a scrapie-susceptible genotype (Pani *et al*., Cholesterol Metabolism in Brain and Skin Fibroblasts from Sarda Breed Sheep With Scrapie-resistant and Scrapie-susceptible Genotypes, Am. J. Infec. Dis., 2007, 3, 143-150; Pani *et al*., Accumulation of Cholesterol Esters in ex vivo Lymphocytes from Scrapie-susceptible Sheep and in Scrapie-infected Mouse Neuroblastoma Cell Lines, Am. J. Infec. Dis., 2007, 3, 165-168). Similar CE alterations were also observed in mouse neuroblastoma N2a cell lines persistently infected with mouse-adapted 22L and RML strains of mouse-adapted scrapie (Pani *et al*., Accumulation of Cholesterol Esters in ex vivo Lymphocytes from Scrapie-susceptible Sheep and in Scrapie-infected Mouse Neuroblastoma Cell Lines, Am. J. Infec. Dis., 2007, 3, 165-168). The treatment of ex vivo PBMCs and skin fibroblasts from scrapie-affected sheep with a number of drugs known to interfere with different steps of cholesterol metabolism strongly reduced the accumulation of CE. In the infected N2a cells, these cholesterol modulators were able to parallel CE reduction to a selective inhibition of the scrapie-like prion protein (PrPres), indicating a direct effect of cholesterol alteration on the misfolding of PrP. This was supported by the finding that PrPres-producing cell populations of subclones from scrapie-infected cell lines were characterized by higher CE levels than clone populations not producing PrPres.

Overall, the results obtained in our previous studies suggested that abnormal cholesterol esterification could indicate an altered metabolic cholesterol arrangement that predispose the cell to the development of pathological processes involving abnormal activation, processing, and/or trafficking of membrane resident proteins. If this was true, then cholesterol homeostasis restoration and in particular the inhibition of cholesterol esterification may represent a nove approach for the control of prion diseases. On these premises, during my PhD, I have continued the studies on the role of cholesterol in the pathogenesis of prion disorders. For clarity sake, description of the whole body of data embedded in this thesis can be subdivided into three different sections. The first one is on the major faced aspect, that is “Studies on the role of cholesterol in the pathogenesis of prion

disorders”(Chapter I). Specific objectives were to evaluate i) gene and protein expression of ACAT-1, Cav-1, and PrPc in brains and skin fibroblasts from scrapie-affected and scrapie-susceptible sheep; ii) the lipid content in cultured scrapie-infected mouse neuroblastoma cell lines, as well as in rodents experimentally infected with scrapie, by different colorimetric and analytical method; iii) the changes in cellular cholesterol pools following treatment with drugs, both in single and dual-drug associations, targeting different steps of the cholesterol metabolism leading to cholesterol esterification (i.e. everolimus, pioglitazone, sandoz 58035, progesterone, verapamil, and others) , and to cholesterol neosynthesis (i.e. pravastatine). The second part of my studies were focused on the characterization of the soluble prion infectivity from scrapie-affected hamster brains (Chapter II). The last part of my researches was devoted to investigate the potential superantigen activity of Alzheimer’s peptides (i.e. sAPPα, Aβ40 and Aβ42) (Chapter III).

2.1 CHAPTER I

STUDIES ON THE ROLE OF CHOLESTEROL IN THE PATHOGENESIS OF PRION DISORDERS

2.1.1 ACAT-1, Cav-1 and PrP expression in scrapie susceptible and resistant sheep (Article I)

As above mentioned, our previous studies on the role of cholesterol homeostasis in the pathogenesis of Scrapie, revealed abnormal accumulation of CE in the brains and in *ex vivo* PBMCs and skin fibroblast cultures from healthy and scrapie-affected sheep carrying a scrapie-susceptible genotype, with respect to samples from sheep with a resistant genotype. In this work we showed that intracellular accumulation of cholesterol esters (CE) in fibroblasts cultures derived from scrapie-susceptible sheep was accompanied by parallel alterations in the expression level of acyl-coenzymeA: cholesterol-acyltransferase (ACAT1) and caveolin-1 (Cav-1), that are respectively involved in the pathways leading to intracellular cholesterol esterification and trafficking. Comparative analysis of cellular prion protein (PrPc) mRNA, showed an higher expression level in cells from animals carrying a susceptible genotype, with or without Scrapie. These data suggest that CE accumulation in peripheral cells, together with the altered expression of some proteins involved in intracellular cholesterol homeostasis, might serve to identify a distinctive lipid metabolic profile associated with increased susceptibility to develop prion disease following infection.

Article I

Cent. Eur. J. Biol. • 5(1) • 2010 • 31–37
DOI: 10.2478/s11535-009-0076-3

VERSITA

Central European Journal of **Biology**

ACAT-1, Cav-1 and PrP expression in scrapie susceptible and resistant sheep

Research Article

Cristina D. Orrù[1#], Claudia Abete[1#], M. Dolores Cannas[1], Claudia Mulas[1], Claudia Norfo[1], Antonella Mandas[2], Sarah Vascellari[1], Paolo La Colla[1], Sandra Dessì[2*], Alessandra Pani[1&]

[1]*Department of Biomedical Science and Technology, University of Cagliari, 09042 Monserrato, Italy*

[2]*Department of Internal Medicine, University of Cagliari, 09042 Monserrato, Italy*

Received 17 June 2009; Accepted 06 October 2009

Abstract: Scrapie is a prion disease for which no means of ante-mortem diagnosis is available. We recently found a relationship between cell susceptibility to scrapie and altered cholesterol homeostasis. In brains and in skin fibroblasts and peripheral blood mononuclear cells from healthy and scrapie-affected sheep carrying a scrapie-susceptible genotype, the levels of cholesterol esters were consistently higher than in tissues and cultures derived from animals with a scrapie-resistant genotype. Here we show that intracellular accumulation of cholesterol esters (CE) in fibroblasts derived from scrapie-susceptible sheep was accompanied by parallel alterations in the expression level of acyl-coenzymeA: cholesterol-acyltransferase (ACAT1) and caveolin-1 (Cav-1) that are involved in the pathways leading to intracellular cholesterol esterification and trafficking. Comparative analysis of cellular prion protein (PrPc) mRNA, showed an higher expression level in cells from animals carrying a susceptible genotype, with or without Scrapie. These data suggest that CE accumulation in peripheral cells, together with the altered expression of some proteins implicated in intracellular cholesterol homeostasis, might serve to identify a distinctive lipid metabolic profile associated with increased susceptibility to develop prion disease following infection.

Keywords: *Scrapie • Prion diseases • Cholesterol homeostasis • Cholesterol esters*

1. Introduction

Prion diseases are fatal neurodegenerative disorders for which no *in vitam* diagnostic tests or effective treatments are currently available. Prion diseases can be inherited, sporadic or transmissible, but in spite of their diverse origins, all forms seem caused by the structural conversion of the cellular prion protein (PrPc) into its pathologic isoform (PrPSc), which is linked to infectivity [1]. PrPc is normally GPI-anchored to specialized cholesterol-rich domains of the plasma membrane, termed lipid rafts or caveolae [2,3]. These membrane domains are detergent-insoluble regions characterized by the presence of free cholesterol (FC), saturated phospholipids and raft-resident proteins [4]. Increasing evidence indicates that subtle intracellular cholesterol changes affect the intracellular processing/trafficking, function and/or activation of raft-resident proteins, including PrPc [2,5-7]. Therefore, a role for cholesterol in the metabolism of PrPc and its conversion into PrPSc has been proposed [7-10].

In normal tissues, approximately 90% of the total cellular cholesterol resides in membrane raft domains as FC, while only a small amount (approximately 1-10%) is found as CE in a cytoplasmic storage form [11]. Because membrane cholesterol appears critical for the function of raft-resident proteins, cells develop

# *These authors contributed equally to this work*
* *E-mail: sdessi@unica.it*
& *E-mail: pania@unica.it*

a highly integrated set of homeostatic mechanisms that finely regulate FC *vs.* CE pools according to the cell's need. In fact, membrane FC is in a dynamic state, moving to the endoplasmic reticulum (ER) in response to changing homeostatic conditions in the cell [12,13]. FC in the ER, if in excess, is converted to CE by ACAT-1, and stored in the cytoplasm as neutral lipid droplets [14]. When cell needs FC for membrane function, or when CE droplets exceed a critical threshold value, CE can be reconverted to FC and recycled to the membrane by cholesterol binding proteins, such as Cav-1 [4,6].

Our recent studies on the role of cholesterol homeostasis in the pathogenesis of Scrapie, revealed abnormal accumulation of CE in the brains and in *ex vivo* peripheral blood mononuclear cells (PBMCs) and skin fibroblast cultures from healthy and scrapie-affected sheep carrying a scrapie-susceptible genotype, when compared to those of sheep with a resistant genotype [15,16]. Similar alterations were observed in mouse neuroblastoma N2a cell lines persistently infected with mouse-adapted 22L and RML strains of scrapie that showed up to 3-fold higher CE levels than parental cells [16]. Moreover, i) scrapie-like prion protein (PrPres)-producing cell populations of subclones from scrapie-infected cell lines were characterized by higher CE levels than clone populations not producing PrPres, and ii) reduction of CE by cholesterol ester metabolism interfering drugs was associated to PrPres inhibition [17]. We thus suggested that abnormal CE levels could identify a phenotype predisposing a cell to the development of pathologic processes involving abnormal activation, and/or processing, and/or trafficking of membrane resident proteins. Other authors, however, found an inhibition of prion infection by using FC lowering drugs (*i.e.* statins) in both *in vitro* [18,19] and *in vivo* [20] prion models.

Thus, in an attempt to better characterize the lipid metabolic state that appears to influence the susceptibility to prion infection, in the present study we compared gene and protein expression of ACAT-1, Cav-1, and PrPc in brains and skin fibroblasts from Sarda sheep carrying scrapie-resistant (ARR/ARR) or scrapie-susceptible (ARQ/ARQ) prion protein genotype, both without (ARQ/ARQ-) and with (ARQ/ARQ+) Scrapie. In addition, the correlation between expression of ACAT-1 and Cav-1 proteins with that of PrPc was evaluated in skin fibroblast cultures from sheep with the different genotypes.

2. Experimental Procedures

2.1 Brain and skin samples

Female Sarda breed ovines ranging from 2 to 4 years of age, and raised in the same environmental conditions, were used in this study. All samples were collected according to the Principles of Laboratory Animal Care at the experimental farms of the Istituto Zooprofilattico Sperimentale of Sardinia (Italy), and kindly provided by Dr. Ciriaco Ligios. Brain samples were obtained from 3 sheep: two sheep carried the susceptible scrapie genotype ARQ/ARQ, 1 sheep was clinically affected by natural scrapie (ARQ/ARQ+) while the other was healthy and negative for PrP^{Sc} in the brain (ARQ/ARQ-); the third sheep carried the resistant genotype ARR/ARR. All sheep were euthanized with a barbiturate followed by 4 ml of embutramide and mebenzonico-iodide (Hoechst Roussel Vet), brain samples were stored at –80°C immediately after collection and thawed just prior to use. Fresh skin biopsies were obtained from 14 sheep and were delivered to our laboratory in transport medium (Eurocollins). Ten biopsies were from sheep with the susceptible genotype ARQ/ARQ; of these, 2 were scrapie-free (ARQ/ARQ-), while 7 developed clinical disease following experimental inoculation of scrapie and 1 had natural scrapie (ARQ/ARQ+). In addition, skin biopsies from 4 scrapie-resistant ARR/ARR sheep, which were experimentally infected with scrapie and remained free of clinical signs, were used as controls. All biopsies were taken at the terminal clinical stage of the scrapie-affected sheep.

2.2 Skin fibroblast cultures

Tissue fragments from skin biopsies were plated into 6-well plates and allowed to adhere to the bottom of the vessels. After 2 h, they were covered with a few drops of Dulbecco's modified Eagle's medium (D-MEM) (Gibco Lab NY, USA) supplemented with 10% fetal bovine serum (FBS) (Sigma), 100 U/ml penicillin/streptomycin (Sigma), and fungizone (Life Technologies, Inc.) and incubated at 37°C in a humidified incubator with 5% CO_2. The following day, tissue fragments were overlaid with culture medium, which was changed every two days. Five to six days later, fibroblasts begun to proliferate from the fragment margins ("halo of cells") and began to form a monolayer. After four weeks, fibroblasts were purified by repeated trypsinization (trypsin-EDTA) and passaging to achieve an homogenous population of spindle cells. Purified fibroblasts were washed twice with sterile PBS and centrifuged. $1x10^6$ cells were then seeded into 25 cm^2 culture flask and grown to confluence. Then, cells were either used for *"in vitro"* experiments or resuspended in cryopreservation medium at a density of $1x10^7$ cells/ml and stored in liquid nitrogen. Analytical assays were carried out using fibroblast cultures between the second and fourth passage. Cells were plated at a density of $5x10^3$ cell/cm^2 in 6-well plates and brought to proliferative quiescence by incubation for 48 h in serum depleted

(0.2% FCS) MEM 199. Then, quiescent cells were stimulated to re-enter cell cycle by addition of 10% FCS and incubation at 37°C for the indicated time intervals.

2.3 RT-PCR and Southern blotting

The expression levels of Cav-1 and PrP mRNAs were evaluated in brain homogenates and skin fibroblasts by reverse transcription polymerase chain reaction (RT-PCR). mRNA levels for the housekeeping gene β-actin were used to normalize the amount of RNA inputs in the RT-PCR. Total RNA was extracted from 10^6 cells using the reagent TRIZOL (Invitrogen Corporation). Equal amounts of total RNA (1 µg) were reverse transcribed into cDNA using the random hexamer method and amplified by PCR in the presence of specific primers, according to the instructions provided by the manufacturer (GeneAmp RNA PCR Kit, Perkin-Elmer Cetus).

PCR was performed using the following ovine-specific primers and conditions: for Cav-1 (258 bp) forward: 5'- GATTAACAGTGGGTACGATA-3', reverse: 5'-TATGTAGTCTTGCGTTATCC-3'; 94°C for 30 s, 59°C for 30 s and 72°C for 45 s, for 30 cycles. For PrP, (341 bp) forward: 5'-ATTGTCACCTAGCAGATAGA-3', reverse: 5'-TTGTTCAGTAGCTCAAGTCT-3'; 94°C for 30 s, 58°C for 1 min, and 72°C for 45 s, for 30 cycles. For β-actin (217 bp) forward: 5'-GATCATGTTTGAGACCTTC-3', reverse: 5'-GAGGATCTTCATGAGGTAGT-3'; 96°C for 30 s, 60°C for 59 s, and 72°C for 45 s, for 20 cycles. Sub-saturation levels of cDNA templates, needed to produce a dose-dependent amount of PCR product, were defined in initial experiments by testing a range of template concentrations. Amplicons were labeled during PCR with Digoxigenin-11-dUTP (DIG; Roche Applied Science), immuno-detected with anti-digoxigenin antibodies conjugated to alkaline phosphatase (Roche Applied Science) and visualized with the chemiluminescent substrate CSPD®. The intensity of the bands was measured after exposure to X-ray film with the Kodak Digital Science Band Scanner Image Analysis System containing HP ScanJet, ID Image Analysis Software. The overall procedure was normalized by expressing the amount of PCR products for each target mRNA relative to the amount of PCR products obtained for the housekeeping gene β-actin.

2.4 Western blotting

Proteins were extracted from brain homogenates and fibroblast monolayers with 0.05 mL per mg of tissue, or cell pellets from 10^6 fibroblasts of RIPA buffer (20 mM Tris-HCl, pH 7.5; 150 mM NaCl, 1 mM Na_2-EDTA; 1 mM EGTA; 1% NP-40; 1% sodium deoxycholate; 2.5 mM sodium pyrophosphate; 1 mM ß-glycerophosphate; 1 mM Na_3VO_4; 1 µg/ml leupeptin). Protein concentration was determined with the Bicinchoninic Acid Protein determination kit (Sigma). Aliquots of protein extracts were separated by 10% SDS polyacrylamide gel electrophoresis and blotted onto nitrocellulose membranes (Millipore, Bedford MA). Blots were subjected to immunoblotting with a 1:5000 dilution of the anti-ACAT-1 antibody (H-125, Santa Cruz Biotechnology, Santa Cruz, CA) and a 1:2000 dilution of the anti-Cav-1 antibody (7C8, Novus Biologicals, Littleton CO), as indicated by the manufacturer. Blots were then reacted with the appropriate dilution of a HRP-conjugated secondary antibody (1:6500 for ACAT-1 and 1: 1000 for Cav-1). Specific bands were detected after addition of the chemiluminescent substrate (Amersham, Freiburg Germany), and analyzed by the NIH Image 1.63 Analysis Software program (Scion Image).

2.5 Statistical analysis

Data are reported as mean ± standard error (SE). Statistical calculations were performed using the statistical analysis software of Origin 7.0 version (Microcal, Inc, Northampton, MA, USA). A value of $P<0.05$ was considered to be statistically significant.

3. Results

3.1 ACAT-1 protein levels in sheep brains

Due to the role of ACAT-1 in the conversion of FC into CE, we investigated whether the different CE levels, previously observed in brains of scrapie-resistant and scrapie-susceptible sheep [15], correlated with the expression of this enzyme. Thus, Western blot analysis of brain protein extracts of ARR/ARR (scrapie-infected; scrapie-free), ARQ/ARQ$^-$ (mock infected) and ARQ/ARQ$^+$ (scrapie-infected; scrapie-affected) sheep was carried out using the anti-ACAT-1 H-125 monoclonal antibody. As shown in Figure 1, lower expression levels of ACAT-1 enzyme were indeed detected in the brains of ARR/ARR sheep, with respect to those of ARQ/ARQ$^-$ and ARQ/ARQ$^+$ animals. When compared to sheep with ARR/ARR genotypes, ARQ/ARQ$^-$ and ARQ/ARQ$^+$ sheep showed 1.7 and 2-fold higher levels of ACAT-1, respectively.

3.2 PrPc and Cav-1 mRNA levels in sheep brains

Based on the knowledge that PrPc is a raft-resident protein [2,3], and that Cav-1 [4,6] is involved in FC trafficking, we next measured mRNA levels of PrPc and Cav-1 in brain homogenates of scrapie-susceptible and scrapie-resistant sheep. Unfortunately, ACAT-1 mRNA levels could not be evaluated because the sequence

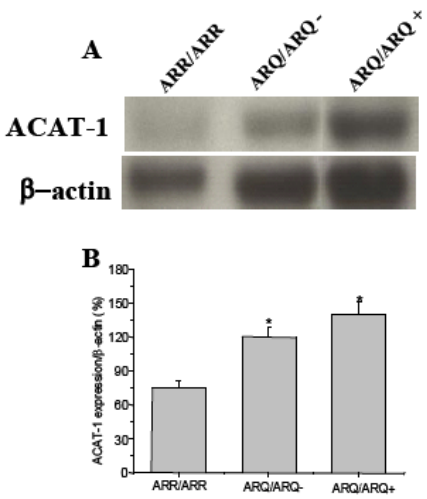

Figure 1. ACAT-1 protein expression in brain extracts of sheep carrying scrapie-resistant (ARR/ARR) or scrapie-susceptible (ARQ/ARQ) genotypes, with (ARQ/ARQ+) or without (ARQ/ARQ-) clinical Scrapie. Proteins were extracted, separated by PAGE and subjected to Western blot as indicated in Materials and Methods. Panel (A) shows representative chemiluminescent Western blots of ACAT-1 and ß-actin, used as an internal control. Panel (B) shows densitometric analyses of the ACAT-1 bands shown in panel A, normalized for the endogenous ß-actin protein content. Data represent mean values ± SE of triplicate determinations of four samples from each brain. *P<0.05 vs. ARR/ARR.

of the ovine ACAT gene is not available. As shown in Figure 2, lower levels of PrPc mRNA, and higher levels of Cav-1 mRNA, were detected in ARR/ARR sheep brains as compared to ARQ/ARQ$^-$ and ARQ/ARQ$^+$ animals.

3.3 ACAT-1 and Cav-1 protein levels in quiescent and replicating sheep skin fibroblasts

Since alterations in cholesterol homeostasis were also found in peripheral cells [15,16], we investigated whether similar expression patterns of ACAT-1 and Cav-1 differentiated skin fibroblasts from sheep with different genetic susceptibility to Scrapie. Due to the fact that cholesterol homeostasis is differently modulated during cell growth [21], the expression level of the two proteins was analysed at various time points after growth stimulation with FCS. Western blot analysis (Figure 3AB) confirmed that, consistent with the results obtained in brains, quiescent (time 0) ARR/ARR fibroblasts contained remarkably lower ACAT-1 expression than ARQ/ARQ fibroblasts. Following FCS stimulation, the above differences in ACAT-1 expression became less prominent, with the exception of ARQ/ARQ$^-$ fibroblasts at 24-48 h. On the contrary, ARR/ARR quiescent fibroblasts showed remarkably higher Cav-1 expression than ARQ/ARQ fibroblasts. Also in this case the above differences became less dramatic 24 h after FCS stimulation. In summary, scrapie-susceptible animals exhibit higher levels of ACAT-1 protein in both fibroblasts and brains. By contrast, significantly lower amounts of Cav-1 protein expression, particularly at 0 time and 24 h after growth stimulation, characterized the scrapie-susceptible sheep fibroblasts.

3.4 Cav-1 and PrPc mRNA levels in quiescent and replicating sheep skin fibroblasts

As shown in Figure 4, with respect to ARR/ARR fibroblasts, ARQ/ARQ cultures associated basal (time 0) had lower mRNA levels of Cav-1 to higher mRNA levels of PrPc. Following FCS stimulation, the differences between scrapie-susceptible and scrapie-resistant sheep in the Cav-1 and PrPc mRNAs diminished or disappeared at 24 and 48 h, to reappear at the 72 h time point.

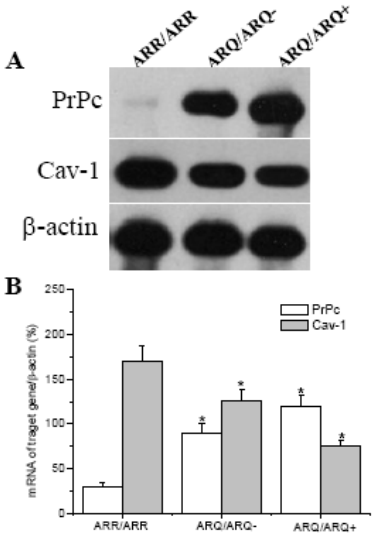

Figure 2. PrPc and Cav-1 mRNA expression in brain extracts of sheep carrying scrapie-resistant (ARR/ARR) or scrapie-susceptible (ARQ/ARQ) genotypes, with (ARQ/ARQ+) or without (ARQ/ARQ-) clinical Scrapie. Panel (A) shows representative RT-PCR chemiluminescent blots of PrPc and Cav-1 (see Experimental Procedures). Panel B shows densitometric analyses of the PrPc and Cav-1 bands shown in panel A, normalized for the endogenous ß-actin mRNA content that was used as an internal control. Data represent mean values ± SE of triplicate determinations of four samples from each brain. *P<0.05 vs. ARR/ARR.

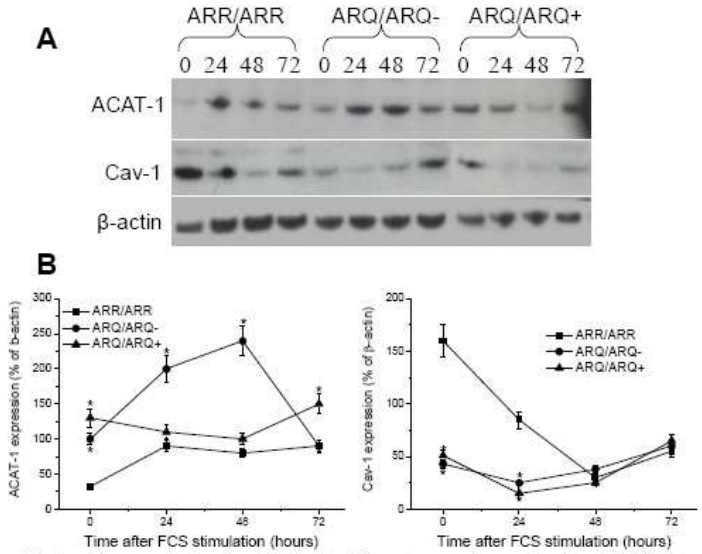

Figure 3. ACAT-1 and Cav-1 protein expression in cultured skin fibroblasts from sheep carrying scrapie-resistant (ARR/ARR) or scrapie-susceptible (ARQ/ARQ) genotypes, with (ARQ/ARQ+) or without (ARQ/ARQ-) clinical Scrapie. Western blots were performed as described (Experimental Procedures) at the time of growth stimulation with FCS (0 h) or 24, 48 and 72 h later. The upper part (A) shows representative chemiluminescent Western blots of ACAT-1 and Cav-1. The bottom parts (B) show densitometric analysis of ACAT-1 and Cav-1 bands, normalized for the endogenous β-actin protein content. Bars indicate mean values ± SE of skin fibroblast samples from 4 ARR/ARR, 4 ARQ/ARQ- and 6 ARQ/ARQ+ sheep. *$P<0.05$ *vs.* ARR/ARR sheep.

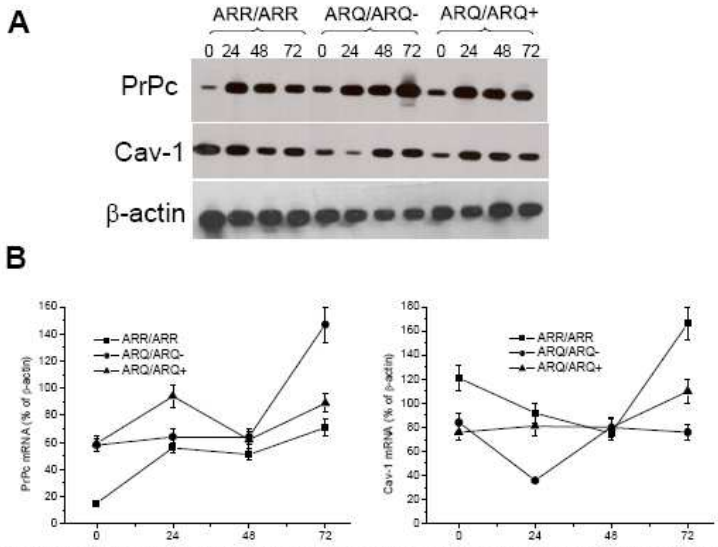

Figure 4. PrPc and Cav-1 mRNA levels in cultured skin fibroblasts from sheep carrying scrapie-resistant (ARR/ARR) or scrapie-susceptible (ARQ/ARQ) genotypes, with (ARQ/ARQ+) or without (ARQ/ARQ-) clinical Scrapie. Analyses were performed at the time of growth stimulation with FCS (0 h) or 24, 48 and 72 h later. The upper part (A) shows representative chemiluminescent blots of RT-PCR analysis of PrPc and Cav-1, respectively. The bottom part (B) shows densitometric analysis of chemiluminescent bands for PrPc and Cav-1 mRNA, normalized for the β-actin mRNA contents. Bars indicate mean values ± SE of skin fibroblast samples from 4 ARR/ARR, 2 ARQ/ARQ- and 8 ARQ/ARQ+ sheep. *$P<0.05$ *vs.* ARR/ARR sheep.

4. Discussion

PrPSc is generally thought to represent the infectious agent of Scrapie, through its ability to promote the structural conversion of the normal cellular prion protein PrPc into a likeness of itself [22]. Although the existence of genetic susceptibility to scrapie infection is well documented [23,24], how particular metabolic states of target cells would modulate degree of susceptibility is not entirely clear. In this context, our previous studies on the role of alterations of intracellular cholesterol homeostasis in the pathogenesis of Scrapie in sheep, revealed a positive correlation between an abnormal accumulation of CE and the genetic susceptibility to infection [15-17]. Of particular relevance, these alterations were found not only in brains but also in peripheral tissues, such as cultured skin fibroblasts and PBMCs, from the scrapie-susceptible sheep (ARQ/ARQ genotype). Moreover, both susceptible and scrapie-affected sheep showed abnormally low levels of high density lipoprotein-cholesterol in their plasma, as compared to resistant animals. Interestingly, Safar *et al.* [25] reported on an interaction of PrPsc with low density lipoprotein suggesting a direct mechanism between cholesterol transport/metabolism and prion biology. In the present study, we found that cellular cholesterol alterations were accompanied by parallel alterations in the expression levels of genes and gene products, ACAT-1 and Cav-1, involved in the pathways leading to intracellular cholesterol esterification and trafficking. In particular, higher ACAT-1 and lower Cav-1 expression characterized cells with scrapie-susceptible genotypes. Interestingly, in fibroblasts carrying the susceptible ARQ/ARQ genotype, we also found that mRNA expression of PrPc was higher than in cultures from scrapie-resistant sheep. These data suggest that genetic PrP polymorphisms and alterations of cholesterol homeostasis may act in concert to create an environment favorable to the initiation and progression of prion disease. Our conclusions are sustained by recent evidence indicating that the metabolic fate of PrPc is dependent on its location at the plasma membrane [26,27], which in turn is mediated by cholesterol levels in the raft domains [28], suggesting that PrP misfolding might be, at least partly, dependent on cholesterol homeostatic regulatory mechanisms. At present, however, although there are clear indications that cholesterol-enriched microdomains (rafts) are essential for the proper folding of nascent PrPc protein, there are divergent findings regarding whether cellular cholesterol depletion or its enrichment would favour the misfolding of PrP. A number of studies have, in fact, shown a decrease of PrPsc generation by lowering the cellular cholesterol content with statins [7,19,20], while other studies produced evidence that cholesterol depletion abolishes PrP-raft association, promotes its accumulation and increases substantially its misfolding [28,29]. In addition, replication of misfolded PrP protein was reported to interfere with the raft composition by displacing raft proteins, such as Cav-1, likely leading to alterations of intracellular cholesterol trafficking and accumulation [30].

In summary, further studies are necessary to elucidate the mechanisms responsible for the cholesterol homeostasis alterations in sheep carrying a genotype susceptible to scrapie, and to unveil possible cause-effect relationships between PrP polymorphisms and cholesterol alterations. Similarly, additional work is needed to reveal the potential implications of this association for prion disease susceptibility. Nonetheless, the data reported in the present paper suggest that accumulation of CE in peripheral cells, together with the altered expression of some proteins implicated in intracellular cholesterol homeostasis, might serve to identify a distinctive lipid metabolic profile (PCT/IT2007/000109; PCT/IT2007/000110) associated with increased susceptibility to develop prion disease following infection.

Acknowledgements

The Authors thank Dr. Ciriaco Ligios of the Experimental Zooprophylactic Institute of Sassari (Italy) for kindly providing tissue samples from Sarda sheep.

References

[1] Prusiner S.B., Prions, Proc. Natl. Acad. Sci. USA, 1998, 95, 13363-13383

[2] Gorodinsky A., Harris D.A., Glycolipid-anchored proteins in neuroblastoma cells form detergent-resistant complexes without caveolin, J. Cell Biol., 1995, 129, 619-627

[3] Loberto N., Prioni S., Bettiga A., Chigorno V., Prinetti A., Sonnino S., The membrane environment of endogenous cellular prion protein in primary rat cerebellar neurons., J. Neurochem., 2005, 95, 771-783

[4] Kurzchalia T.V., Parton R.G., Membrane microdomains and caveolae, Curr. Op. Cell Biol., 1999, 11, 424-431

[5] Vey M., Pilkuhn S., Wille H., Nixon R., DeArmond S.J., Smart E.J., et al., Subcellular colocalization of the cellular and scrapie prion proteins in caveolae-like membranous domains, Proc. Natl. Acad. Sci. USA, 1996, 93, 14945-14949
[6] Simons K., Ehehalt R., Cholesterol, lipid raft and disease, J. Clin. Invest., 2002, 110, 597-603
[7] Taraboulos A., Scott M., Semenov A., Avrahami D., Laszlo L., Prusiner S.B., Cholesterol depletion and modification of COOH-terminal targeting sequence of the prion protein inhibit formation of the scrapie isoform, J. Cell Biol., 1995, 129, 121-132
[8] Diomede L., Forloni G., Bugiani O., Tagliavini F., Salmona M., The prion protein and cellular cholesterol homeostasis, Neurobiol. Lipids, 2002, 1, 8-14
[9] Prado A.M., Silva J.A., Magalhaes A.C., Prado V.F., Linden R., Martins V.R., et al., PrPc on the road: trafficking of the cellular prion protein, J. Neurochem., 2004, 88, 769-781
[10] Critchley P., Kazlauskaite J., Eason R., Pinheiro T.J., Binding of prion protein to lipid membranes, Biochem. Biophys. Res. Commun., 2004, 313, 559-567
[11] Schmitz G., Orso E., Intracellular Cholesterol and Phospholipid Trafficking: Comparable Mechanisms in Macrophages and Neuronal Cells, Cell Mol. Life Sci., 2001, 26,1045-1068
[12] Maxfield, F.R., Tabas I., Role of cholesterol and lipid organization in disease, Nature, 2005, 438, 612-621
[13] Simons K., Ikonen E., How cell handle cholesterol, Science, 2000, 290, 1721-1726
[14] Binder W.H., Barragan V., Menger F.M., Domains and raft in lipid membrane. Angewandte chemie-international edition, 2003, 42, 5802-5827
[15] Pani A., Abete C., Norfo C., Mulas C., Laconi S., Cannas M.D., et al., Cholesterol Metabolism in Brain and Skin Fibroblasts from Sarda Breed Sheep With Scrapie-resistant and Scrapie-susceptible Genotypes, Am. J. Infec. Dis., 2007, 3, 143-150
[16] Pani A., Norfo C., Abete C., Mulas C., Putzolu M., Laconi S., et al., Accumulation of Cholesterol Esters in ex vivo Lymphocytes from Scrapie-susceptible Sheep and in Scrapie-infected Mouse Neuroblastoma Cell Lines, Am. J. Infec. Dis., 2007, 3, 165-168
[17] Pani A., Norfo C., Abete C., Mulas C., Putzolu M., Laconi S., et al., Anti-prion activity of cholesterol esterification modulators: a comparative study in ex vivo sheep fibroblasts and lymphocytes and in mouse neuroblastoma cell lines, Antimicrob. Agents Chemother., 2007, 51, 4141-4147
[18] Bate C., Williams A., Role of glycosylphosphatidylinositols in the activation of phospholipase A2 and the neurotoxicity of prions, J. Gen. Virol., 2004, 85, 3797-3804
[19] Gilch S., Kehler C., Schätzl H.M., The prion protein requires cholesterol for cell surface localization, Mol. Cell. Neurosci., 2006, 31, 346-353
[20] Mok S.W., Thelen K.M., Riemer C., Bamme T., Gültner S., Lütjohann D., et al., Simvastatin prolongs survival times in prion infections of the central nervous system, Biochem. Biophys. Res. Commun., 2006, 348, 697-702
[21] Pani A., Dessì S., Cell Growth and Cholesterol Esters, Kluwer Academic Press/Plenum Publishers, New York, NY, USA, 2004
[22] Soto C., Castilla J., The controversial protein-only hypothesis of prion propagation, Nat. Med., 2004, 10, S63-S67
[23] Wickner R.B., Edskes H.K., Roberts B.T., Baxa U., Pierce M.M., Ross E.D., et al., Prions: proteins as genes and infectious entities, Genes Dev., 2004, 18, 470-485
[24] Goldmann W., Baylis M., Chihota C., Stevenson E., Hunter N., Frequencies of PrP gene haplotypes in British sheep flocks and the implications for breeding programmes, J. Appl. Microbiol., 2005, 98, 1294-1302
[25] Safar J.G., Wille H., Geschwind M.D., Deering C., Latawiec D., Serban A., et al., Human prions and plasma lipoproteins, Proc. Natl. Acad. Sci. USA, 2006, 103, 11312-11317
[26] Harris D.A., Trafficking, turnover and membrane topology of PrP, Brit. Med. Bull., 2003, 66, 71-85
[27] Sarnataro D., Campana V., Paladino S.M., Stornaiuolo M., Nitsch L., Zurzolo C., PrPC Association with Lipid Rafts in the Early Secretory Pathway Stabilizes Its cellular conformation, Mol. Biol. Cell., 2004, 15, 4031-4042
[28] Campana V., Sarnataro D., Fasano C., Casanova P., Paladino S., Zurzolo C., Detergent-resistant membrane domains but not the proteasome are involved in the misfolding of a PrP mutant retained in the endoplasmic reticulum, J. Cell Sci., 2006, 119, 433-442
[29] Abid K., Soto C., The intriguing prion disorders, Cell. Mol. Life Sci., 2006, 63, 2342-2351
[30] Russelakis-Carneiro M., Hetz C., Maundrell K., Soto C. Prion replication alters the distribution of synaptophysin and caveolin 1 in neuronal lipid rafts, Am. J. Pathol., 2004, 165, 1839-1848

2.1.2 In vitro synergistic anti-prion effect of cholesterol ester modulators in combination with chlorpromazine and quinacrine (Article II)

Our previous studies also showed that a number of drugs which inhibit cholesterol esterification by targeting different steps of cholesterol metabolism/trafficking were able to reduce CE levels in both PBMCs and skin fibroblasts isolated from scrapie-affected sheep, and to determine a parallel inhibition of PrPres in prion infected 22L-N2a cell lines. In the article below, in these prion-infected cell lines, we reported increased anti-prion activity of dual-drug combinations consisting of cholesterol ester modulators associated with prion inhibitors. In these experiments, the synergistic activity was obtained with the cholesterol ester modulators everolimus, pioglitazone, progesterone, and verapamil associated with the anti-prion chlorpromazine, and with everolimus and pioglitazone associated with the anti-prion quinacrine. In addition, comparative lipid analyses in prion-infected *vs.* uninfected N2a cells by different lipid probes (Oil red O; Nile red and filippin), lipid separation techniques (TLC), and lipid precursors (labelled actetate and oleate), demonstrated a general derangement of type and distribution of the cholesterol ester (CE), free cholesterol (FC), and triglyceride pools in the infected cells. Single-drug treatments differently affected synthesis of the various lipid forms, whereas combined drug treatments appeared to restore a lipid profile similar to that of the untreated-uninfected cells. We concluded that anti-prion synergistic effects of cholesterol ester modulators associated with the cholesterol-interfering anti-prion drugs chlorpromazine and quinacrine, may arise from the ability of combined drugs to re-establish lipid homeostasis in the prion-infected cells. Overall, these data suggest that inhibition of prion replication can be readily potentiated by combinatorial drug treatments, and that steps of cholesterol/cholesterol ester metabolism may represent suitable targets.

Article II

Cent. Eur. J. Biol. • 5(2) • 2010 • 151–165
DOI: 10.2478/s11535-009-0070-9

VERSITA

Central European Journal of **Biology**

In vitro synergistic anti-prion effect of cholesterol ester modulators in combination with chlorpromazine and quinacrine

Research Article

Christina D. Orrù[1°], M. Dolores Cannas[1°], Sarah Vascellari[1], Fabrizio Angius[1], Pier Luigi Cocco[1], Claudia Norfo[1], Antonella Mandas[2], Paolo La Colla[1], Giacomo Diaz[1], Sandra Dessì[1], Alessandra Pani[1*]

[1]*Department of Biomedical Science and Technology, University of Cagliari, 09042 Monserrato (CA), Italy*

[2]*Department of Internal Medicine, University of Cagliari, 09042 Monserrato (CA), Italy*

Received 06 October 2009; Accepted 16 December 2009

Abstract: Our studies on the role of cholesterol in prion infection/replication showed that brains and peripheral cells of sheep susceptible-to or suffering-from Scrapie were characterized by an altered cholesterol homeostasis, and that drugs affecting cholesterol ester pool were endowed with selective anti-prion activity in N2a cell lines infected with the 22L and RML prion strains. In these prion-infected N2a cell lines, we now report increased anti-prion activity of dual-drug combinations consisting of cholesterol ester modulators associated with prion inhibitors. Synergism was obtained with the cholesterol ester modulators everolimus, pioglitazone, progesterone, and verapamil associated with the anti-prion chlorpromazine, and with everolimus and pioglitazone associated with the anti-prion quinacrine. In addition, comparative lipid analyses in prion-infected *vs.* uninfected N2a cells, demonstrated a derangement of type and distribution of cholesterol ester, free cholesterol, and triglyceride pools in the infected cells. Single-drug treatments differently affected synthesis of the various lipid forms, whereas combined drug treatments appeared to restore a lipid profile similar to that of the untreated-uninfected cells. We conclude that the anti-prion synergistic effects of cholesterol ester modulators associated with the cholesterol-interfering anti-prion drugs chlorpromazine and quinacrine may arise from the ability of combined drugs to re-establish lipid homeostasis in the prion-infected cells. Overall, these data suggest that inhibition of prion replication can be readily potentiated by combinatorial drug treatments and that steps of cholesterol/cholesterol ester metabolism may represent suitable targets.

Keywords: *Prions • Cholesterol metabolism • Cholesterol esters • Prion inhibitors • Drug combinations*

Abbreviations

PrP^{res}	- PK-resistant prion protein;
TL	- total lipids;
TC	- total cholesterol;
FC	- free cholesterol;
NL	- neutral lipids;
CE	- cholesterol esters;
TG	- triglycerides;
PL	- phospholipids;
DX 500	- dextran sulphate 500,000;
TA	- tannic acid;
CP	- chlorpromazine;
Q	- quinacrine;
EVE	- everolimus;
PIO	- pioglitazone;
PG	- progesterone;
VP	- verapamil.

* *E-mail: pania@unica.it*
° *These authors contributed equally to this work.*

1. Introduction

Prions are unconventional infectious agents involved in a number of fatal neurodegenerative diseases of mammals whose replication implies conversion of cellular prion protein isoforms, named PrP^{C}, into disease-specific isoforms, designated PrP^{Sc} [1]. Although no treatment is currently available, several compounds have been identified in prion-cell systems as inhibitors of the scrapie-like PK-resistant prion protein (PrP^{res}), some of which have shown a protective effect in rodent prion models. In no case, however, have inhibitors showed ability to hamper disease progression when treatment was given to animals at the time of symptoms development [2-3]. In humans, single intraventricular pentosan polysulphate (PPS) treatment was reported to increase the mean survival of seven prion-diseased individuals [4]; yet, due to the lack of formal drug evaluation in controlled randomized studies, it is not possible to draw any conclusion on the real effectiveness of PPS or that of several other agents tested [5,6]. The results of a patient-preference quinacrine trial in the UK (PRION-1; ISRCTN 06722585) in patients with Creutzfeldt-Jacob disease (CJD; sporadic, iatrogenic, variant, inherited) were recently published and indicated that a tolerated dose (*i.e.* 300 mg/day) of quinacrine did not significantly affect the clinical course of disease [7]. This study, however, initially intended to be a partially randomised patient-preference treatment trial, resulted in an observational study and thus, was fraught with confounding factors [7,8]. More conclusive information on quinacrine effectiveness should be available at the end of a randomised, double-blinded, placebo-controlled study in sporadic CJD (NCT 00183092) started this year in the USA [9].

Besides the limits of therapies given to individuals with established disease, the clinical relevance of available drugs might be hindered by monotherapy-based approaches. From the experience accumulated from other complex diseases, such as cancer and AIDS, one can in fact speculate that any identified pharmacological intervention able to effectively combat the chronic progression of brain damage during prion disease would imply polychemotherapy. Actually, based on this concept, Kocisko *et al.* found in mice enhanced anti-scrapie effect by using combinations of PPS and porphyrin FeTSP [10]. Thus, efforts should be made to identify more successful therapeutic approaches, as well as novel molecular targets of prion generation. In this context, our studies on the role of cholesterol in cell susceptibility to prion infection/replication showed that brains and *ex vivo* dermal fibroblasts and peripheral blood mononuclear cells (PBMCs) from sheep genetically susceptible-to or suffering-from scrapie, displayed higher cholesterol ester (CE) levels than sheep carrying a scrapie-resistant genotype, and altered expression levels of the acyl-coenzymeA:cholesterol-acyltransferase (ACAT-1; up-regulated) and caveolin-1 (Cav-1; down-regulated) involved in cholesterol esterification and trafficking, respectively [11-13]. In addition, in persistently prion-infected N2a cells, we found that drugs able to reduce the CE pool, *i.e.* everolimus, pioglitazone, Sandoz 58035, progesterone, and verapamil, were also able to inhibit PrP^{res} formation [14].

We now report on the anti-prion effect of everolimus, pioglitazone, progesterone, and verapamil in dual-drug combinations with selected prion inhibitors. Quinacrine and chlorpromazine were used as anti-prion agents known to prevent PrP^{res} formation in the endocytic compartment [15], whereas dextran sulphate 500,000 (DX500) and tannic acid (TA) were used as inhibitors acting on PrP^{res} formation at the plasma membrane site. Like PPS, DX500 is a sulphated polyanion which is thought to bind to PrP^{C} or PrP^{res} [16,17], whereas polyphenol tannic acid is known to stabilize plasma-membrane saturated phosphatidylcholine residues, thereby affecting PrP^{C} to PrP^{res} conversion [18]. Our data indicate that, compared to uninfected N2a cells, the prion-infected cultures display general alteration of lipid homeostasis, which can be reverted by treatments with CE modulators combined with the cholesterol-interfering anti-prion drugs chlorpromazine and quinacrine.

2. Experimental Procedures

2.1 Chemicals

Dextran sulphate sodium salt (MW 500 000), verapamil hydrochloride (98%), chlorpromazine hydrochloride, quinacrine dihydrochloride, and progesterone, were purchased from Sigma-Aldrich (Italy). Tannic acid was purchased from MP Biomedicals (USA). Everolimus was provided by Novartis (Switzerland), and pioglitazone by Takeda (Japan). Dextran sulphate 500 was solubilised in OptiMEM, and stored at -20°C. Everolimus was solubilised in 100% ethanol and stored at +4°C. Pioglitazone was solubilised in 100% ethanol and stored at room temperature. Stock solutions of the other compounds were prepared in DMSO and stored at -20°C.

2.2 Cell lines and PrP analysis

Mouse neuroblastoma N2a cell line and sublines persistently infected with the 22L and RML strains of mouse-adapted scrapie (22L-N2a, RML-N2a), were

a generous gift by Byron Caughey, NIH/NIAID Rocky Mountain Laboratories, USA. Cells were grown at 37°C, 5% CO_2, in OptiMEM supplemented with 10% FBS (Gibco, Invitrogen; Italy), 2mM L-glutamine, 50 U/ml penicillin G sodium and 50 µg/ml streptomycin sulphate (Gibco, Invitrogen; Italy), and split every 3 to 4 days. Cell lines were stored in liquid nitrogen and working cultures were replaced every two-three months. All experiments were carried out in exponentially growing cells or sub-confluent cultures. PrP^{C} and PK-resistant PrP (PrP^{res}) were detected in cell lysates by dot blot procedure with the mouse anti-PrP antibody 6H4 (Prionics, Zurich; 1:5.000) as previously described [14].

2.3 Effect of single *vs.* dual drug treatments on PrP^{res} formation

Approximately 5.000 of prion-infected N2a cells in 90 µl of growth medium were added to each well of a Microtest flat-bottom 96-well plate with a low-evaporation lid (Becton Dickinson, USA). The cells were allowed to settle overnight before addition of 10 µl (10x solutions) of different concentrations of the drugs. For dual drug combinations, cell cultures were treated with 5 µl (20x solutions) of serial sub-active drug concentrations; *i.e.* serial ½ fractions of the EC_{50} of each compound. Cells were either exposed to both drugs at the same time or pre-treated for 8 hours with one inhibitor before addition of the second one. DMSO in the cell medium was never higher than 0.2% (v/v). Each drug combination was tested in duplicate and each experiment was performed at least twice. After 96-hour incubation at 37°C in 5% CO_2, cells were processed for PrP^{res} detection. Autoradiography films of PrP^{res} blots were captured in TIFF format and intensity of each dot was determined through the Scion Image software (NIH). The mean value of PrP^{res} at each drug concentration and at each drug combination was expressed as a percentage of control cultures (*i.e.* untreated and single-drug treated cultures, respectively). EC_{50} values (50% inhibition) were determined by linear regression analysis. Duplicate cultures were drug treated as above and after 96 hours processed for evaluation of cell viability at each drug concentration/combination with the MTT method as described [14].

2.4 Type of interaction of dual drug treatments on PrP^{res} formation

The results of dual drug treatments on the generation of PrP^{res} were plotted according to the isobole method [19], a well-known procedure for the evaluation of synergism, additivity, indifference, or antagonism which requires experimental data for the agent used alone and in different dose combinations at equal-effective levels (fractions of EC_{50s}). According to this procedure, a combination is said to show zero interaction (*i.e.* additive) if the data points are on the straight line connecting the EC_{50} of the single agents; the points below this line correspond to synergistic interactions; those above the line indicate indifference and antagonism. To measure the degree of drugs interaction, FIC index was calculated according to the equation: $FIC = (EC50_A^{comb} / EC50_A^{alone}) + (EC50_B^{comb} / EC50_B^{alone})$. By this method, interactions are considered synergistic if the FIC index is <1, additive to indifferent if the FIC index is comprised between 1 and 2, and antagonistic if the FIC index is >2. The reduction in the EC_{50s} of the anti-prion drugs when they were given in combination compared to the EC_{50s} when given alone, were compared through a paired rank test, a non parametric test for comparison between two related samples. A P value <0.05 was considered significant.

2.5 Evaluation of drug efflux activity

Drug efflux activity of P-gp protein was determined by measuring intracellular accumulation of radioactive vinblastine as previously described [20]. In brief, 22L-N2a cells were seeded at $1x10^4$ cells/ml in growth medium (OptiMEM supplemented with 10% FCS, 100 units/ml penicillin, 100 µg/ml streptomycin) in a Microtest flat-bottom 24-well plate with a low-evaporation lid (Becton Dickinson, USA). Cultures were allowed to settle overnight and then further incubated in the absence and in the presence of different concentrations of the cholesterol inhibitors. After 96 hours of incubation, cell cultures were washed twice with PBS and re-incubated at 37°C in ½ final volume of fresh growth medium with or without the drugs. One hour later, cells were re-fed with equal volume of identical pre-warmed medium supplemented with 0.1 µCi/ml [G-^{3}H]vinblastine sulfate (15.5 Ci/millomole; Amersham Life Sci.). After 1-hour pulse, cell monolayers were rapidly washed 3 times with ice-cold PBS, solubilized in 0.1 N NaOH, and analyzed for protein and [G-^{3}H]-vinblastine content in a Beckman β-Counter. The amount of intracellular [G-^{3}H]-vinblastine is reported as CPM per µg of total cellular protein, as determined by the bicinchoninic acid (BCA) protein assay (Sigma-Aldrich) [14]. Each determination was performed in triplicate.

2.6 Staining of intracellular lipids

To visualize intracellular lipids, N2a and 22L-N2a cells were seeded at $1x10^4$/ml in growth medium in Microtest flat-bottom 24-well plates (Becton Dickinson, USA). After overnight settlement, 22L-N2a cultures were drug-treated under conditions used for evaluation of anti-PrP^{res} activity. Each drug and drug combination was tested

in triplicate. After 96-hour incubation, untreated and drug treated cultures were washed with PBS, fixed by soaking in 10% formalin and then stained with Oil red-O (ORO) (Sigma), Nile red (9-diethylamino-5H-benzo[α] phenoxazine-5-one, Fluka, Buchs, SG, Switzerland) and filipin (Sigma). ORO is a lipid-soluble dye which stains NL (*i.e.* CE and triglycerides, TG), but not free cholesterol (FC). ORO staining was performed in 60% isopropyl alcohol, followed by Mayer's hematoxylin counterstaining for nuclei [14]. After staining, cells were imaged using a Leitz inverted-phase microscope fitted with a digital camera. Neutral lipids (NL) appear as bright red spots in the cell cytoplasm. At least two different fields per sample were imaged and analyzed. Red ORO intensity was quantified by NIH Image J software utilizing four different selected regions of interest (ROIs), and values expressed as integrals of the intensity given as 'arbitrary units' (pixels/cm2) ± SE of triplicate wells.

Nile red is a fluorescent dye that stains differentially polar lipids (*i.e.* phospholipids, PL) and NL (*i.e.* CE and TG) [21]. PL show a prevalent red emission, while NL show both red and green emission. Red emission was observed with 540±12.5 excitation and 590 LP emission filters. Green emission was observed with 460±25 excitation and 535±20 emission filters. Filipin is a fluorescent dye which stains only free cholesterol (FC; blue emission). Filipin was observed with 360±20 excitation and 460±25 emission filters. Filipin and Nile red emissions were completely separated by the above indicated filters, so the two fluorochromes could be used in combination on the same cells [22]. Quantitative image analysis was performed with the ImagePro Plus package (Media Cybernetics, Silver Springs, MD).

2.7 Cellular lipid content, synthesis, and efflux

For determinations of the different lipid subclasses in N2a and 22L-N2a cells, total lipids (TL) were extracted with cold acetone from a total of $30x10^6$ of each cell line collected from sub-confluent flasks. Extracted lipids were split into two equal aliquots and air dried: one aliquot was used to determine total cholesterol (TC) by the cholesterol oxidase method (Sclavo Diagnostics, Siena, Italy); the other aliquot, after drying, was resuspended in 100 µl of chloroform and analysed for lipid subclasses by thin layer chromatography (TLC) on kiesegel plates using a solvent system containing n-heptane/isopropyl ether/formic acid (60:40:2 v/v/v). Separated bands were identified as FC, CE, and TG by comparison with reference standards run simultaneously side-by-side and visualized under iodine vapors. Bands were excised and their masses determined by the cholesterol oxidase (for FC and CE) and peroxidase (for TG) assay methods (Sclavo Diagnostics, Siena, Italy).

To determine the effect of drugs and drug combinations on lipid synthesis and efflux, N2a and 22L-N2a cells were seeded at $1x10^4$/ml in growth medium in Microtest flat-bottom 24-well plates (Becton Dickinson, USA). After overnight settlement, 22L-N2a cultures were drug-treated and incubated under the condition used for evaluation of anti-PrP^{res} activity. Each drug and drug combination was tested in triplicate. Six hours before harvesting, 5 µCi/ml sodium ^{14}C-acetate (DuPont, NEN; specific radioactivity 50 mCi/mmol) were added to each well. At the end of labelling, TL in the cell monolayers and in the growth media were extracted with cold acetone and lipid subclasses separated by TLC as described above. The incorporation of ^{14}C-acetate into lipid sub fractions was measured in a Liquid Scintillation Counter. Efflux of ^{14}C-TL was expressed as the percentage of the radioactivity recovered in medium/total radioactivity (cells + medium).

2.8 Statistical analysis

Unless otherwise indicated, data are reported as mean ± standard error (SE). Statistical calculations were performed using the statistical analysis software Origin 8.0 version (Microcal, Inc, Northampton, MA, USA). Data analysis was done using the Student t-test. A value of $P<0.05$ was considered statistically significant.

3. Results

3.1 Anti-PrP^{res} activity of prion inhibitors in combination with CE modulators

The inhibitory effect of single *vs.* dual-drug treatments on PrP^{res} generation was evaluated in 22L-infected cells by dot blot procedure [23], a method equally reliable but more suitable than Western blot-based assay for comparative studies of multiple drugs. 22L-N2a cell cultures were exposed to fractions of the EC_{50} (serial ½ drug dilutions) of each compound, alone and in association. Dual-drug treatments were either performed at the same time or in sequential order: 8 hrs treatment with one drug before adding the second drug. Type and degree of drug interactions were analyzed by both isobole and FIC index methods [19]. The effect of combined treatments ranged from synergism to indifference, depending on the prion inhibitor considered, drug concentration, and the temporal sequence of drug addition. Simultaneous treatments, as well as sequential combination with prion inhibitors that preceded CE modulators, always resulted in an additive or indifferent type of interaction (not shown). Sequential combinations comprising any

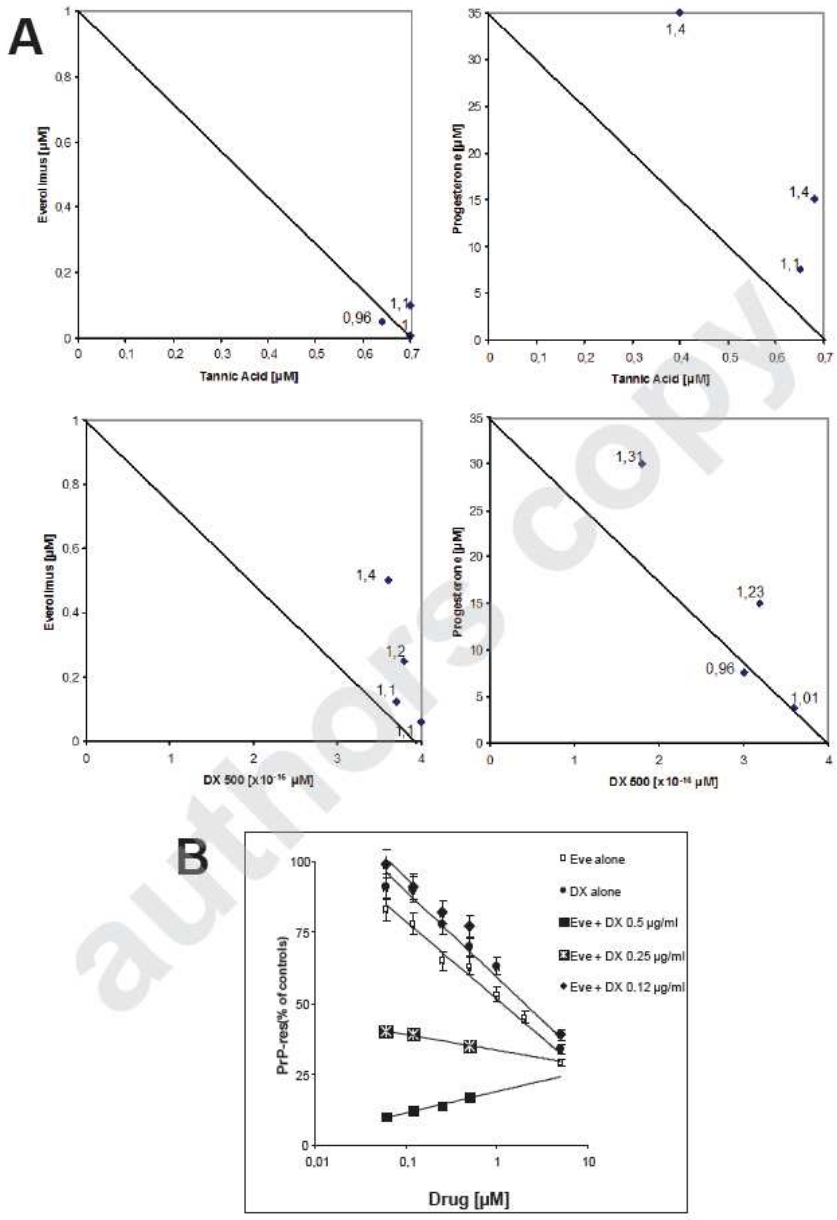

Figure 1. Anti-prion activity of tannic acid and DX500 in combination with everolimus and progesterone. Prion-infected 22L-N2a cells were pre-treated for 8 hours with different concentrations of everolimus (EVE) or progesterone (PG) prior to the addition of different concentrations of tannic acid (TA) or dextran sulphate (DX500). After 96 hours, cells were lysed and processed for detection of PrP^{res} by dot blot with mouse monoclonal 6H4 antibody (Prionics). (A) Isoboles and FIC indices of drug combinations. (B) Representative dose-response curves of EVE and DX500 alone and in combination one with another. Each point is the mean of three independent experiments ± SE.

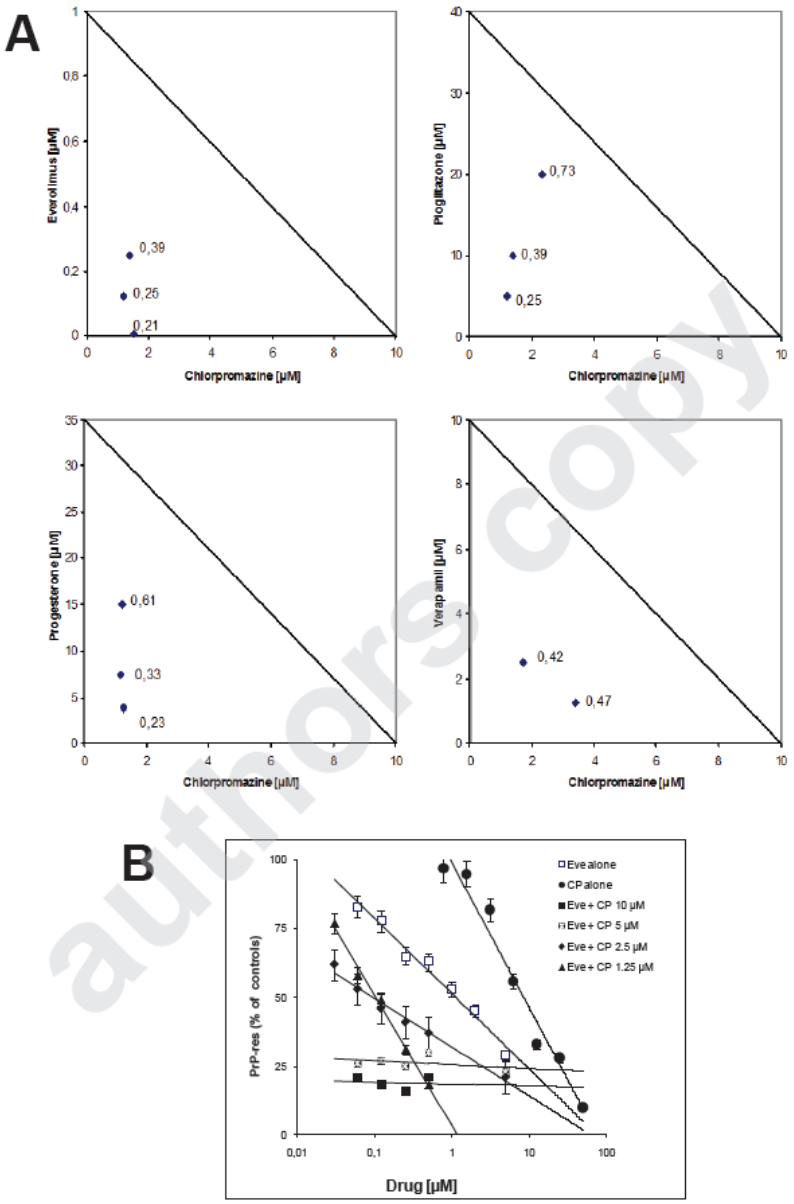

Figure 2. Anti-prion activity of chlorpromazine in combinations with everolimus, pioglitazone, progesterone, and verapamil. Prion-infected 22L-N2a cells were treated for 8 hours with different concentrations of everolimus (EVE), pioglitazone (PIO), progesterone (PG), and verapamil (VP) prior to the addition of different concentrations of chlorpromazine (CP). After 96 hours cells were lysed and processed for detection of PrP^{res} by dot blot with mouse monoclonal 6H4 (Prionics). (A) Isoboles and FIC indices of combinations. (B) Representative dose-response curves of EVE and CP, alone and in combination one with another. Each point is the mean of three independent experiments ± SE.

CE modulator followed by dextran sulphate or tannic acid also resulted in an additive or indifferent type of interaction. Isoboles and FIC indices of combinations comprising everolimus and progesterone followed by dextran sulphate and tannic acid are shown in Figure 1A. By contrast, a marked enhancement of the anti-prion effect was obtained when cells were treated with any CE modulator followed by chlorpromazine. Pre-treatments with everolimus, pioglitazone, progesterone, or verapamil, resulted in anti-prion effects in the range of synergism, as indicated by either FIC values (0.21-0.73) or data points in isoboles (Figure 2A). Significant reduction of chlorpromazine EC_{50} (CP, 10 to 1.8 μM [P<0.01]), everolimus (EVE, 1 to 0.1 μM [P<0.01]), pioglitazone (PIO, 40 to 5 μM [P<0.05]), progesterone (PG, 35 to 5 μM [P<0.05]), and verapamil (VP, 10 to 2.5 μM [P<0.05]) was observed. Sequential combinations of CE modulators followed by quinacrine resulted in different drug interactions, depending on the dose and type of CE modulator. Pre-treatments with low doses of everolimus, pioglitazone, and progesterone resulted in synergistic interactions (FIC values: 0.18-0.25, EVE; 0.29-0.5, PIO; 0.70-0.71, PG), while higher doses resulted in additive effects. Verapamil showed additive interaction at any concentration (FICs 0.95-1.13) (Figure 3A). Significant reduction of quinacrine EC_{50} (Q, 1 to 0.1 μM [P<0.01]), everolimus (EVE, 1 to 0.08 μM [P<0.01]), and pioglitazone (PIO, 40 to 5 μM [P<0.05]) was observed. Representative dose-response curves of single and dual-drug combination treatments of everolimus, dextran sulphate, chlorpromazine, and quinacrine are shown (Figure 1-3B). Notably, similar drug interactions against PrP^{res} formation were also obtained in N2a cells infected with the RML prion strain (data not shown). Anti-prion effects were not due to cytotoxicity, as neither single nor dual-drug treatments affected MTT viability at active concentrations (Table 1).

3.2 Effect of CE modulators on P-gp drug efflux activity

In multidrug-resistant cell lines, progesterone and verapamil are chemo-sensitizers of unrelated cytotoxic agents *via* the inhibition of membrane drug-efflux P-gp protein [24, refs therein]. To investigate whether synergistic anti-prion effects were due to increased cell retention of chlorpromazine and quinacrine induced by P-gp inhibition, the overall drug-efflux potential of 22L-N2a cells was investigated. Cells were exposed to the CE modulators for either 1 hour (*i.e.* standard procedure for measuring drug-efflux P-gp activity) or 96 hours (*i.e.* our test condition to evaluate anti-prion activity), and then pulse-labelled with ^{3}H-vinblastine, a known P-gp substrate [20,24]. Actually, both verapamil and progesterone, at concentrations close to their EC_{50s} (*i.e.* 10 μM and 35 μM, respectively), increased labelled vinblastine content with respect to untreated cultures (Table 2). Verapamil was a better P-gp inhibitor than progesterone and determined higher vinblastine retention after both short (1 h) and prolonged (96 h) exposure to the drug. However, treatments with concentrations (*i.e.* 7.5 μM and 2.5 μM, respectively) closer to synergistic ones, had no effect on vinblastine retention. Everolimus showed negligible anti-P-gp activity following treatments with 1 μM and 0.5 μM, and had no effect at a dose (0.05 μM) higher than that showing the strongest anti-prion synergism in combination with both chlorpromazine and quinacrine. Intriguingly, a high dose of pioglitazone (40 μM), while not affecting vinblastine influx after short treatment, determined a marked retention of labelled vinblastine after prolonged treatment.

3.3 Effect of single *vs.* dual-drug combinations on intracellular lipids

Given that observed synergism was unlikely due to increased cell retention of chlorpromazine or quinacrine, we investigated whether combined drugs interacted at the level of lipid metabolism. The effect on intracellular lipids of a drug combination with marked anti-PrP^{res} synergism, such as everolimus (EVE, 0.02 μM) and chlorpromazine (CP, 2 μM), was evaluated by staining the cells with dyes with affinity for different lipids (Oil Red O for neutral lipids; Nile red for neutral lipids and phospholipids; Filipin for free cholesterol). As expected [14], Oil Red O (ORO) staining revealed significantly higher neutral lipids (NL) in the 22L-infected than in the uninfected N2a cells (Figure 4A and B). However, both single and combined drug treatments markedly reduced red ORO intensity in the 22L-infected cell line. More detailed information was obtained with Nile red, a fluorescent hydrophobic probe that, being based on the different sensitivity of red and green emissions to low- and high-hydrophobic lipids, respectively, allowed us to distinguish neutral from polar lipids. Combined staining with Nile red and Filipin, a fluorescent sterol binding agent, allowed us to also co-localize free cholesterol (FC; blue emission). With respect to uninfected cells, 22L-infected N2a showed an increase in both polar (phospholipids, PL) and NL (*i.e.* CE and triglycerides, TG), as well as in FC (Figure 5A and B). In agreement with ORO data, 22L-N2a cells showed a higher green emission signal - indicative of higher NL content. In addition, Nile-red staining in the infected cells appeared as spread greenish fluorescence, rather than being

	CC_{50}	DX 500 µg/ml 0.5	0.25	0.12	0.06	CC_{50} 50±0.9	CP µM 10	5	2.5	1.25	CC_{50} 98±11	Q µM 1	0.50	0.25	0.12	CC_{50} 4.5±1.3
							Mean cell viability (MTT OD 570 nm) ± SD									
EVE µM	1.2±0.2															
0.5		1.07±0.02	1.12±0.01	1.07±0.04	1.09±0.02		0.88±0.03	0.97±0.02	0.98±0.02	0.98±0.02		0.97±0.04	1.03±0.01	1.05±0.01	1.09±0.01	
0.25		1.11±0.01	1.16±0.04	1.13±0.03	1.14±0.04		0.90±0.01	0.99±0.01	1.06±0.01	1.05±0.04		0.99±0.01	1.06±0.04	1.05±0.01	1.06±0.03	
0.12		1.11±0.03	1.16±0.02	1.14±0.03	1.14±0.01		0.92±0.03	1.05±0.04	1.00±0.02	1.05±0.03		1.08±0.03	1.06±0.04	1.09±0.03	1.12±0.04	
0.06		1.16±0.03	1.20±0.02	1.09±0.01	1.12±0.01		0.93±0.01	0.97±0.03	0.94±0.03	0.98±0.04		1.10±0.02	1.11±0.03	1.18±0.01	1.08±0.02	
		mean controls 1.07±0.05					mean controls 0.90±0.04					mean controls 1.05±0.05				
PIO µM	53±4.1															
40		0.81±0.02	0.80±0.01	0.82±0.04	0.79±0.01		0.81±0.03	0.77±0.03	0.77±0.04	0.79±0.01		0.81±0.05	0.83±0.04	0.80±0.03	0.81±0.01	
20		0.91±0.01	0.90±0.03	0.86±0.01	0.90±0.02		0.84±0.02	0.87±0.01	0.84±0.02	0.85±0.01		0.93±0.03	0.97±0.02	0.98±0.01	1.02±0.01	
10		1.09±0.04	1.10±0.01	1.12±0.03	1.08±0.01		0.84±0.03	0.84±0.03	0.84±0.03	0.89±0.02		0.97±0.02	1.03±0.03	1.05±0.04	1.04±0.01	
5		1.18±0.02	1.21±0.03	1.17±0.02	1.13±0.01		0.92±0.04	0.95±0.01	0.92±0.01	0.91±0.03		1.03±0.02	1.08±0.01	1.05±0.02	1.05±0.02	
		mean controls 1.08±0.07					mean controls 0.84±0.05					mean controls 1.03±0.06				
VP µM	97±8.7															
10		1.10±0.01	1.14±0.03	1.05±0.02	1.04±0.04		1.09±0.01	1.07±0.01	1.06±0.03	1.08±0.01		0.93±0.04	1.04±0.01	1.07±0.02	1.04±0.03	
5		1.07±0.04	1.12±0.01	1.07±0.03	1.07±0.03		1.08±0.02	1.07±0.04	1.10±0.01	1.07±0.03		0.97±0.03	1.05±0.03	1.10±0.01	1.06±0.01	
2.50		1.21±0.04	1.22±0.03	1.05±0.04	1.06±0.03		1.07±0.02	1.06±0.02	1.09±0.02	1.06±0.02		0.97±0.02	1.05±0.02	1.05±0.03	1.04±0.02	
1.25		1.10±0.02	1.15±0.03	1.08±0.04	1.06±0.04		1.10±0.01	1.11±0.04	1.10±0.02	1.13±0.04		1.07±0.04	1.10±0.02	1.04±0.02	1.09±0.02	
		mean controls 1.04±0.06					mean controls 1.06±0.05					mean controls 1.04±0.06				
PG µM	135±8.8															
30		1.13±0.03	1.14±0.04	1.12±0.02	1.09±0.01		0.73±0.05	0.87±0.03	0.95±0.01	1.05±0.04		0.97±0.03	1.03±0.01	1.08±0.01	1.11±0.02	
15		1.10±0.03	1.09±0.02	1.10±0.01	1.07±0.04		0.96±0.03	1.04±0.01	1.09±0.02	1.12±0.03		1.00±0.01	1.07±0.01	1.11±0.01	1.13±0.02	
7.5		1.05±0.02	1.06±0.03	1.06±0.01	1.03±0.04		1.03±0.03	1.07±0.02	1.08±0.02	1.09±0.01		0.99±0.01	1.11±0.01	1.13±0.02	1.14±0.03	
3.75		1.08±0.05	1.11±0.01	1.09±0.01	1.07±0.02		1.06±0.01	1.13±0.04	1.12±0.03	1.16±0.04		1.11±0.05	1.15±0.01	1.09±0.03	1.13±0.02	
		mean controls 1.03±0.09					mean controls 1.06±0.06					mean controls 1.08±0.07				

Table 1. Cytotoxicity of single and dual drug treatments in 22L-infected N2a cells.

Values represent the mean ±SD of duplicates from three independent experiments.

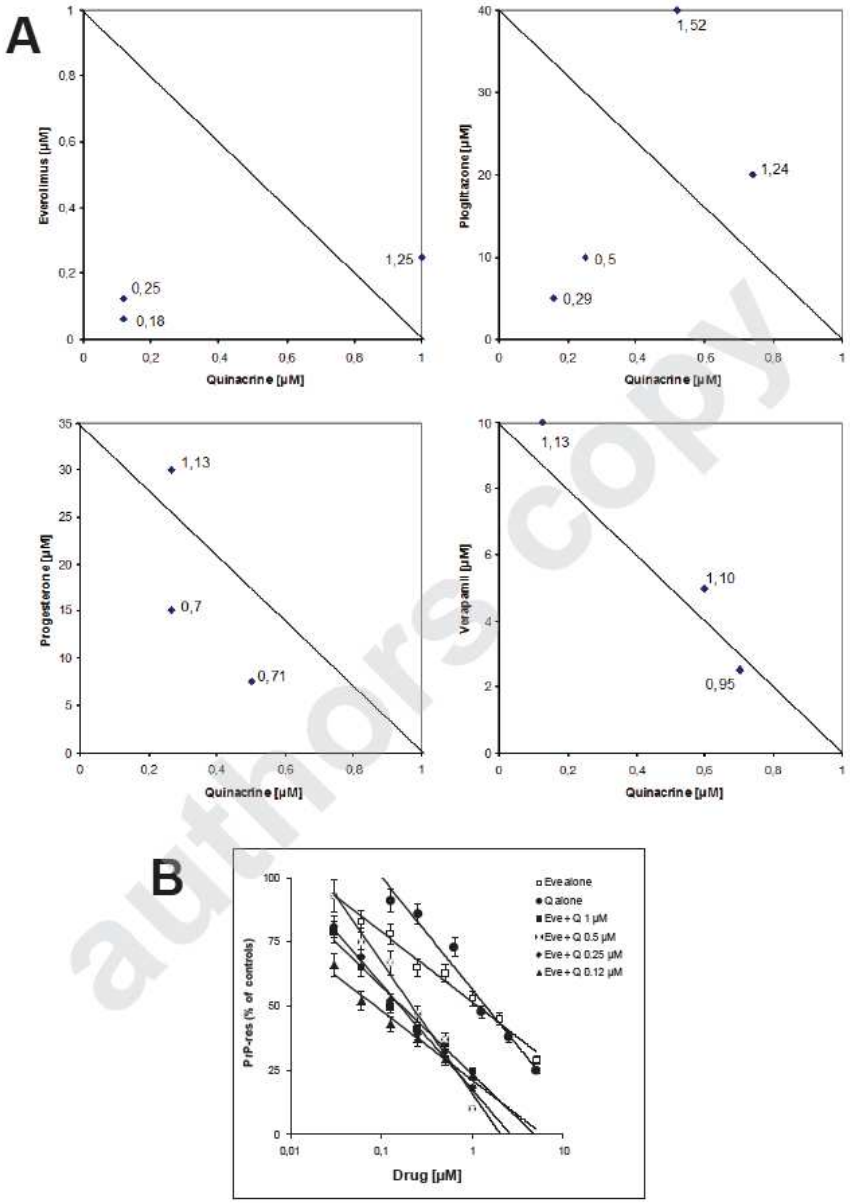

Figure 3. Anti-prion activity of quinacrine in combination with everolimus, pioglitazone, progesterone and verapamil. Prion-infected 22L-N2a cells were treated with different concentrations of everolimus (EVE), pioglitazone (PIO), progesterone (PG) and verapamil (VP) for 8 hours prior to the addition of different concentrations of quinacrine (Q). After 96 hours, cells were lysed and processed for detection of PrP^{res} by dot blot with mouse monoclonal 6H4 (Prionics). (A) Isoboles and FIC indices of combinations. (B) Representative dose-response curves of EVE and Q, alone and in combination one with another. Each point is the mean of three independent experiments ± SE.

Drug	[μM]	[³H]-VBL CPM/μg protein ± SD 1 hour	96 hours
No drug	-	28.11±3.3	36.30±2.2
Progesterone	35	37.28±3.1	41.85±2.2
	15	32.18±2.5	36.10±1.6
	7.5	28.43±2.9	36.32±2.5
Verapamil	10	60.68±4.2	63.79±3.9
	5	45.77±3.3	39.21±3.6
	2.5	28.34±1.7	36.06±1.0
Everolimus	1	30.59±1.9	35.85±2.4
	0.5	28.32±2.1	33.63±2.2
	0.05	28.04±2.8	34.87± 1.7
Pioglitazone	40	30.39± 2.2	50.73±3.8
	20	28.65±3.1	37.33±3.3
	10	28.88±2.0	36.73±1.1

Table 2. MDR1/P-gp drug efflux activity in 22L-infected N2a cell lines.

Values represent the mean ±SD of triplicate determinations from three independent experiments.

localized in the cytoplasm as lipid droplets (Figure 5C, compare N2a with 22L-N2a). 22L-N2a cells showed a more intense Filipin fluorescence - indicative of a higher FC content, some of which was also dispersed in the cytoplasm. Single treatment of infected cultures with everolimus determined a marked reduction of all forms of intracellular lipids, whereas treatment with chlorpromazine had a lower, although significant, effect on both PL and CE, but no significant effect on FC. Interestingly, combined treatments of infected cells with everolimus and chlorpromazine appeared to generate a lipid profile similar to that of the untreated-uninfected cells.

3.4 Lipid content in N2a *vs.* 22L-N2a by TLC

The above data clearly indicated that 22L-infected cells displayed higher NL compared to uninfected cells. However, there was a marked difference in dye intensity values of ORO *vs.* Nile red staining; compared to N2a, 22L-N2a cells showed over 5-fold-higher ORO stain and only approximately 1.5-fold-higher green Nile-red fluorescence. This discrepancy led us to more accurately

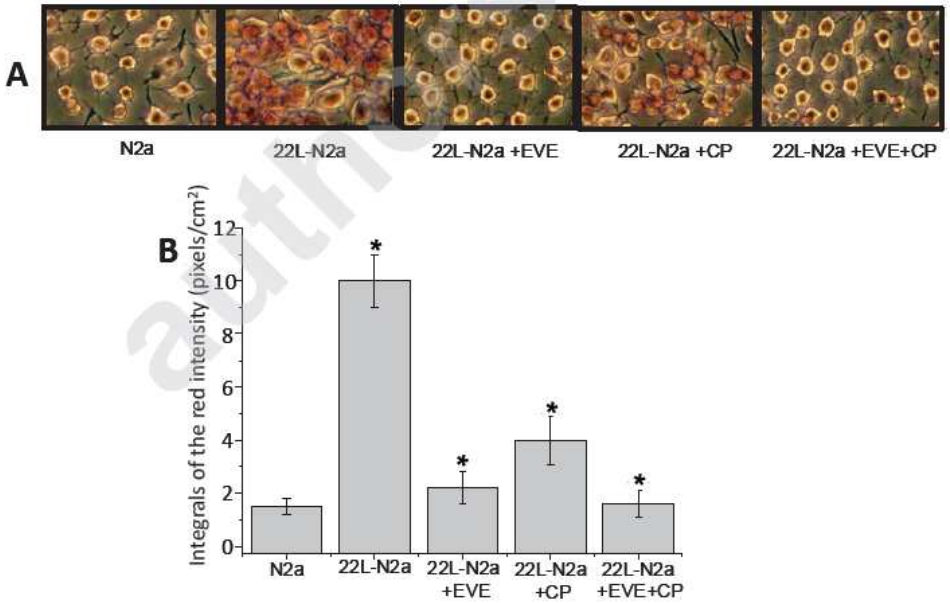

Figure 4. Oil red O staining of 22L-infected N2a cells after single and dual drug treatments. 22L-infected cells were incubated in the absence or in the presence of everolimus (EVE, 0.02 μM) and chlorpromazine (CP, 2 μM), alone or in combination. Control uninfected N2a cells were incubated in drug-free medium. After 96 hours, cell cultures were processed for evaluation of neutral lipid-bound Oil Red O. (A) Representative microscopic visualization of neutral lipid accumulation. (B) Quantitative measurements of Oil Red O staining. Data are expressed as integrals of the intensity given as 'arbitrary units' (pixels/cm²) ± SE. *P<0.05: (22L-N2a *vs.* N2a); (treated *vs.* untreated 22L-N2a).

analyse lipids in cell extracts. As seen in Figure 6 (A and B), the cholesterol oxidase assay revealed 1.7-fold higher content of total cholesterol (TC) in the lysates of infected cells. Separation of lipid subclasses by TLC showed higher levels not only of FC (1.6-fold) and CE (5.5-fold), but also of TG (1.9-fold). Thus, lipid analysis by enzymatic and chemical means confirmed, even though not in a stoichiometric manner, that prion infected cells display increased levels of all lipid sub-fractions, and additionally identified the CE pool as the most altered.

3.5 Effect of single *vs.* dual-drug combinations on lipid synthesis and efflux in 22L-N2a

To draw more consistent conclusions regarding the effects of drugs and drug combinations on cellular lipid homeostasis, we compared neosynthesis of lipids (FC, CE, TG) and lipid efflux (mainly FC) in N2a *vs.* 22L-infected N2a cells, either untreated or treated with single and dual-drug combinations of everolimus (EVE, 0.02 μM), chlorpromazine (CP, 2 μM), and quinacrine (Q, 0.2 μM). Once again, ^{14}C-acetate incorporated into total lipids (TL) was higher in the 22L-N2a than in N2a cells (Figure 7A). In spite of a slight increase in TL efflux in the 22L-infected cultures, the percentage of TL efflux did not significantly differ between the two cell lines. TLC separation of lipid subclasses showed that the higher lipid syntheses in the 22L-N2a cells was due to increased neosynthesis of FC (1.5-fold), CE (2-fold), and TG (1.6-fold) (Figure 7B). Although syntheses of uninfected N2a were also affected by single and combined drug treatments (not shown), in the prion-infected cultures combined drugs seemed to act in concert triggering lipid syntheses back at levels of untreated-uninfected cells (Figure 7A and B).

4. Discussion

In the present study we found that drugs targeting steps of cholesterol metabolism/esterification were able to enhance the anti-prion activity of chlorpromazine and quinacrine by reducing their EC_{50s} up to 10-fold. Synergistic drug interactions were obtained in sequential combination of chlorpromazine or quinacrine with i) everolimus, an immunosuppressant agent that

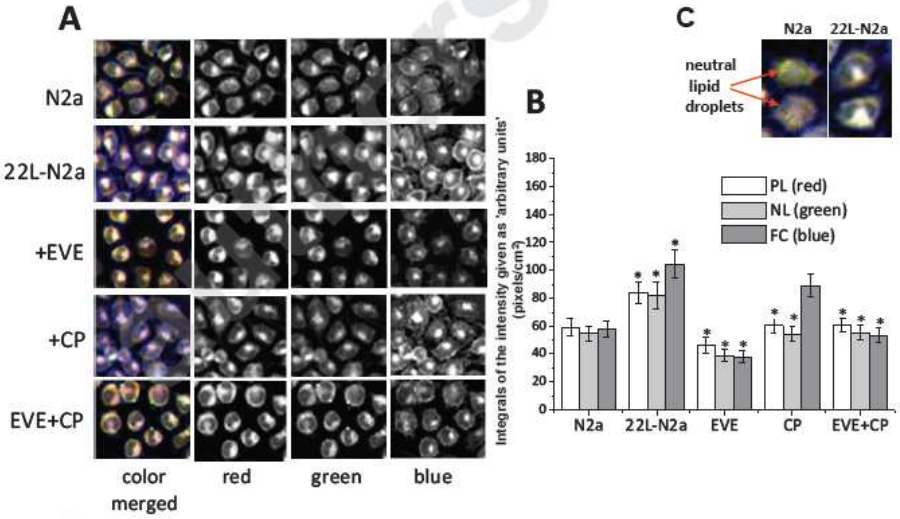

Figure 5. Nile red and Filipin staining of 22L-infected N2a cells after single and dual drug treatments. 22L-infected cells were incubated in the absence or in the presence of everolimus (EVE, 0.02 μM) and chlorpromazine (CP, 2 μM), alone or in combination. Control uninfected N2a cells were incubated in drug-free medium. After 96 hours, cell cultures were stained with Nile red and Filipin. (A) Representative microscopic visualization of stained cultures. NR-590 and NR-535 represent the red and green Nile red emissions which distinguish low-hydrophobic (*i.e.* phospholipids, PL) and high-hydrophobic (*i.e.* triglycerides, TG; cholesterol ester, CE) lipids, respectively. Filipin stains free cholesterol (FC). The three pictures are merged in the colour picture. Note that the white colour, prevalent in 22L-infected cultures, is given by the overlay of the three signals. (B) Quantitative analysis of Nile red and Filipin staining. (C) Single cell enlargements of Nile red stained N2a *vs.* 22L-N2a cells. Note that in the cytoplasm of N2a cells neutral lipids are visible as green droplets (arrows), while in the 22L-N2a green fluorescence is spread throughout the cytoplasm. Data are the mean ± SE of the fluorescence intensity of NR-590, NR-535 and Filipin staining, expressed as integrals of the intensity given as 'arbitrary units' (pixels/cm²). *P<0.05: (22L-N2a *vs.* N2a); (treated *vs.* untreated 22L-N2a).

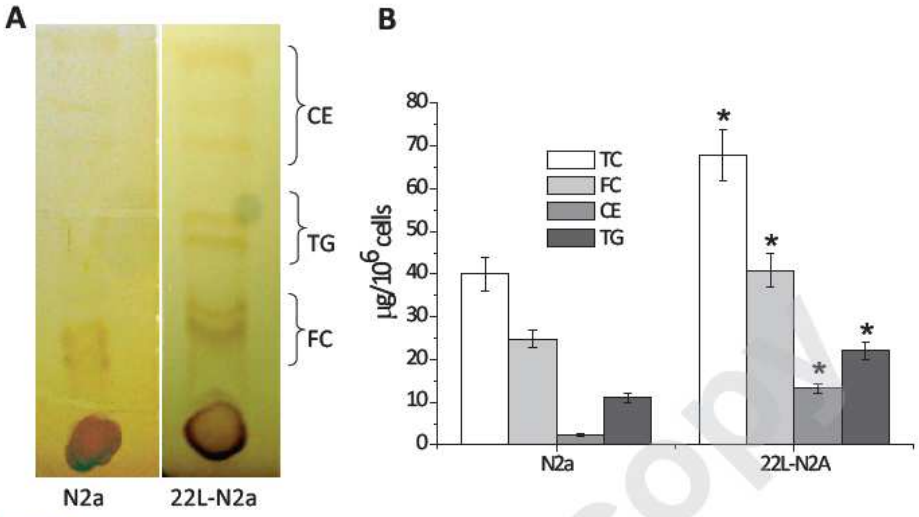

Figure 6. N2a *vs.* 22L-N2a lipid content by TLC. Total lipids (TL) were extracted with cold acetone from triplicate N2a and 22L-N2a cell cultures. A total of $30x10^6$ of each cell culture was collected from sub-confluent flasks. Extracted lipids were split into two equal aliquots and air dried: one aliquot was used to determine total cholesterol (TC) by the cholesterol oxidase method; the other aliquot was resuspended in 100 µl of chloroform and analysed for lipid subclasses by TLC (see section 2.7). (A) TLC separated bands as visualized by iodine vapor. (B) TC, cholesterol ester (CE), free cholesterol (FC), and triglycerides (TG) as determined by enzymatic methods. Data are the mean ± SE of triplicate cultures. *P<0.05: (22L-infected N2a *vs.* N2a); (treated *vs.* untreated 22L-infected N2a).

inhibits cholesterol esterification by an as yet unknown mechanism [25,26]; ii) pioglitazone, an anti-diabetic drug that induces cell redistribution of free fatty acids [27]; iii) verapamil, a calcium-blocking drug that inhibits cholesterol trafficking from the plasma membrane to the endoplasmic reticulum [21, refs therein]; and iv) progesterone, a sterol hormone that affects cholesterol trafficking from both the plasma membrane and lysosomes [28,29]. Chlorpromazine and quinacrine are known to inhibit prions *in vitro* and to some extent also *in vivo* [2,30]. Although the exact mechanism(s) remains to be established, these drugs have been involved in i) competitive inhibition of endogenous sulfated glycosaminoglycans (GAGs)-PrP interaction, essential for PrP^{res} formation or stabilization in the endosomes; ii) unfolding of PrP^{res} by drug-induced endosome/lysosome accumulation of chaperone-like factor(s); iii) destabilization of PrP^{res} by alteration of lysosomal pH [15]. Recent evidence, however, not formally excluding the above mechanisms, indicates that quinacrine and chlorpromazine might exert anti-prion effect by additional mechanisms that involve interference with intracellular cholesterol. Quinacrine has been reported to determine destabilization of cholesterol-rich membrane domains (DRMs or rafts) [31]. Worthy of mention, these Authors also described the anti-prion activity of progesterone and the synergistic anti-prion effect of quinacrine in combination with the cholesterol biosynthesis inhibitor simvastatin. As for chlorpromazine, a study on the role of cellular cholesterol in the pathogenesis of schizophrenia, indicated that drug-induced transcriptional activation of cholesterol biosynthesis could represent a novel mechanism of action for some antipsychotic drugs, chlorpromazine being one of the most potent [32]. Moreover, more recently Vik-Mo *et al.* [33] showed that antipsychotic and antidepressant drugs also induce transcriptional activation of genes involved in cholesterol transport and efflux. Hence, the observed anti-prion synergistic effects may arise from pharmacologic-induced cholesterol homeostasis. Compared to parental uninfected N2a cells, in fact, prion-infected cultures displayed a general derangement of type and distribution of most intracellular lipids, including free cholesterol, cholesterol esters, phospholipids, and triglycerides.

These results confirm and extend our previous findings in the same cell model [14] and in the ovine scrapie [11-13], and further support the presence of a tight association between prion infection/susceptibility and altered cholesterol homeostasis. In agreement with our results, altered cholesterol metabolism/esterification with over-expression of ACAT-1 (*soat1*) was reported in mice brains during the course of experimental scrapie [34, refs therein], and up-regulation of cholesterol biosynthesis was recently described following prion

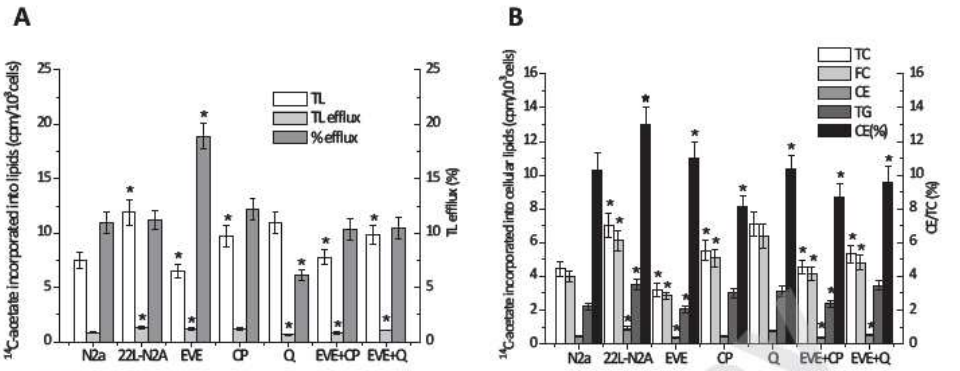

Figure 7. Effect of single *vs.* dual drug combinations on lipid synthesis and efflux. N2a and 22L-N2a cells were seeded at 1x10^4/ml in growth medium in Microtest flat-bottom 24-well plates (Becton Dickinson, USA). After overnight settlement, a set of 22L-N2a cultures were drug-treated (everolimus, EVE 0.02 μM; chlorpromazine, CP 2 μM; quinacrine, Q 0.2 μM) and further incubated for 72 hours. Cellular lipid syntheses (TC, FC, CE, TG) were evaluated by incubating cells for 6 hours in medium containing [1-^{14}C]acetate at a final concentration of 2 μCi/ml. After labelling, cells were washed with PBS and lipids extracted with cold acetone. Lipid subclasses were separated by TLC and [^{14}C]acetate incorporation into the various lipid fractions was measured. Efflux from the cells into the medium was expressed as the percentage of radioactivity in medium/total radioactivity (cells + medium). Each drug and drug combination was tested in triplicate. (A) Total lipids and efflux; (B) FC, CE, and TG. Data shown are the mean ± SE of triplicate cultures. *P<0.05: (22L-infected N2a *vs.* N2a); (treated *vs.* untreated 22L-infected N2a).

infection in various types of neuronal cells, N2a included [35]. Interestingly, Bach *et al.* [35] presented evidence that modification of cholesterol biosynthesis appears a characteristic response of neurons and neuronal cell lines to prion challenge, and suggested that prions themselves may have the potential to alter cell cholesterol homeostasis in a cell-type specific manner. Although at present we have no mechanistic explanation for the association found in sheep between cholesterol alteration and scrapie-susceptible prion genotype [11-13], we can speculate that prions may as well have the potential to alter cholesterol homeostasis in a genotype-type specific manner. Whatever mechanism is involved, the emerging picture is that of a direct relationship between prion infection/replication and lipid homeostasis alterations. These modifications, likely translating into changes in the raft-membrane integrity, may in turn support the aberrant processing of prion protein [36]. The ability of combined treatments of everolimus and chloropromazine, or everolimus and quinacrine, to trigger lipid homeostasis in the prion-infected cells, supports this hypothesis and may account for the enhanced anti-prion effect of these drug combinations. On the other hand, a mechanism involving inhibition of the drug-efflux pump P-gp seems unlikely. Firstly, most synergistic effects against PrP^{res} were obtained with P-gp inhibitors (progesterone and verapamil) at concentrations 4/5-fold lower than those required to increase vinblastine influx. Secondly, everolimus, at the highest concentration tested (*i.e.* 1 μM) increased vinblastine retention by only 10%. Worthy of note, a recent study by Bate *et al.* reported a higher toxicity of some ACAT inhibitors (*i.e.* TMP-153, FR179254 and YIC-C8-434) in prion-infected ScGT1 and ScN2a cell lines *vs.* uninfected cells [37]. However, none of the cholesterol ester modulators used in the present study affected viability of 22L-infected and uninfected N2a cells, neither in single nor in combinatory experiments.

Taken together these results indicate that inhibition of prion generation can be readily potentiated by combinatorial drug treatments, and that steps of cholesterol/cholesterol esterification metabolism may represent suitable targets. While these findings are suggestive, the potential effectiveness of these drugs and drug-combinations yet remains to be confirmed in other prion models as well as in cell conditions that may better reflect the *in vivo* prion biology. In this respect, an interesting study in prion-infected N2a cells showed that cell division strongly influences the accumulation of PrP^{res} and suggested that, since the process of cell division may intensify the kinetics of PrP^{Sc} clearance, inhibitory activity in neuronal cell lines may not reflect real effectiveness in the neurons [38]. Moreover, our previous studies on the role of cholesterol metabolism during cell proliferation indicated an association between the cell capability to synthesize and retain cholesterol esters and the cell growth rate potential [20,24,25]. Therefore, given that inhibitory activity of anti-prion compounds in culture seems to be influenced by the growth phases of target cells, and given that cell cycle

progression appears itself associated with changes of cholesterol homeostatic mechanisms, the evaluation of these drugs and drug combinations in non-dividing stationary cultures may provide further insight on the mechanism(s) linking cholesterol metabolism to the processing of prion protein.

Acknowledgements

This work was in part supported by a grant from Regione Autonoma Sardegna. The Authors are indebted with Byron Caughey (NIH/NIAID Rocky Mountain Laboratories, USA) for kindly providing mouse neuroblastoma cell lines. We also thank Marina Julian and Edward Steeden for excellent English revision.

References

[1] Prusiner S.B., Prions, Proc. Natl. Acad. Sci. USA, 1998, 95, 13363-13383
[2] Trevitt C.R., Collinge J., A systematic review of prion therapeutics in experimental models, Brain, 2006, 129, 2241-2265
[3] Doh-ura K., Ishikawa K., Murakami-Kubo I., Sasaki K., Mohri S., Race R., et al., Treatment of transmissible spongiform encephalopathy by intraventricular drug infusion in animal models, J. Virol., 2004, 78, 4999-5006
[4] Bone I., Belton L., Walker A.S., Darbyshire J. Intraventricular pentosan polysulphate in human prion diseases: an observational study in the UK, Eur. J. Neurol., 2008, 15, 458-464
[5] Love R., Old drugs to treat new variant Creutzfeldt-Jakob disease, Lancet, 2001, 358, 563-574
[6] Stewart L.A., Rydzewska L.H.M., Keogh G.F., Knight R.S.G., Systematic review of therapeutic interventions in human prion disease, Neurology, 2008, 70, 1272-1281
[7] Collinge J., Gorham M., Hudson F., Kennedy A., Keogh G., Pal S., et al., Safety and efficacy of quinacrine in human prion disease (PRION-1 study): a patient-preference trial, Lancet Neurol., 2009, 8, 334-344
[8] Geschwind M.D., Clinical trials for prion disease: difficult challenges, but hope for the future, Lancet Neurol., 2009, 8, 304-306
[9] CJD (Creutzfeldt-Jakob disease) quinacrine study. (accessed March 4, 2009). http://clinicaltrials.gov/ct2/show/NCT00183092
[10] Kocisko D., Caughey B., Morrey J.D., Race R.E., Enhanced antiscrapie effect using combination drug treatment, Antimicrob. Agents Chemother., 2006, 50, 3447-3449
[11] Pani A., Abete C., Norfo C., Mulas C., Putzolu M., Laconi S., et al., Cholesterol metabolism in brain and skin fibroblasts from Sarda breed sheep with scrapie resistant or susceptible genotype, Am. J. Infect. Dis., 2007, 3, 143-150
[12] Pani A., Abete C., Norfo C., Mulas C., Putzolu M., Laconi S., et al., Accumulation of CE in ex vivo lymphocytes from scrapie-susceptible sheep and in scrapie-infected mouse neuroblastoma cell lines, Am. J. Infect. Dis., 2007, 3, 165-168
[13] Orrù C.D., Abete C., Cannas M.D., Mulas C., Norfo C., Mandas A., et al., ACAT-1, Cav-1 and PrP expression in scrapie susceptible and resistant sheep, Cent. Eur. J. Biol., 2010, 5, 31-37
[14] Pani A., Norfo C., Abete C., Mulas C., Putzolu M., Laconi S., et al., Anti-prion activity of cholesterol esterification modulators: a comparative study in ex vivo sheep fibroblasts and lymphocytes and in mouse neuroblastoma cell lines, Antimicrob. Agents Chemother., 2007, 51, 4141-4147
[15] Doh-ura K., Iwaki T., Caughey B., Lysosomotropic Agents and Cysteine Protease Inhibitors Inhibit Scrapie-Associated Prion Protein Accumulation, J. Virol., 2000, 74, 4894-4897
[16] Caughey B., Raymond G.J., Sulfated polyanion inhibition of scrapie-associated PrP accumulation in cultured cells, J. Virol., 1993, 67, 643-650
[17] Caughey B., Brown K., Raymond G.J., Katzenstein G.E., Thresher W., Binding of the protease-sensitive form of PrP (prion protein) to sulfated glycosaminoglycan and congo red, J. Virol., 1994, 68, 2135-2141
[18] Kocisko D.A., Engel A.L., Harbuck K., Arnold K.M., Olsen E.A., Raymond L.D., et al., Comparison of protease-resistant prion protein inhibitors in cell cultures infected with two strains of mouse and sheep scrapie, Neurosci. Lett., 2005, 388, 106-111
[19] Suhnel J., Evaluation of synergism or antagonism for the combined action of antiviral agents, Antiv. Res., 1990, 13, 23-40
[20] Pani A., Batetta B., Putzolu M., Sanna F., Spano O., Piras S., et al., MDR1, cholesterol esterification and cell growth: a comparative study in normal and multidrug-resistant KB cell lines, Cell. Mol. Life Sci., 2000, 57, 1094-1102

[21] Greenspan P., Fowler S.D., Spectrofluorometric studies of the lipid probe, Nile red, J. Lipid Res., 1985, 26, 781-789
[22] Diaz G., Batetta B., Sanna F., Uda S., Reali C., Angius F., et al., Lipid droplet changes in proliferating and quiescent 3T3 fibroblasts, Histochem. Cell Biol., 2008, 129, 611-621
[23] Kocisko D.A., Baron G.S., Rubenstein R., Chen J., Kuizon S., Caughey B., New inhibitors of scrapie-associated prion protein formation in a library of 2000 drugs and natural products, J. Virol., 2003, 77, 10288-10296
[24] Pani A., Dessì S., (Eds.), Cell Growth and Cholesterol Esters, New York: Landes Bioscence & Kluwer Academic Press Publishers, 2004
[25] Batetta B., Mulas M.F., Sanna F., Putzolu M., Bonatesta R.R., Casperi-Campani A., et al., Role of cholesterol ester pathway in the control of cell cycle in human aortic smooth muscle cells, FASEB J., 2003, 17, 746-748
[26] Varghese Z., Fernando R., Moorhead J.F., Powis S.H., Ruan X.Z., Effects of sirolimus on mesangial cell cholesterol homeostasis: a novel mechanism for its action against lipid-mediated injury in renal allografts, Am. J. Physiol. Renal Physiol., 2005, 289, 43-48
[27] Freeman D.A., Romero A., Effects of troglitazone on intracellular cholesterol distribution and cholesterol-dependent cell functions in MA-10 Leydig tumor cells, Biochem. Pharmacol., 2003, 66, 307-313
[28] Debry P., Nash E.A., Neklason D.W., Metherall J.E., Role of multidrug resistance P-glycoproteins in cholesterol esterification, J. Biol. Chem., 1997, 272, 1026-1031
[29] Butler J.D., Banchette-Mackie J., Golden E., O'Neill R.R., Carstea G., Roff C.F., et al., Progesterone blocks cholesterol translocation from lysosomes, J. Biol. Chem., 1992, 267, 23797-23805
[30] Barret A., Tagliavini F., Forloni G., Bate C., Salmona M., Colombo L., et al., Evaluation of quinacrine treatment for prion diseases, J. Virol., 2003, 77, 8462-8469
[31] Klingenstein R., Lober S., Kujala P., Godsave S., Leliveld S.R., Gmeiner P., et al., Tricyclic antidepressants, quinacrine and a novel, synthetic chimera thereof clear prions by destabilizing detergent-resistant membrane compartments, J. Neurochem., 2006, 98, 748-759
[32] FernØ J., Skrede S., O Vik-Mo A., Havic B., Steen V.D., Drug-induced activation of SREBP-controlled lipogenic gene expression in CNS-related cell lines: marked differences between various antipsychotic drugs, BMC Neuroscience, 2006, 7, 69-80
[33] Vik-Mo A.O., Fernø J., Skrede S., Steen V.M., Psychotropic drugs up-regulate the expression of cholesterol transport proteins including ApoE in cultured human CNS- and liver cells, BMC Pharmacol., 2009, 9, 10
[34] Kumar R., McClain D., Young R., Carlson G.A., Cholesterol transporter ATP-binding cassette A1 (ABCA1) is elevated in prion disease and affects PrPC and PrPSc concentrations in cultured cells, J. Gen. Virol., 2008, 89, 1525-1532
[35] Bach C., Gilch S., Rost R., Greenwood A.D., Horsch M., Hajj G.N., et al., Prion-induced activation of cholesterogenic gene expression by Srebp2 in neuronal cells, J. Biol. Chem., 2009, 284, 31260-31269
[36] Taylor D.R., Hooper N.M., Role of lipid rafts in the processing of the pathogenic prion and Alzheimer's amyloid-β proteins, Sem. Cell. Develop. Biol., 2007, 18, 638-648
[37] Bate C., Tayebi M., Williams A., Cholesterol esterification reduces the neurotoxicity of prions, Neuropharmacology, 2008, 54, 1247-1253
[38] Ghaemmaghami S., Phuan P.W., Perkins B., Ullman J., May B.C., Cohen F.E., et al., Cell division modulates prion accumulation in cultured cells, Proc. Natl. Acad. Sci. USA., 2007, 104, 17971-17976

2.1.3 Pharmacologic Cholesterol Homeostasis Affects Prion Generation in a Synergistic Manner (Article III)

In this article we discuss all previous results pointing to a direct link between systemic metabolic lipid alterations and the pathogenesis of prion diseases. At the cellular level, our findings indicate that prion infection/replication is likely associated with a lipid environment that involve changes both in the content and distribution of the different pools of cellular cholesterol, as well as of other cellular lipids, including phospholipids and triglycerides. The synergic anti-prion effect showed by drug combinations affecting cholesterol metabolism at different levels suggest that pharmacologic interventions restoring lipid homeostasis may represent a more successful therapeutic approach than drug treatments lowering cholesterol content. Notably, our data also point to neutral lipid accumulation in peripheral cells as an easy-to-detect hallmark associated with disease and/or indicative of increased susceptibility to develop disease following infection.

Article III

Pharmacologic Cholesterol Homeostasis Affects Prion Generation in a Synergistic Manner

Christina D. Orru[1], M. Dolores Cannas[1], Sarah Vascellari[1], Claudia Abete[1], Antonella Mandas[2], Fabrizio Angius[1], Pierluigi Cocco[1], Paolo La Colla[1], Sandra Dessi'[1] and Alessandra Pani*[,1]

[1]*Department of Biomedical Science & Technology;* [2]*Department of Internal Medicine University of Cagliari, Italy*

Abstract: It is generally recognised that prion replication in the brain is associated with cholesterol changes. We now show that prion diseases are likely associated with systemic metabolic alterations that involve changes both in the content and distribution of the different pools of cellular cholesterol, free cholesterol and cholesterol esters, as well as of other cellular lipids, including phospholipids and triglycerides. The synergic anti-prion effect showed by drug combinations affecting cholesterol metabolism at different levels suggest that pharmacologic interventions restoring lipid homeostasis may represent a more successful therapeutic approach than drug treatments lowering cholesterol content *per se* (i.e. statins). Notably, our data also point to neutral lipid accumulation in peripheral cells as an easy-to-detect hallmark associated with disease and/or indicative of increased susceptibility to develop disease following infection.

Keywords: Prions, prion disorders, cholesterol homeostasis, cholesterol modulators, drug combinations.

INTRODUCTION

The elucidation of the cellular prion protein (PrP^C) metabolism and of the mechanism(s) of its structural conversion into pathogenic isoforms (PrP^{Sc}) remains a fundamental target for developing therapeutic and prophylactic strategies against prion diseases. Numerous studies hint at lipid rafts, i.e. membrane microdomains enriched in cholesterol and sphingolipids, as possible sites of prion conversion [1,2], and many lines of evidence indicate that intracellular cholesterol changes readily affect the processing/trafficking of PrP^C [3-5], suggesting that the process of PrP misfolding might be modulated by cholesterol homeostatic mechanisms. At present, however, although there are clear indications that raft composition is essential for the proper folding of nascent PrP^C, there are divergent findings on whether depletion of membrane cholesterol or its enrichment would favour PrP misfolding. A number of studies have shown a decrease in PrP^{Sc} generation by lowering the cellular cholesterol content with statins [5-7], while other studies produced evidence that cholesterol depletion abolishes PrP-raft association, promotes its accumulation and increases substantially its misfolding [8,9]. The overall complexity of the mechanism(s) linking PrP metabolism to cellular cholesterol changes is even more complicated by the fact that prion infection/replication itself seems to have the potential to induce modifications in the cholesterol metabolism [10,11]. In this context, our recent findings in sheep scrapie indicated that modifications of cholesterol metabolism, rather than being limited to the brain, appear to be a systemic trait since also *ex vivo* dermal fibroblasts and blood lymphocytes of sheep suffering-from or susceptible-to scrapie display similar alterations [12-14].

*Address correspondence to this author at the Dept. Biomedical Science & Technology, University of Cagliari, Italy; Tel: +39 070 675 4209; Fax: +39 070 675 4210; E-mail: pania@unica.it

2210-2892/10

In addition, in prion/cell systems we found that persistent infection is associated to metabolic changes involving, besides cholesterol, all major classes of intracellular lipids, and that treatments with drug combinations triggering lipid homeostasis determine a synergic inhibition of prion generation [13,15,16].

SYSTEMIC CHOLESTEROL ALTERATIONS IN SHEEP SCRAPIE

Abnormal accumulation of cholesterol esters characterizes brain biopsies and *ex vivo* skin fibroblasts from sheep susceptible-to (ARQ/ARQ-) or suffering-from (ARQ/ARQ+) scrapie, with respect to scrapie-resistant sheep (ARR/ARR), Fig. (**1**).

In brains and skin fibroblasts from scrapie susceptible/infected sheep, the accumulation of cholesterol esters is accompanied by altered expression levels of enzymatic activities involved in cholesterol esterification (ACAT-1; up-regulated) and cholesterol trafficking (Cav-1; down-regulated), and by that of PrP^C itself (up-regulated), Fig. (**2**).

CHOLESTEROL ALTERATIONS IN PRION-INFECTED NEURONAL CELL LINES

In prion-infected N2a cells, Nile red and filipin staining of intracellular lipids reveals changes both in the content and distribution of most intracellular lipids, Fig. (**3**). Notably, besides cholesterol esters and free cholesterol, also phospholipids and triglycerides appear up-regulated.

ANTI-PRION ACTIVITY OF CHOLESTEROL MODULATORS

Cell treatments with cholesterol/cholesterol ester modulators, alone or in combination with the cholesterol-interfering prion inhibitors chlorpromazine and quinacrine, show marked anti-prion activity, Figs. (**4**) and (**5**).

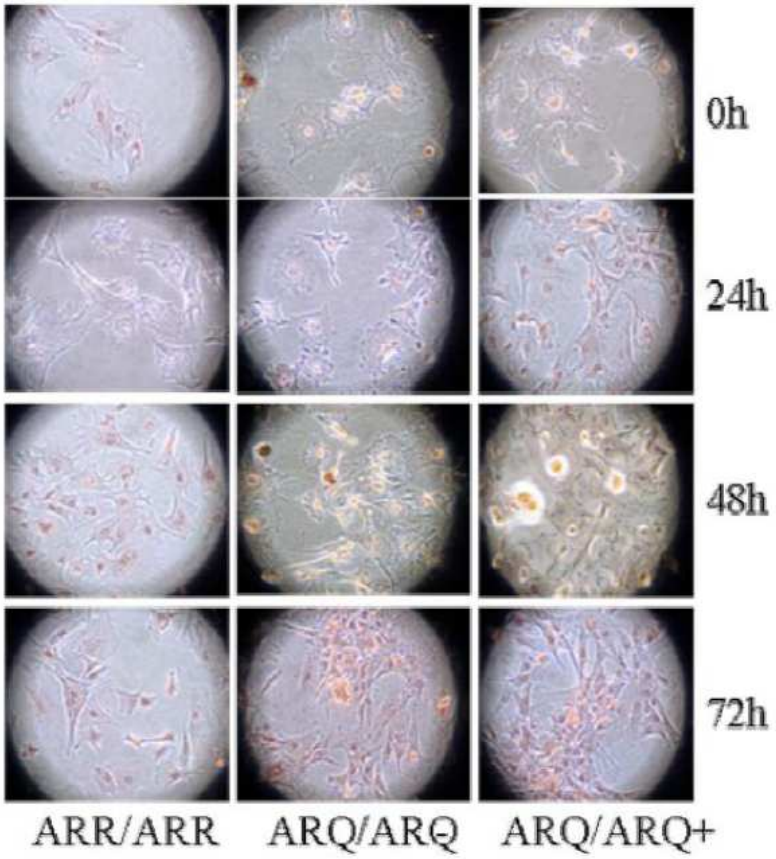

Fig. (1). Oil-red O-stained neutral lipids of cultured serum-stimulated skin fibroblasts from sheep carrying scrapie-resistant (ARR/ARR) or -susceptible (ARQ/ARQ) genotypes.

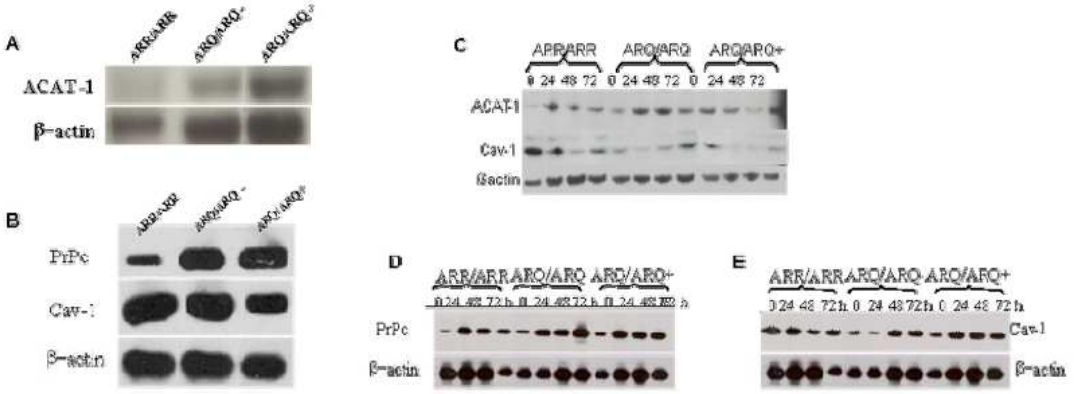

Fig. (2). ACAT-1, Cav-1 and PrP in brains (**A** and **B**) and skin fibroblasts (**C**-**E**) of sheep carrying scrapie-resistant (ARR/ARR) or -susceptible (ARQ/ARQ) genotypes.

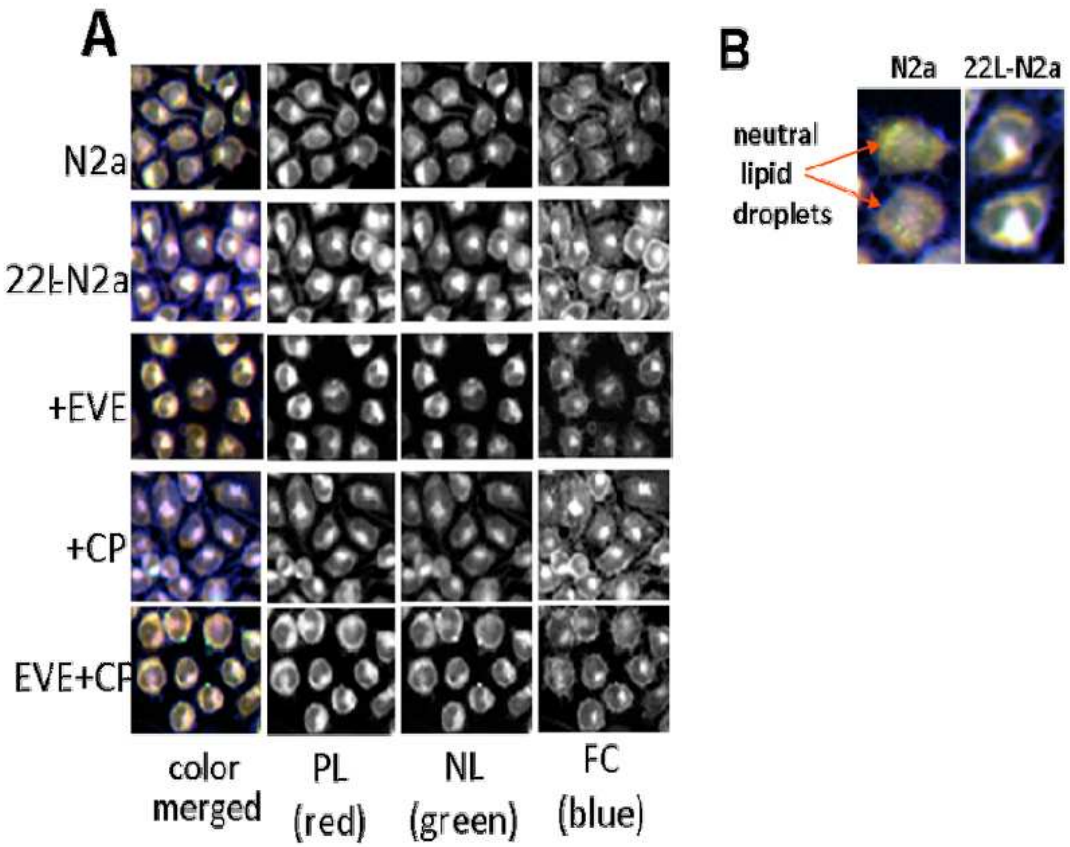

Fig. (3). Nile red and Filipin lipid staining of N2a cells.

Notably, drug combinations determine a strong synergistic anti-prion effect apparently by triggering a lipid profile similar to that of uninfected-untreated cells, see Fig. (**3**).

The most potent synergism is obtained with everolimus, an immunosuppressant agent that inhibits cholesterol esterification by an yet unknown mechanism, in combination with both chlorpromazine and quinacrine. Synergic interaction of the latter anti-prion drugs are also observed with pioglitazone, an anti-diabetic drug that induces redistribution of free fatty acids within the cell; verapamil, a calcium-blocking drug that inhibits cholesterol trafficking from the plasma membrane to the ER, and progesterone, a sterol hormone that affects cholesterol trafficking both from the plasma membrane and lysosomes.

As for chlorpromazine and quinacrine themselves, recent evidence, not formally excluding other reported mechanisms, indicates that these drugs might exert anti-prion effect by interfering with intracellular cholesterol: quinacrine through destabilization of cholesterol-rich membrane domains (rafts), and chlorpromazine by inducing transcriptional activation of genes involved in cholesterol biosynthesis, transport, and efflux.

CHOLESTEROL HOMEOSTASIS NETWORK

In normal condition, since membrane cholesterol appears critical for the function of raft-resident proteins, highly integrated sets of homeostatic mechanisms finely regulate free cholesterol vs. cholesterol ester pool according to the cells' need. Approximately 90% of the total cellular cholesterol resides in the membrane raft domains as free cholesterol, while only a minor amount (approximately 1-10%) is found as cholesterol esters in cytoplasmic lipid droplets [17]. Membrane cholesterol is in a dynamic state, moving to the endoplasmic reticulum (ER) in response to changing homeostatic conditions in the cell [18,19]. Free cholesterol in the ER, if in excess, is converted to cholesterol esters by ACAT-1, and stored in the cytoplasm [20]. When cells need cholesterol for membrane biogenesis/function, or when cholesterol esters exceed critical threshold values, esterified cholesterol can be reconverted to free cholesterol and recycled to the membrane by cholesterol binding/transport proteins, such as Cav-1 and, for cell efflux *via* HDL, ABCA-1 [5,20], Fig. (**6**).

In pathologic condition, synthesis, esterification, and trafficking of cholesterol is deregulated leading to altered

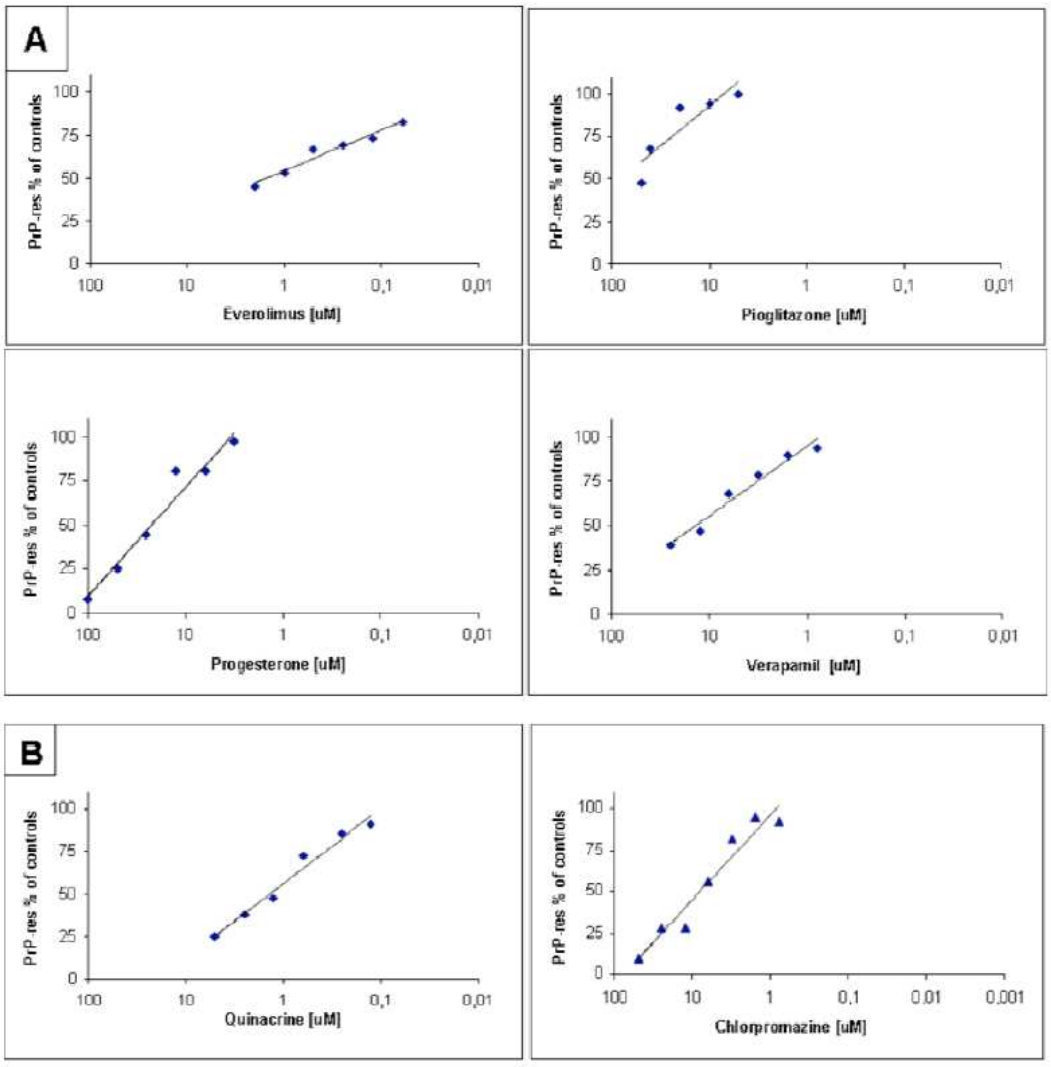

Fig. (4). Dose-response curves of anti-prion activity of cholesterol ester modulators (**A**) and prion inhibitors (**B**).

content and distribution of free cholesterol and to abnormal cytoplasmic accumulation of cholesterol esters.

The altered cholesterol homeostasis, in turn, likely affects the metabolism of other cellular lipids, such as phospholipids and tryglicerides, altogether creating in the cell a lipid environment apparently more suitable for aberrant prion protein conversion. The strong synergistic anti-prion effect of drug combinations restoring lipid homeostasis in the infected cell, supports this hypothesis.

CONCLUDING REMARKS

Altogether our results indicate that prion infection/susceptibility is associated with systemic lipid alterations and that pharmacologic cholesterol homeostasis may represent a more successful way to hamper prion generation than drug treatments lowering cholesterol content *per se* (i.e. statins). Overall, these data support the idea that prion infection, as well as particular cellular-PrP polymorphisms, may take advantage of preexistent and/or induced modifications of cholesterol homeostasis to create a lipid environment favorable to the initiation/progression of the aberrant processing of prion protein.

Besides the potential significance of these results in the clinic of prion disease, our data point to neutral lipid accumulation in peripheral cells as an easy-to-detect

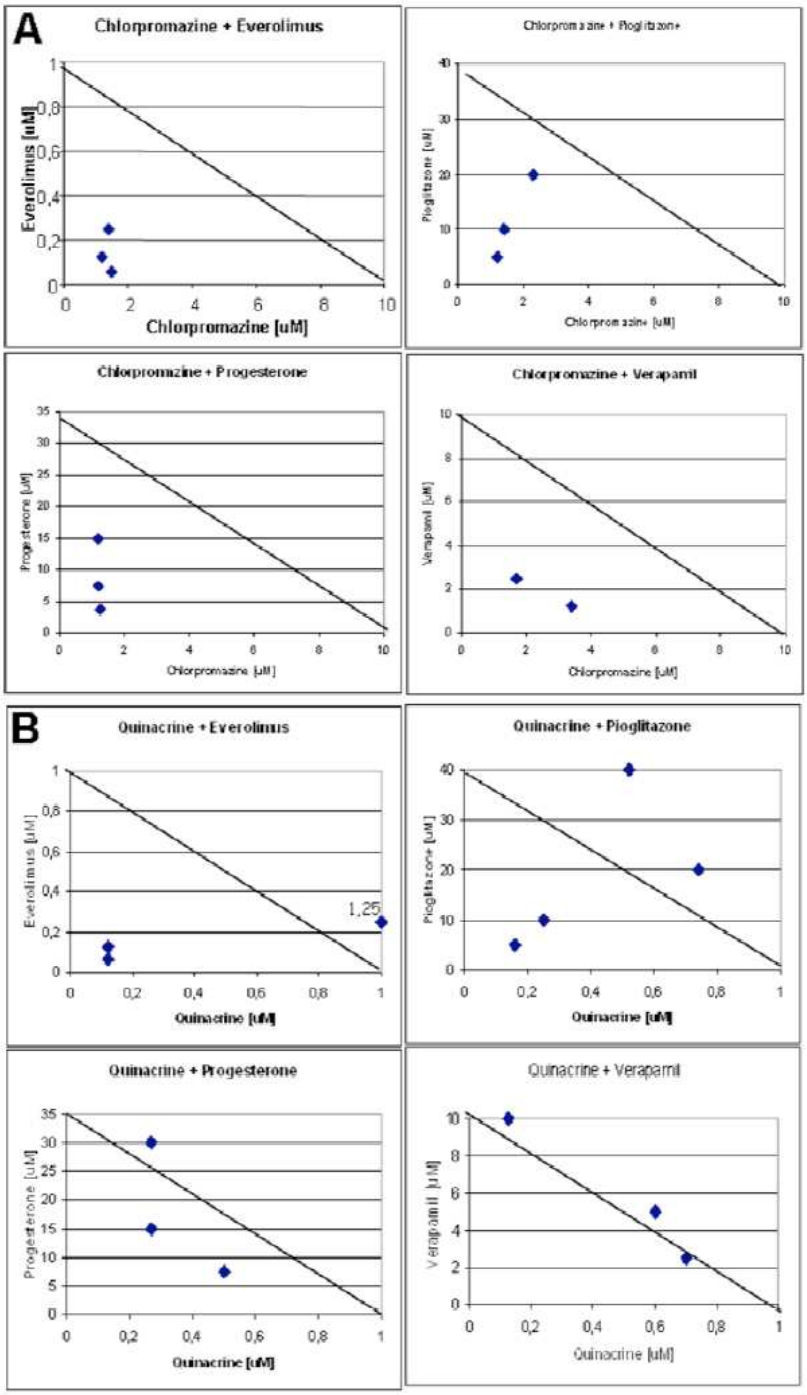

Fig. (5). Anti-prion activity of chlorpromazine (**A**) and quinacrine (**B**) in combination with the cholesterol ester modulators everolimus, pioglitazone, progesterone, and verapamil.

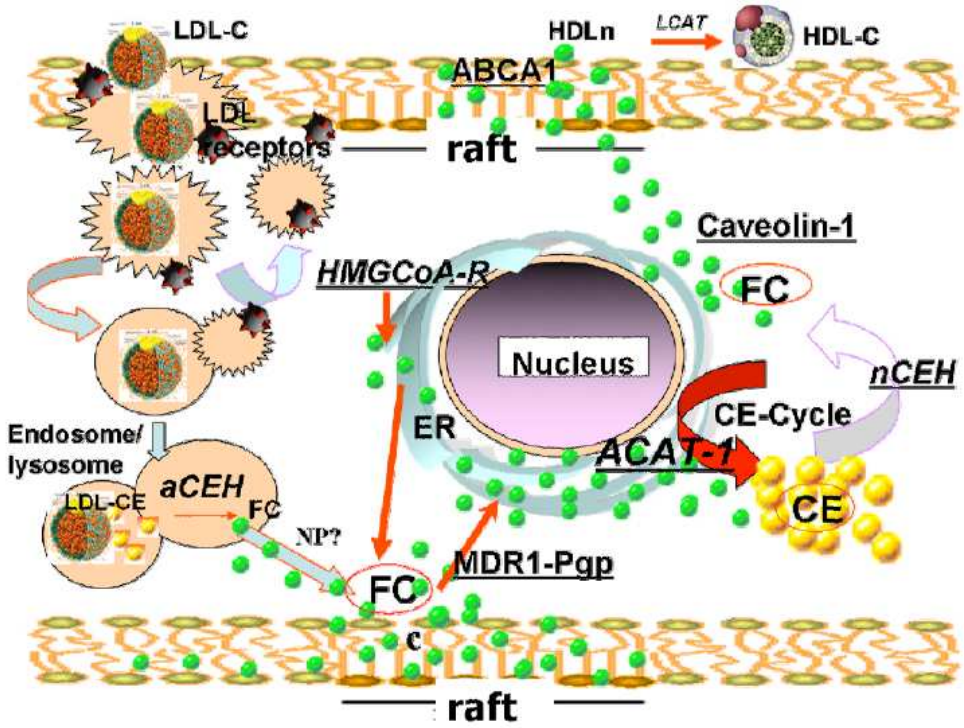

Fig. (6). Cholesterol homeostasis network.

hallmark associated with disease, and/or indicative of increased risk to develop disease following infection.

REFERENCES

[1] Simons, K.; Ehehalt R. Cholesterol, lipid rafts, and disease. *J. Clin. Invest.*, **2002**, *110*, 597-603.

[2] Critchley, P.; Kazlauskaite, J.; Eason, R.; Pinheiro, T.J. Binding of prion protein to lipid membranes. *Biochem. Biophys. Res. Commun.*, **2004**, *313*, 559-67.

[3] Gorodinsky, A.; Harris, D.A. Glycolipid-anchored proteins in neuroblastoma cells form detergent-resistant complexes without caveolin. *J. Cell Biol.*, **1995**, *129*, 619-27.

[4] Vey, M.; Pilkuhn, S.; Wille, H.; Nixon, R.; DeArmond, S.J.; Smart, E.J.; Anderson, R.G.; Taraboulos, A.; Prusiner, S.B. Subcellular colocalization of the cellular and scrapie prion proteins in caveolae-like membranous domains. *Proc. Natl. Acad. Sci. U S A*, **1996**, *93*, 14945-49.

[5] Taraboulos, A.; Scott, M.; Semenov, A.; Avrahami, D.; Laszlo, L.; Prusiner, S.B. Cholesterol depletion and modification of COOH-terminal sequence of the prion protein inhibit formation of the scrapie isoform. *J. Cell Biol.*, **1995**, *129*, 121-32.

[6] Gilch, S.; Kehler C.; Schätzl, H.M. The prion protein requires cholesterol for cell surface localization. *Mol. Cell. Neurosci.*, **2006**, *31*, 346-53.

[7] Mok, S.W.; Thelen, K.M.; Riemer, C.; Bamme, T.; Gültner, S.; Lütjohann, D.; Baier, M. Simvastatin prolongs survival times in prion infections of the central nervous system. *Biochem. Biophys. Res. Commun.*, **2006**, *348*, 697-702.

[8] Campana, V.; Sarnataro, D.; Paladino, S.; Zurzolo ,C. Detergent Resistant Domains but not the proteasome are involved in the misfolding of a PrP mutant retained in the Endoplasmic Reticulum. *J. Cell Sci.*, **2006**, *119*, 433-442.

[9] Abid, K.; Soto, C. Biomedicine and diseases: Review the intriguing prion disorders. *Cell. Mol. Life Sci.*, **2006**, 63, 2342-2351.

[10] Russelakis-Carneiro, M.; Hetz, C.; Maundrell, K. Prion replication alters the distribution of synaptophysin and caveolin 1 in neuronal lipid rafts. *Am. J. Pathol.*, **2004**, *165*, 1839-1848.

[11] Bach, C.; Gilch, S.; Rost, R.; Greenwood, A.D.; Horsch, M.; Hajj, G.N.; Brodesser, S.; Facius, A.; Schädler, S.; Sandhoff, K.; Beckers, J.; Leib-Mösch, C.; Schätzl. H.M.; Vorberg, I. Prion-induced activation of cholesterogenic gene expression by SREBP2 in neuronal cells. *J. Biol. Chem.*, **2009**, *284*, 31260-31269.

[12] Pani, A.; Abete, C.; Norfo, C.; Mulas, C.; Putzolu, M.; Laconi, S.; Cannas, M.D.; Orrù, C.D.; La Colla, P.; Dessi, S. Cholesterol metabolism in brain and skin fibroblasts from sarda breed sheep with scrapie-resistant and scrapie-susceptible genotypes. *Am. J. Infect. Dis.*, **2007**, *3*, 143-150.

[13] Pani, A.; Norfo, C.; Abete, C.; Mulas, C.;, Putzolu, M.; Laconi, S.; Orrù, C.D.; Cannas, M.D.; Vascellari, S.; La Colla, P.; Dessi, S. Accumulation of cholesterol esters in *ex vivo* lymphocytes from scrapie-susceptible sheep and in scrapie-infected mouse neuroblastoma cell lines. *Am. J. Infect. Dis.*, **2007**, *3*, 165-168.

[14] Orrù, C.D.; Abete, C.; Cannas, M.D.; Mulas, C.; Norfo, C.; Mandas, A.; Vascellari, S.; La Colla, P.; Dessì, S.; Pani, A. ACAT, Cav1 and PrP expression in scrapie susceptible and resistant sheep. *Cent. Eur. J. Biol.*, **2010**, *5*, 31-37.

[15] Pani, A.; Norfo, C.; Abete, C.; Mulas, C.; Putzolu, M.; Laconi, S.; Orrù, C.D.; Canna, M.D.; Vascellari, S.; La Colla, P.; Dessi, S. Anti-prion activity of cholesterol esterification modulators: a comparative study in ex vivo sheep fibroblasts and lymphocytes and in mouse neuroblastoma cell lines. *Antimicrob. Agents Chemother.*, **2007**, *51*, 4141-4147.

[16] Orrù, C.D.; Cannas, M.D.; Vascellari, S.; Angius, A.; Cocco, P.G.; Norfo, C.; Mandas, A.; La Colla, P.; Diaz, G.; Dessì, S.; Pani, A. In vitro synergistic anti-prion effect of cholesterol ester modulators in combination with chlorpromazine and quinacrine. *Cent. Eur. J. Biol.*, **2010**, *5*, 151-165.

[17] Schmitz, G.; Orso, E. Intracellular cholesterol and phospholipid trafficking: comparable mechanisms in macrophages and neuronal cells. *Cell. Mol. Life Sci.*, **2001**, *26*,1045-1068.
[18] Maxfield, F.R.; Tabas, I. Role of cholesterol and lipid organization in disease. *Nature*, **2005**, *438*, 612-621.
[19] Simons, K.; Ikonen, E. How cell handle cholesterol. *Science*, **2000**, *290*, 1721-1726.
[20] Kurzchalia, T.V.; Parton, R.G. Membrane microdomains and caveolae. *Curr. Opin. Cell Biol.*, **1999**, *11*, 424-431.

Received: April 12, 2010 Revised: July 09, 2010 Accepted: July 12, 2010

2.1.4 Comparative analysis of the variation of cholesterol in prion-infected N2a cells and in scrapie-affected mouse brains (Manuscript)

2.1.4.1 Introduction

Although our findings are in line with those by others that associated prion infections with altered cholesterol content, there is still no general agreement on the intracellular cholesterol forms (FC and CE) affected by prion infection. Contrasting results in the literature may be due not only to the complexity of prion biology, but also to intrinsic limitations of the diverse methods for cholesterol measurements in the various samples.

2.1.4.1.a Methods for Measuring Cholesterol in tissues.

Because of the broad involvement of cholesterol in normal and pathophysiological processes in the nervous system, its quantification under different conditions is critical to understand cholesterol role in the brain function. Methods to determine the cholesterol content of various cellular compartments are subjected to technical limitations. So far, several methods for measuring lipid in brain tissues have been used. Earlier cholesterol tissues staining techniques were based on chemical reactions such as the Schultz reaction, Lieberman-Burchard reaction, or reaction with fluoric–chloride–sulphuric acid and perchloric acid (Cossec *et al*., 2010). Currently, the methods for measuring lipids in brain tissues can be classified into two groups: non enzymatic methods and enzymatic methods. The enzymatic methods are direct assays amenable to automated procedures, suitable for the rapid and direct automated analysis of cholesterol using a limited amount of sample, and have largely replaced the more laborious non-enzymatic methods in clinical laboratories. In the enzymatic assay, cholesteryl esters are hydrolyzed by cholesterol esterase into fatty acid and free cholesterol; the latter is then oxidized by cholesterol oxidase (CO) to yield the corresponding ketone and hydrogen peroxide coproducts. Thus, the enzymatic methods for assaying cholesterol are based on the measurement of H_2O_2 by way of horseradish peroxidase (HRP)-coupled oxidation of H_2O_2 sensitive probes (Drake *et al*., 1999). By these technique, CE are not direcly determined.

In contrast, the non enzymatic methods are time-consuming multiple-step assays, and require the use of corrosive chemicals. These methods include colorimetric and fluorescent probes that allow visualization of cholesterol in tissues. Filipin is the most widely used fluorescent probe for visualizing free cholesterol (FC) because it binds with high affinity to the 3β-hydroxyl group of cholesterol (Rudolf and Curcio, 2009). Enzymatic and colorimetric methods are limited by the rapid bleaching of filipin under confocal microscopy, and the lack of specificity of both fillipin and cholesterol oxidase staining, respectively (Lebouvier *et al*., 2009).

Several other methods involve i) preliminary column chromatography of the total lipid into three or more fractions, which are then analyzed separately (Privett *et al*., 1971); ii) three or more solvent systems for TLC (Downing *et al.,* 1968; Pernes *et al.,* 1980); iii) a chemical pre-treatment of the TLC plate; iv) HPLC lipid separation with ultraviolet light, fluorescence, or mass spectrometric detection, and gas chromatography with mass spectrometric or flame ionization detection, which altogether represent the most selective and sensitive technicques for lipid studies (Cossec *et al*., 2010).

2.1.4.1.b Targeting Cholesterol to Prevent Protein Misfolding

With respect to cholesterol metabolism as potential therapeutic target in prion diseases, in our studies suggested that cell treatments with various cholesterol interfering drugs, as cholesterol ester inhibitor everolimus, the cholesterol-trafficking modulators progesterone and verapamil, and pioglitazone, a drug which induces the cell redistribution of free fatty acids, in combination with prions inhibitors, as the lysosomotropic drugs quinacrine and chlorpromazine, which, in addition to several other effects, respectively determine cell cholesterol redistribution and activation of cholesterol biosynthesis, transportation and efflux, showed synergic anti-prion effects, apparently by restoring cholesterol homeostasis in infected cells. Other authors, however, found an inhibition of prion infection by using FC-lowering drugs (*i.e.* statins) in both *in vitro* (Taraboulos *et al*., 1995; Bate *et a.*, 2004), and *in vivo* (Mok *et al*., 2006) prion models. A number of studies, in fact, have revealed that cholesterol-lowering drugs prevent prion replication *in vitro*, presumably by redistribution of PrPc out of the rafts (Taraboulos et al., 1995), while other studies produced evidence that cholesterol depletion abolishes PrP-raft association, promotes its accumulation and increases substantially its misfolding. After more than a decade of investigations in cell-based and *in vivo* models of PD, no conclusive and unequivocal answer is yet available. The promising early studies on the anti-amyloidogenic activity of cholesterol biosynthesis inhibitors, statins, and on their beneficial effects in experimental rodent Scrapie, have been followed by studies producing mixed results and inconclusive information on the statins' mode of action *in vivo* (Table 2).

Table 2. Effect of Cholesterol-Interfering Drugs in AD and PrD Models.

Cholesterol interfering drug	PrD models		Comments
	In vitro	*In vivo*	
Statins	+	+/-	They inhibit cholesterol biosynthesis
CP-113,818	nd	nd	It inhibits ACAT1 activity It reduces cholesterol esters
Avasimibe	nd	nd	It inhibits ACAT1 activity It inhibits also ACAT2 It reduces cholesterol esters
Sandoz 58-035	+	nd	It inhibits ACAT activity It reduces cholesterol esters
Quinacrine	+	+/-	Antidepressant, anti-malaria Cross BBB It induces cholesterol redistribution It is synergic anti-prion effect in combination with simvastatin, everolimus, pioglitazone *Multimeric quinacrine conjugate inhibits Abeta(1-40) fibril formation Trial ongoing in CJD
Chlorpromazine	+	-	Anti-psychotic drug Cross BBB It activates transcription of cholesterol synthesis, transport, efflux genes It shows synergic anti-prion effect in combination with everolimus, pioglitazone, verapamil, and progesterone
Everolimus	+	nd	Antiproliferative agent It is reduces cholesterol esters (molecular target unknown)
Progesterone	+	nd	Sterol hormone It affects cholesterol trafficking It reduces cholesterol esters
Verapamil	+	nd	Calcium-blocking drug It affects cholesterol trafficking It reduces cholesterol esters
Pioglitazone	+	nd	Anti-diabetic drug It induces redistribution of free fatty acids It reduces cholesterol esters

Statins act as reversible competitive inhibitors of 3-hydroxy-3-methylglutaryl coenzyme A (HMG-CoA) reductase, the key rate-controlling enzyme in cholesterol biosynthesis, that catalyzes the conversion of HMG-CoA to mevalonic acid. They are pharmacologically categorized as lipophilic (e.g. *Lovastatin, Simvastatin*) or hydrophilic (e.g.*Pravastatin*) compounds, depending upon their solubility in lipid solvents or water (Schachter, 2004). Lipophilic statins, as Simvastatin, are commonly considered able to cross promptly the blood-brain barrier (BBB) by passive diffusion. However, it was shown in rodents that hydrophilic statins, such as Pravastatin (PRV), may enter hepatic cells (Nezasa *et al.*, 2003; Evers & Chu, 2008) as well as brain capillary endothelial cells at BBB (Kikuki *et al.*, 2004; Cheng *et al.*, 2005) via an ATP dependent anion transport polypeptidic system (Oatps). These transporters, expressed in a variety of different tissues, including gut, kidney and brain, play important roles in drug absorption, distribution and excretion (Seithel *et al.*, 2008; Kivisto & Niemi, 2007). In cell-prion systems, different statins proved to be selective inhibitors of the scrapie-like prion protein (PrPres), indicating that *in vitro* statin anti-prion activity is linked to their lowering of cellular cholesterol levels (Taraboulos *et al*., 1995; Bate *et a.*, 2004).

However, *in vivo* studies in rodent scrapie models showed that statins delayed disease progression, and prolonged survival time (Mok *et al*., 2006; Kempster *al*., 2006; Vetrugno et al., 2009) through pleiotropic neuroprotective effects (Bate *et al*., 2007; Haviv *et al*., 2008), rather than by lowering brain cholesterol levels.Therefore, in spite of the increasing data in literature the clinic utility of drugs affecting cholesterol neosynthesis, in prion disorders, is being re-examined. Moreover, many aspects of the mechanisms that link cholesterol homeostasis alterations and pathologic conversion of prion protein yet remain unclear, probably also due to the lack of sensitive and specific methods for assessing cholesterol levels in the brain at subcellular resolution.

During my PhD, in the ambit of the "Master and Back program" of the Sardegna region, I carried out a research intership at the "Istituto Superiore di Sanità", Department of "Clinica, Diagnostica e Terapia delle Malattie Neurodegenerative del Sistema Nervoso Centrale", directed by Professor Maurizio Pocchiari. Recently, Pocchiari's research group showed delayed disease symptoms and prolonged survival times of 139A strain scrapie-infected mice treated orally with Pravastatin (PRV) (Vetrugno *et al*., Oral pravastatin prolongs survival time of scrapie infected mice. Journal of General Virology, 2009, 90, 1775–1780, DOI 10.1099/vir.0.009936-0). On these premises, I investigated the cholesterol metabolism alterations in an *in vivo* murine model of prion infection, by comparative analysis of the total, free and cholesterol esters content with two different methods for measuring cholesterol in tissue (by enzymatic and non-enzymatic method), in Normal C57BL mice vs terminally ill C57BL/6 mice inoculated with the 139A scrapie strain, and in brains from terminally ill C57BL/6 Pravastatin-treated mice inoculated with the 139A scrapie strain.

Therefore, the purpose of this study was *1*) to compare the cholesterol analysis in N2a cell line vs 22L-N2a scrapie-infected and uninfected vs scrapie infected mice by Fluorometric and HPLC-MS method; *2*) to evaluate the cholesterol content in infected untreated vs scrapie infected Pravastain-treated mice. As expected, HPLC anlysis has shown advantages for its high selectivity, its high sensitivity, and its potential for simultaneous quantification for several lipid classes. In present study, the lipid analysis showed that neuronal cultures and mouse brains prion-infected, were characterized by an altered cholesterol metabolic profile associated with increased of TC, FC and a higher CE pool, confirm our previous evidence of a relationship between abnormal accumulation of cholesterol esters and cell susceptibility to scrapie infection/replication. Treatment with cholesterol synthesis inhibitor Pravastatin slightly reduced the cholesterol free content but no total cholesterol content in brain homogenates of scrapie infected mice.

Our findings seems to indicate that brain cholesterol alterations during PrD involve dynamic modifications in cholesterol homeostatic networks. These data confirm our hypothesis that steps of cholesterol/cholesterol ester metabolism may represent suitable targets of potential clinical importance.

Manuscript

COMPARATIVE ANALYSIS OF THE VARIATION OF CHOLESTEROL IN PRION-INFECTED N2a CELLS AND IN SCRAPIE-AFFECTED MOUSE BRAINS

Sarah Vascellari[a*], Sebastiano Banni[b], Claudia Vacca[b], Christina Doriana Orrù[a], Vito Vetrugno[c], Franco Cardone[c], Maurizio Pocchiari[c], Paolo La Colla[a], Sandra Dessì[a], Alessandra Pani[a]

[a] Department of Biomedical Science and Technology, [b]Department of Experimental Biology, University of Cagliari, 09042-Monserrato, Italy, [c]Department of Cell Biology and Neurosciences, Istituto Superiore di Sanità, Viale Regina Elena 299, 00161 Rome, Italy.

Abstract

Increasing data in the literature suggest a role of cholesterol in the pathogenesis of prion diseases, and indicate that cholesterol metabolic network could represent a promising drug target for more successful therapeutic approaches. At present, however, which specific changes are at play during prion infection, and how they are relevant to the pathologic process, yet remain unclear. Beside the overall complexity of prion biology, intrinsic limitations of the methods used to measure cholesterol variations may hamper unequivocal answers. In the present study we analysed total cholesterol, free cholesterol, cholesteryl esters, and fatty acids, in whole brain homogenates of terminally ill C57BL/6 mice inoculated with the 139A scrapie strain, either untreated and treated with pravastatin, and in mouse neuroblastoma N2a cell line infected with the 22L prion strain. Lipid analyses were performed by two different methods, the widely used fluorometric enzymatic cholesterol assay Amplex red, and the highly selective and sensitive HPLC-MS technique. Our results showed that, with respect to controls, significative cholesterol variations in both the prion-infected cells and brains could be reproducibly seized by HPLC-MS analyses only. Major cholesterol modifications with significative increases of the total cholesterol content, as well as of both free cholesterol and cholesterol esters pool, was detected in brains of infected mice and in prion-infected N2a cells. Consistent with an increased cholesterol ester fraction, HPLC-MS analyses of prion-infected vs. uninfected N2a cell extracts, highlighted a parallel increase of the whole fatty acid fraction, and that palmithic, oleic, and miristic acids were the most raised. Concerning the yet unclear relationship between the beneficial effect of statins in experimental mouse scrapie and their lowering effect on cerebral cholesterol, HPLC-MS analysis in 139A-infected C57BL/6 mice treated with PRV showed a significative reduction of free cholesterol, and a moderate, although not significative, decrease of total cholesterol. Somehow unexpectedly, a parallel increase of the cholesterol esters was also detected. Although their variation was modest in terms of absolute values, the CE/TC ratio in PRV-treated vs. untreated 139A-infected mice was highly significative ($p<0.005$). Altogether these data indicate that prion infection is associated with an altered arrangement of cholesterol metabolism characterized by increased cellular pools of both free and esterified cholesterol, and aware on the central importance of the analytical methods chosen to discriminate and measure different cholesterol intracellular forms.

Keywords: Prion Disease• Cholesterol metabolism • Cholesterol esters • 24*S* hydroxycholesterol • Fatty acids • Cholesterol synthesis inhibitors

Abbreviations: Prion Disease (PrD); prion protein (PrP^{C}); scrapie-like prion protein (PrP^{res}); total cholesterol (TC); free-cholesterol (FC); cholesterol esters (CE); Fatty acids (FAs); 24*S* hydroxycholesterol (24*S*-OH-chol); Pravastatin (PRV)

1. Introduction

Prion diseases (PrD) are a group of progressive and fatal protein-based neurodegenerative disorders that affect humans and several other mammals. Hallmark of all PrDs is the structural conversion of a (GPI)-anchored membrane protein, the cellular prion protein (PrP^{C}), into misfolded, disease-related isoform(s), termed PrP^{Sc} (Prusiner 1998; Weissmann *et al*., 2002; Aguzzi *et al*., 2004). It has been established that the catalytic formation of PrP^{Sc} is dependent upon its interaction with PrP^{C} molecules within specific membrane microdomains enriched in cholesterol and sphingolipids, commonly called lipid rafts (Vey *et al.,* 1996; Naslavsky *et al.,* 1997). Cholesterol, a key molecule for the correct membrane structuring and raft function, has been reported to be essential also for the cell-surface localization of PrP^{C} (Bate et al., 2004; Gilch et al., 2006). According to a role for membrane cholesterol in the misfolding process of PrP, drug-induced changes of intracellular cholesterol have been reported to affect the generation of PrP^{Sc} (Pani *et al*, 2007, Orrù *et al*., 2010). At present, however, it is still matter of debate whether depletion of cellular cholesterol or its enrichment would favour the misfolding process of PrP^{C}. While several studies have shown a decrease in PrP^{Sc} generation by lowering the cellular cholesterol content (Mattson *et al*., 1999; Stefani *et al*., 2007), other studies produced evidence that cholesterol depletion abolishes PrP-raft association, promotes PrP accumulation and increases substantially its misfolding (Koudinov *et al.*, 2005; Sjögren *et al.*, 2006). The promising early findings on the anti-prion activity of the cholesterol biosynthesis inhibitors, statins, have been followed by studies producing contrasting results. Although in cell-prion systems different statins generally were reported to inhibit the accumulation of the scrapie-like prion protein (PrP^{res}), indicating that *in vitro* statin anti-prion activity is linked to lowering cholesterol levels (Taraboulos *et al.*, 1995; Bate *et a.,* 2004), the *in vivo* studies, while describing the ability of these drugs to delay disease progression and to prolong the survival time in scrapie-infected rodents (Mok *et al*., 2006; Kempster *al*., 2006, Vetrugno *et al*., 2009), failed to demonstrate a direct effect of statins on the level of brain cholesterol, and attributed their beneficial activity to pleiotropic neuroprotective effects (Bate *et al.*, 2007; Haviv *et al*., 2008). Despite that, several independent lines of evidence pointed to an increased content of cellular cholesterol during prion infection, thus supporting the presence of a tight link between cholesterol and the misfolding of PrP at the cellular level (Pani *et al*, 2007; Bate *et al* 2008; Orrù *et al.*, 2010; Bach *et al.*, 2009). In this context, our studies in in vitro and ex vivo scrapie models, highlighted that prion infection is accompanied by a general derangement of cellular cholesterol homeostasis as the observed modifications of cholesterol metabolism included an increase of the free cholesterol (FC) pool (i.e. the cholesterol form in membranes), as well as that of the storage form of cellular cholesterol, the cytoplasmic colesteryl ester (CE) pool (Orrù *et al.*, 2010). In addition, we found that a number of drugs that affect steps of the cholesterol metabolism/trafficking other than biosynthesis, are also endowed with anti-prion activity in N2a cell lines, and that selected combinations of cholesterol modulating drugs produced strong synergistic anti-prion effects, apparently by restoring cholesterol homeostasis in the infected cell (Pani *et al*, 2007, Orrù *et al*., 2010). Hence, available data suggest that the continuous misfolding of PrP might be governed by an altered, and possibly prion-induced (Bach *et al*., 2009, Arispe *et al*., 2002; Stefani *et al*., 2009), arrangement of cholesterol homeostasis that creates a misfolding-favoring lipid environment in the cell. Since the elucidation of the mechanism(s) that regulate structural conversion of PrP^{C} into the pathogenic isoform(s) remains a fundamental target also for the development of novel therapeutic and prophylactic strategies, it is crucial to define the specific cholesterol metabolic arrangement that sustains PrP^{Sc} generation. Unfortunately, the understanding of the mechanism(s) linking PrP and cholesterol metabolisms is also complicated by the fact that the claimed prion-induced cholesterol modifications (Arispe *et al*., 2002; Stefani *et al.*, 2009) likely encroaches upon the physiologic cholesterol homeostatic changes that go with the cell's response to various stimuli (e.g. growth factors) and processes (e.g. progression through the cell cycle phases), especially when studies are performed in actively growing cell cultures (Pani *et al.*, 2004). Moreover, beside the use of different prion strains in different prion models, different methods used for cholesterol measurements may

contribute to unclear results. In particular, at present it is not yet generally accepted that prion infection is associated with an increase of the cytoplasmic CE pool as other Authors indicated that its reduction characterizes prion-infected neuronal cells (Bate *et al*., 2008). Although our data are consistent with those reported in a recent systems biology study (Hwang *et al*, 2009), showing that the *SOAT1* gene, encoding for the enzyme (i.e. ACAT1) responsible for cholesterol esterification, was the first one of all cholesterol-related genes to be up-regulated in the brain of scrapie-infected mice, the mouse neuroblastoma cell model remains widely used to investigate many aspects of the prion biology, as well as to screen novel prion inhibitors.
For these reasons, and with the aim to better define the modified cellular cholesterol arrangement that accompanies, and possibly sustains, the accumulation of pathologic prion isoforms, we deemed useful to comparatively analyze in the mouse neuroblastoma N2a cell model (i.e. 22L-infected vs. uninfected N2a cells), and in brains of experimentally scrapie-infected C57BL/6 mice (untreated and pravastatin treated 139A-infected vs. uninfected), the qualitative and quantitative variations of the intracellular cholesterol forms by two methods: the widely used fluorometric enzymatic assay (i.e. Amplex Red Cholesterol Assay kit), and HPLC-MS analyses. While fluorometric enzymatic based cholesterol assays are amenable to automated procedures and suitable for the rapid and direct analysis of cholesterol using a limited amount of samples, the pairing of HPLC lipid separation with mass spectroscopy (HPLC-MS) quatification is a highly sensitive and selective analytical method as it allows the simultaneous separation and quantification of several lipid classes beside cholesterol as such and its cellular derivatives, thus representing the most reliable approach for the study of lipids.

2. METHODS

2.1 Chemical Reagents

The solvents (Chloroform, Methanol, N-Heptane, Diisopropyl Ether, Formic Acid, Acetonitrile) and Iodine Bisublimate were purchased from Carlo Erba, (Italy). PRV kindly was provided by Bristol–Myers Squibb.

2.2 Cell lines

The mouse neuroblastoma N2a cell line and the 22L-N2a infected with the mouse-adapted 22L strains of scrapie, were a generous gift of Byron Caughey, Rocky Mountain Laboratories, National Institute of Allergy and Infectious Diseases, NIH, USA. The cells were grown and maintained at 37°C and 5% CO2 in OptiMEM supplemented with 10% fetal bovine serum (Gibco-Invitrogen, Italy), 2 mM L-glutamine, 50 U/ml penicillin G sodium, and 50 μg/ml streptomycin sulphate (Gibco-Invitrogen, Italy) and splitted every 3 to 4 days at a 1:10 or 1:20 dilution, respectively. All experiments were carried out in exponentially growing cell cultures or sub-confluent cultures.

2.3 Brains

One-month-old female C57BL/6 mice (Charles River) weighing 18–20 g, identified individually by a passive integrated transponder, were inoculated intracerebrally (i.c.) in the left hemisphere with 1% (w/v) brain homogenate prepared from terminally ill, strain 139A scrapie-infected mice as described previously (Vetrugno *et al*., 2005) and assigned randomly to the control or PRV-treated groups. PRV sodium salt (mouse oral LD50, 8939 mg kg21), was administered in the drinking water at a dose of 200 mg (kg body weight) 21 day 21 from the time of scrapie inoculation. Water consumption was monitored twice weekly and drug concentration was adjusted as required. Control animals received water without PRV. Mice were examined twice weekly until the appearance of scrapie clinical signs and then observed daily until they reached the terminal stage of the disease, when they were euthanized by carbon dioxide. Brains were collected as described previously (Vetrugno et al ., 2009). Each brain was divided into the two hemispheres; one was used for

immunoblot analysis and the other for lipid analysis. The brains was frozen at – 80°C until performing the analytical protocol.

2.4 Preparation of brain homogenates.

Mid-brain tissues from Normal, 139A and 139A PRV mice were thawed, weighed, and homogenized in nine volumes (10% w/v) of phosphate-buffered saline (PBS, Invitrogen) and 0,1% Triton X-100 by sonication pulses (Vibra Cell, Sonics & Materials Inc., Newtown, CT) while kept on ice and then boiled for 15 min to inactivate endogenous cellular cholesterol esterase. The resulting 10% homogenate was stored at - 80°C until further analysis by the fluorometric enzymatic and HPLC methods.

2.5 Lipid Extraction from brain homogenates.

Cholesterol, and its metabolite 24S-OH-Chol, were extracted from brain homogenates by the method of Folch (Folch J. *et al*, 1957). In brief, brain homogenates from Normal, 139A and 139A PRV mice were mixed with chloroform-methanol (2:1 v/v). Vitamin E was added as antioxidants to prevent lipid degradation during analysis. After 1 hour incubation in the dark, was added water (Clor/MeOH/H2O, 2:1:1 v/v/v) and the sample were incubated for another hour in the dark. Subsequently, samples were centrifuged at 1500 rpm for 1 hour at RT and the organic phase, containing lipids, was recovered. Total lipid extracts were dried in an evaporator and resuspended in methanol to HPLC/MS analysis.

2.6 Lipid Extraction from cell cultures

The mouse neuroblastoma N2a cell line and the 22L-Sc$^+$ infected with the mouse-adapted strains were seeded at density of 1x10^{5}cells/ml in T-75 flasks. After four day incubation at 37°C in a humidified 5% CO2 atmosphere, the sub-confluent cultures were trypsinized, washed twice in sterile PBS and centrifuged at 1300 rpm for ten minutes to eliminate all residual of growth medium containing fetal bovine serum. After two washes, pellets were resuspended in PBS and the cellular suspension was separed in two aliquots. After centrifugation, one pellet, corresponding approximately to 1 x 10^6 cells, was resuspended in 500 µl of NaOH to the total protein concentration determination by the bicinchoninic acid protein assay (Sigma) and the other pellet, corresponding approximately to 30-40 x 10^6 cells for the HPLC/MS analysis, and to 4 x 10^6 cells for the fluorometric-enzymatic assay, was collected and total lipids extracted by Folch method as described above. Total lipid extracts were dried in an evaporator and re-suspended in methanol for HPLC-MS analysis, or re-suspended in Reaction buffer for the florometric-enzymatic cholesterol assay.

2.7 Analysis of Cholesterol content, TC, FC and CE fractions in mouse brains and cell extracts by HPLC-MS

The cholesterol content was determined from total lipid extracts of Normal, 139A, 139A PRV mouse brains and N2a, 22L-Sc$^+$ cell extracts by HPLC-MS as reported previously (Banni et al).

Separation of total cholesterol (TC), and FC and CE fractions was carried out with an Agilent 1100 HPLC system (Agilent, Palo Alto, CA) equipped with a diode array detector. A C-18 Inertsil 5 ODS-2 Chrompack column, (Chrompack International BV, Middleburg, the Netherlands), 5 µm particle size, 150 . 4.6 mm. Thirty microliters of sample was injected onto a chromatographic column. The solvent program for elution was composed of 0.1% formic acid in water (solvent A) and 0.1% formic acid in acetonitrile (solvent B). FC were detected at …nm. Spectra (195-315 nm) of the eluates were obtained every 1.28 s and were electronically stored. CE fractions CE-14:0, CE-16:0,CE-18:1, CE-18:2, CE-18:3, CE-20:4, CE-22:6 were detected at …nm. Spectra (195-315 nm) of the eluate were obtained every 1.28 s and were electronically stored. These spectra were taken to confirm the identification of the HPLC peaks. MS analysis was performed using a quadrupole mass spectrometer (API3000; Applied Biosystems, Foster City, CA) equipped with a TurboIonSpray

ionization source. Each sample was duplicated in the assays and at least three independent experiments were performed.
The 24S-OH-Cholesterol content was determined from total lipid extracts of Normal, 139A and 139A PRV mouse brains by HPLC-MS as reported previously (Banni *et al*., 2004). The solvent program for elution was composed of 0.1% formic acid in water (solvent A) and 0.1% formic acid in acetonitrile (solvent B). The 24S-OH-Chol was detected at …nm. Spectra (195-315 nm) of the eluate were obtained every 1.28 s and were electronically stored. These spectra were taken to confirm the identification of the HPLC peaks. Each sample was duplicated in the assays and at least three independent experiments were performed.

2.10 Analysis of TC, FC and CE fractions in mouse brains and cell extracts by the fluorometric-enzymatic Amplex red method.
Cholesterol content in the brain tissue samples and cultured cells was evaluated by the fluorometric enzymatic method using the Amplex Red Cholesterol Assay kit (Invitrogen, Italy) according to the manufacturer's instructions with a minor modification as described (Xiong et al., 2008). In the Amplex Red Cholesterol Assay, cholesteryl esters are hydrolyzed by cholesterol esterase into cholesterol, which is then oxidized by cholesterol oxidase to yield H_2O_2 and the corresponding ketone product. The H_2O_2 is then detected using 10-acetyl-3,7-dihydroxyphenoxazine, a highly sensitive and stable probe for H_2O_2 that in the presence of horseradish peroxidase reacts with H_2O_2 with a 1:1 stoichiometry to produce highly fluorescent resorufin. The amounts of cholesterol esters are calculated by subtracting the amounts of free cholesterol in each sample from those of total cholesterol. Briefly, brain homogenates of Normal, 139A, 139A PRV mice and N2a, 22LN2a cell extracts were1:10 diluted with 1× cholesterol reaction buffer (0.1 M potassium phosphate, pH 7.4, 0.05 M NaCl, 5 mM cholic acid, 0.1% Triton X-100). Fifty microliter of 150 µM Amplex Red reagent, 1 U/ml horseradish peroxidase, 1 U/ml cholesterol oxidase and 1 U/ml cholesterol esterase were added to 50 µL sample in 96 well plates. After 60-min incubation in the dark at 37 °C, sample fluorescence was measured using a microplate reader (Victor 3V 1420 Multilabel Counter, Perkin Elmer) at 530/25 nm excitation and 590/35 nm emission wavelengths. The total cholesterol content of samples was determined by measuring the cholesterol concentration following digestion with cholesterol esterase. To measure free cholesterol, cholesterol esterase was omitted from the assay. Values obtained from a cholesterol standard curve were normalized to protein content measured by the bicinchoninic acid protein assay according to the manufacturer's instructions (Sigma, Italy). Each sample was triplicated in the assays and at least three independent experiments were performed.

2.11 Statistical analysis
All statistical comparisons were calculated using a two-way, unpaired Student's t-test or a one-way ANOVA and a Tukey- Kramer posthoc test when appropriate, using Instat II (Graphpad, San Diego, CA). Data analysis was done using the Student t-test. Statistical significance was assigned to $p < 0.05$. All values are expressed as the means of values ± standard error (SD).

3. RESULTS

3.8 Cholesterol analysis by HPLC-MS in 22L-infected vs. uninfected N2a cells
HPLC-MS analysis was adopted for its high sensitivity and selectivity as it allows simultaneous separation and quantification of several lipid classes. This method involves the fractionation of lipid classes by high-pressure liquid chromatography followed by qualitative/quantitative analysis of injected lipid extracts by mass spectrometry. The identification of chromatographic peaks is based on comparison of retention times of samples with those of reference standards. Table 1 shows the TC, FC and CE contents, normalized both to million of cells and to mg of protein, and the ratios of CE/TC and FC/TC expressed in percentages, in the infected vs. uninfected N2a cells.

Table 1. Content of TC, FC and CE levels in 22L-infected vs. uninfected N2a cells by HPLC-MS.

	Tot Cholesterol	Free Cholesterol	Cholesterol esters	CE/TC
	(ug/million cells)	(ug/million cells)	(ug/million cells)	%
N2a	4,52 ± 2,24	2,90 ± 1,27	1,62 ± 0,97	36
22L-Sc	6,63± 3,24	4,15 ± 2,05	2,48 ± 1,19	37
	(ug/mg protein)	(ug/mg protein)	(ug/mg protein)	%
N2a	6,47 ± 1,41	4,19 ± 0,65	2,28 ± 0,76	35
22L-Sc	9,58 ± 4,14	6,00 ± 2,63	3,59 ± 1,51	37

The table shows mean values ± SE of cholesterol content normalized to million of cells (top panel), and to mg of protein (below panel).

With respect to control N2a, 22L-infected cells showed higher content of TC, as well as of the FC and CE fractions: TC increased by 148%; FC increased by 143%; CE increased by 157%.
HPLC-MS analyses allowed us to also define the quali-quantitative modifications of the fatty acid (FA) fraction bond to the cholesterol moiety (CE-FA). As expected, compared to control cells, the prion-infected cultures showed also a higher content of the total FA-CE fraction (Table 2). Qualitatively, however, two FAs appeared more markedly modified: the palmithic acid (C16:0) increased from 0,30% to 2,07% (mean difference +1,77%), and the oleic acid (C18:1) that increased from 1,44% to 2,65% (mean difference +1,21%). Although less marked, increased contents were observed also for miristic acid (C14:0; from 0,91% to 1,43%); linoleic acid (C18:2; from 1,08% to 1,40%); α-linolenic acid (C18:3; from 0,74% to 0,98%); and docosaesaenoic acid (DHA) (C22:**6;** from 1% to 1,47%), while content of the arachidonic acid (C20:4) remained unchanged (Table 2 and Figure 1).

Table 2. CE Fat acids composition in 22L-infected vs. uninfected N2a cells by HPLC-MS

	CE-22:6	CE-18:3	CE-20:4	CE-18:2	CE-14:0	CE-18:1	CE-16:0
N2a	1,00%	0,74%	1,27%	1,08%	0,91%	1,44%	0,30%
22L-Sc	1,47%	0,98%	1,28%	1,40%	1,43%	2,65%	2,07%

Percent composition of Fas respect to total FA-CE fraction

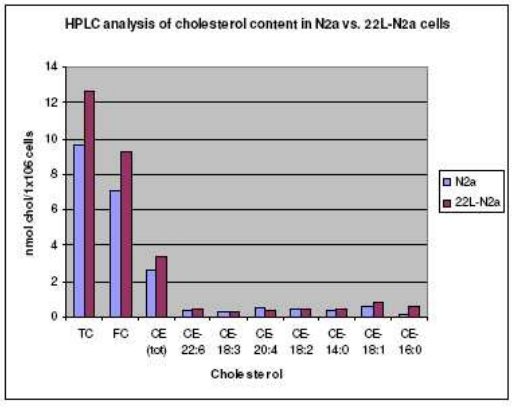

Figure 1. HPLC-MS analysis in 22L-infected vs. uninfected N2a cells. The bars represent the mean values ± SE of cholesterol content of three different cell preparations, normalized to million of cells.

3.11 Cholesterol analysis by a fluorometric enzymatic assay in 22L-infected vs. uninfected N2a cells.

Cholesterol measurements in 22L-infected vs. uninfected N2a cells by the Amplex Red cholesterol assay, produced different results depending on whether cholesterol values were normalized to million of cells or, rather, to mg of protein (Table 3; Figure 2A,B). Although in no case the data obtained were significative, mean values normalized to million of cells showed a slight increase of both TC and FC, and a marked increase of CE (+250%). On the contrary, normalization of cholesterol measures to mg of protein showed slight decreases of TC and FC, and an increase of CE (+125%). Although the variation of the CE fraction was confirmed by either types of normalization, it is worth mentioning that CE values are not directly determined as they are calculated by subtraction of the FC values from those of TC. Thus, in our opinion, these results cannot be considered reliable as they may be subjected to not irrelevant variations depending on even slight changes in the TC and/or FC values. As a matter of fact, out of the three cell pools analyzed by this method, one showed increased content of both TC and FC, one showed increased content of the FC fraction only, and one showed no variation of any cholesterol forms between the infected and uninfected N2a cells.

Table 3. Content of TC, FC and CE levels in 22L-infected vs. uninfected N2a cells by Fluorometric - enzymatic method

	Tot Cholesterol	Free Cholesterol	Cholesterol esters	CE/TC
	(ug/million cells)	(ug/million cells)	(ug/million cells)	%
N2a	2,08 ±0,11	2,04 ±0,01	0,04 ±0,08	2,0
22L-Sc	2,20 ±0,11	2,10 ±0,01*	0,10 ±0,11	4,7
	(ug/mg protein)	(ug/mg protein)	(ug/mg protein)	%
N2a	1,98 ± 0,11	1,94 ± 0,01	0,04 ± 0,07	2,0
22L-Sc	1,69 ± 0,08	1,61 ± 0,01*	0,05 ± 0,08	2,3

The table shows mean values ± SE of cholesterol content normalized to million of cells (top panel), and to mg of protein (below panel). *p < 0.05 versus N2a control group

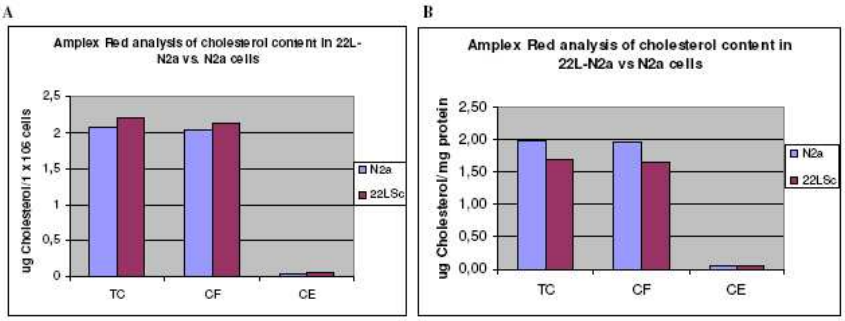

Figure 2. Amplex Red analysis in 22L-infected vs. uninfected N2a cells. The bars represent the mean values ± SE of TC, FC and CE content in three independent experiments, normalized to g of tissue (A) or to mg of protein (B).

3.1 Cholesterol analysis by HPLC-MS in brains of uninfected vs. 139A-infected, pravastatin treated or untreated, mice

HPLC-MS lipid analyses of brain homogenates from C57BL/6 mice infected with the 139A strain of scrapie, confirmed the data obtained in the N2a cell model by the same method, showing a significative enrichment of TC (+127-133%), FC (+122-129%) and CE (+168-177 %) contents in

the brains of the scrapie-ill mice, with respect to the mock-infected control mice (Table 4). With respect to control values, the increasing of CE fractions in brains of scrapie-infected mice were significative either with respect to absolute CE values ($p < 0.01$), and to the CE/TC ratio ($p < 0.05$). Figure 3 (A,B,C) shows the content of lipid subclasses in 139A-infected vs. control mouse brains. The bars represent the mean values of five control and four 139A-infected brains. shows the mean ± SE of the contents of TC, FC, and CE, normalized to both gram of tissue and mg of protein.
Consistent with the cholesterol lowering effect of statins, HPLC-MS analysis of brains from infected mice treated with pravastatin (PRV; 200 mg/ kg bw/day) [Vetrugno et al ., 2009], showed a significative ($p<0.05$) decrease of the FC (77-76%) content, accompanied by a moderate, although not significative reduction of TC (86-84%) (Table 4 and Figure 3D). Unexpectedly, PRV treatment appeared to determine a parallel increase of the CE level (+146-144%), whose CE/TC ratio in PRV-treated vs. untreated 139A-infected mice was highly significative ($p<0.005$).

Table 4. Content of TC, FC, CE in brains of uninfected vs. 139A-infected, pravastatin treated or untreated mice by HPLC-MS.

	Tot Cholesterol	Free Cholesterol	Cholesterol esters	CE/TC
	(mg/g tissue)	(mg/g tissue)	(mg/g tissue)	%
Normal (n = 5)	4,81 ± 0,78	4,37 ± 0,67	0,74 ± 0,2	15
139A (n = 4)	6,06 ± 0,67*	5,31 ± 0,65	1,24 ±0,21**	20*
139A PRV (n = 4)	5,19 ± 0,73	4,10 ± 0,52*	1,81 ± 0,43	35***
	(ug/mg protein)	(ug/mg protein)	(ug/mg protein)	%
Normal (n = 5)	32,51 ± 5,49	29,51 ± 4,70	4,99 ± 1,47	15
139A (n = 4)	43,36 ± 5,37*	38,03 ± 5,27*	8,85 ±1,22***	21*
139A PRV (n = 4)	36,53 ± 5,07	28,84 ± 3,32*	12,77 ± 3,25	35***

The table shows mean values ± SE of cholesterol content normalized to g of tissue (top panel), and to mg of protein (below panel). *p < 0.05 and p** < 0.01 and p***< 0.005 versus Normal control group; *p < 0.05 and p***< 0.005 versus 139A-infected untreated mice control group

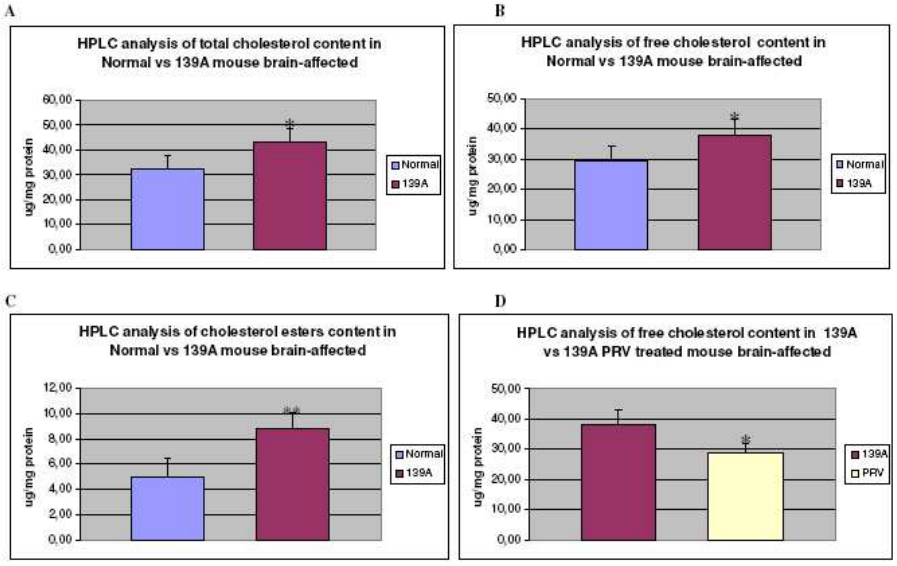

Figure 3. HPLC-MS analysis in brains of uninfected vs. 139A-infected, pravastatin treated or untreated, mice:
(A) shows total cholesterol content in brains from uninfected vs. 139A-infected mice, normalized to mg of protein. The bars represent the mean values ± SE of cholesterol content in 5 Normal and four 139A infected brains,*$p < 0.05$ versus Normal control group; (B) shows free cholesterol content in brains from uninfected vs. 139A-infected mice, *$p < 0.05$ versus Normal control group; (C) shows cholesterol esters content in brains from uninfected vs. 139A-infected mice, ***$p < 0.005$ versus Normal control group; (D) shows free cholesterol content in brains from 139A-infected, pravastatin treated or untreated mice. The bars represent the mean values ± SE of cholesterol content in four 139A infected untreated mice and four 139A infected pravastatin treated mice,*$p < 0.05$ versus 139A-infected untreated mice control group.

3.7 Cholesterol analysis by a fluorometric-enzymatic method in brains of uninfected vs. 139A-infected, pravastatin treated or untreated, mice

Similarly to the results obtained in the N2a model, the analysis and quantification of TC, FC and CE in the mouse scrapie model by the Amplex red cholesterol assay resulted in no reproducible cholesterol variations between scrapie-infected and control brain homogenates (Table 5 and Figure 4 A,B). No modifications of the TC and FC contents were observed in brains of PRV-treated infected mice. Again, the only exception was the calculated CE content, whose increase resulted highly significative ($p<0.005$). As already stated for the CE data obtained in N2a cells by the enzymatic method, brain CE values are not directly determined; thus, although no great variations of TC and FC absolute values were detected within triplicates of each sample, as well as among samples of homogenous mouse groups, they may be sufficient to perceive relevant changes of the CE content.

Table 5. Content of TC, FC, CE in brains of uninfected vs. 139A-infected, pravastatin treated or untreated, mice by Fluorometric - enzymatic method.

	Tot Cholesterol	Free Cholesterol	Cholesterol esters	CE/TC
	(mg/g tissue)	(mg/g tissue)	(mg/g tissue)	%
Normal (n = 5)	7,46 ± 0,23	7,43 ± 0,26	0,06 ± 0,09	0,8
139A (n = 4)	7,01 ± 0,31	6,98 ± 0,38	0,13 ± 0,14	1,2
139A PRV (n = 4)	7,24 ± 0,18	6,86 ± 0,23	0,28 ± 0,01	3,9
	(ug/mg protein)	(ug/mg protein)	(ug/mg protein)	%
Normal (n = 5)	50,38 ± 2,12	50,25 ± 1,92	0,63 ± 0,94	2,10
139A (n = 4)	52,06 ± 3,79	51,77 ± 4,22	0,59 ± 0,80	2,20
139A PRV (n = 4)	51,11 ± 4,72	48,48 ± 4,82	2,64 ± 0,27**	5,16*

The table shows mean values ± SE of cholesterol content normalized to g of tissue (top panel), and to mg of protein (below panel). p** < 0.005 versus 139A-infected untreated mice control group.

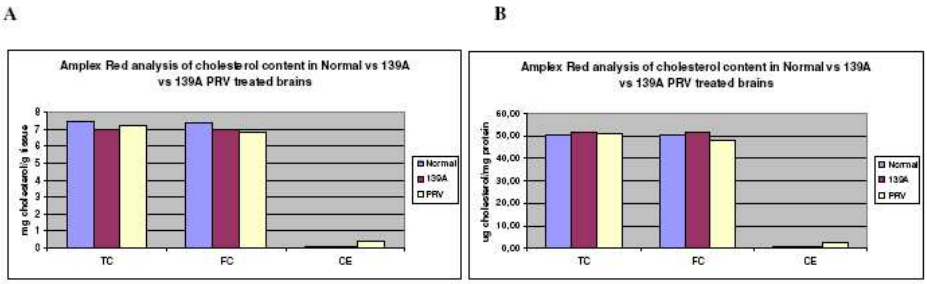

Figure 4. Amplex Red analysis in brains of uninfected vs. 139A-infected, pravastatin treated or untreated, mice. The bars represent the mean values ± SE of cholesterol content in 5 Normal and four 139A infected and four 139A infected pravastatin treated brains, normalized to g of tissue (A) or to mg of protein (B).

4. DISCUSSION

Contrarily to other body tissues, brain cholesterol appears to come entirely from cellular de novo synthesis. In neurons, cholesterol is essentially all in the un-esterified form (FC) (Xie *et al.*, 2003) as its excess, rather than being esterified to free fatty acids (CE) and stored in cytoplasmic lipid droplets, it is converted into 24*S*-hydroxycholesterol, the cholesterol form able to cross the blood-brain barrier and leave CNS through the bloodstream (Björkhem et al., 1998). Although it seems established that brain cholesterol modifications play an important role in the PrPsc generation, two alternative and opposite scenarios involving disturbance of the cholesterol-rich raft domains describe the role of cholesterol in the pathogenesis of PrD. The high membrane cholesterol model implies that cholesterol enrichment would favour contact between PrP and misfolded PrPsc isoforms, by triggering the raft-clustering process, while the low membrane cholesterol model claims that undesired amyloidogenic protein-protein interactions are favoured by raft disassembly caused by cholesterol depletion (Simons et al 2002). After more than a decade of investigations in cell-based and *in vivo* models of PrD, no conclusive and unequivocal answer is yet available. Beside the overall complexity of the prion biology, technical limitations of the methods used for accurate cholesterol measurements may have hampered the definition of this particular aspect. Our results showed that, with respect to controls, significative cholesterol variations in the prion-infected cells and tissues could be reproducibly seized by HPLC-MS analyses only. By this method, we were able to confirm the findings previously obtained in prion-infected N2a cells and in brains of ovine affected sheep by several methodological approaches (Orrù *et al.*, 2010), that are: neutral lipid stain (i.e. Oil Red O), fluorescent cholesterol probes (i.e. Nile red and filippin), TLC lipid separation, and labelled cholesterol and cholesterol ester precursors (i.e. ^{14}C-acetate and ^{14}C-oleate). HPLC-MS study of cholesterol changes in prion-infected mouse brains and neuronal cells showed in fact major cholesterol modifications with significative increases of the total cholesterol content, as well as of both the FC and CE pools. Also in agreement with our previous findings, HPLC-MS analysis of lipid extracts from prion-infected mouse brains and N2a cells, indicated that the most significantly changed cholesterol form following prion infection was represented by the CE fraction (Pani *et al.*, 2007; Orrù *et al.*, 2010). Consistent with an increased CE pool, HPLC-MS analyses of prion-infected vs. uninfected N2a cell extracts, highlighted an increased content of the fatty acid (FA) fraction. Palmithic, oleic, and miristic acids were the most dramatically FA increased in the CE pool, while the polyunsaturated linoleic, α-linolenic and docosaesaenoic (DHA) acids were only slightly increased, and arachidonate remained unchanged.

In contrast with HPLC-MS data, the fluorometric enzymatic cholesterol measurements did not allow us to define a clear cut picture of the cholesterol modifications following in vitro and in vivo prion infection. In our hands, cholesterol determinations showed in fact variability, either among brain samples within otherwise homogeneous mice groups (i.e. control; scrapie-infected; scrapie-infected and PRV-treated), and among the different cell preparations of prion-infected and uninfected N2a cells. In our opinion, these results may be due to the intrinsic limitation of the enzymatic-based method that, although very sensitive among the available fluorescent probes for the enzymatic determination of H_2O_2 (Drake *et al.*, 1999), it is probably not suitable to reproducibly measure the content of different intracellular cholesterol forms starting from too small amount of samples, and to appreciate their proportional variations in different samples, especially with respect to changes in the CE fraction. As above mentioned, in the normal brain, CE is present, if any, only in traces; therefore methods that allow direct and sensitive determination of the CE content is required to appreciate its variation.

Concerning the yet unclear relationship between the beneficial effect of statins in experimental mouse scrapie and their lowering effect on cerebral cholesterol, our HPLC-MS analysis in 139A-infected C57BL/6 mice treated with PRV showed a significative reduction of the FC levels, but not of those of TC. Somehow unexpectedly, a parallel increase of the CE fraction was also observed. Although the CE content variations were moderate in terms of absolute values, the calculated

CE/TC percentage ratio in the PRV-treated vs. untreated 139A-infected mice was highly significative ($p<0.005$). Kirsch and colleagues reported that lovastatin and simvastatin slightly enhanced CE levels, and suggested that these statins shuttle free plasma membrane cholesterol (FC) to the CE pool, possibly via an ER cycling route (Liscum *et al.*, 1992), and that net cholesterol levels across the membrane may remain unchanged under statin treatment as free cholesterol and its esters build up a dynamic equilibrium (Liscum *et al.*, 1992; Simons *et al.*, 2000). This may explain why we showed that PRV treatment affected FC but not TC levels.

5. Conclusions

Altogether our data on cholesterol modifications in the brains of scrapie-affected mice and in prion-infected neuronal cells confirm that prion diseases are associated with an altered arrangement of cholesterol metabolism leading to increased cellular pools of both free and esterified cholesterol, and aware on the central importance of the analytical methods chosen to discriminate and measure the different cholesterol intracellular forms. Above all, our results support previous indications that re-engineering cholesterol homeostasis with drug cocktails which simultaneously target the altered metabolic pathways could represent a more successful approach to treatment/prevention of prion disorders.

Acknowledgements

This study was supported by funds of the Regione Autonoma of the Sardinian Region and of the Sardinian Bank Foundation. Authors wish to thank Mrs. Angelina Valanzano for her excellent technical assistance in the in vivo experiments.

References

Aguzzi A, Polymenidou M. Mammalian prion biology: one century of evolving concepts. Cell, 2004, 116:313–327

Akhlaq A. Farooqui, Lloyd A. Horrocks. Glycerophospholipids in the brain: phospholipases A2 in Neurological Disorders Springer 2007

Anuna Johnson, Eckert L. N., Keller G. P, Igbavboa J. H, Franke U., Fechner C., Schubert-Zsilavecz T., Karas M., Muller M., W. E. & Wood, W. G. Chronic administration of statins alters multiple gene expression patterns in mouse cerebral cortex. J Pharmacol Exp Ther 2005,312, 786–793.

Arispe N, Doh M. Plasma membrane cholesterol controls the cytotoxicity of Alzheimer's disease AßP (1–40) and (1–42) peptides. FASEB J 2002; 16: 1526-1536.

Bach, C.; Gilch S.; Rost R, *et al.* Prion-induced activation of cholesterogenic gene expression by SREBP2 in neuronal cells. J Biol Chem 2009; 284: 31260-31269]

Banni S, Petroni A, Blasevich M, Carta G, Angioni E, Murru E, Day BW, Melis MP, Spada S, Ip C. Detection of conjugated C16 PUFAs in rat tissues as possible partial beta-oxidation products of naturally occurring conjugated linoleic acid and its metabolites. Biochim Biophys Acta. 2004 Jun 1;1682(1-3):120-7.

Bate C, Salmona M, Diomede L, Williams A. Squalestatin cures prion-infected neurons and protects against prion neurotoxicity. J Biol Chem 2004; 279: 14983–14990

Bate C, Rumbold L, Williams A. Cholesterol synthesis inhibitors protect against platelet-activating factor-induced neuronal damage. J Neuroinflam 2007, 4:5. Doi:10.1186/1742-2094-4-5;

Bate C., Tayebi M., Williams A. Cholesterol esterification reduces the neurotoxicity of prions. Neuropharmacology 54, 2008 1247–1253

Bate B, Tayebi M, Williams A. Sequestration of free cholesterol in cell membranes by prions correlates with cytoplasmic phospholipase A2 activation. BMC Biol 2008; 6: 8. Doi:10.1186/1741-7007-6-8

Bate Clive, Mourad Tayebi, Salmona Mario, Diomede Luisa, Williams Alun. Polyunsaturated Fatty Acids Protect Against Prion-Mediated Synapse Damage In Vitro Neurotox Res (2010) 17:203–214DOI 10.1007/s12640-009-9093-2

Björkhem, I., D. Lütjohann, U. Diczfalusy, L. Ståhle, G. Ahlborg, and J. Wahren. Cholesterol homeostasis in the human brain: turnover of 24S-hydroxycholesterol and evidence for a cerebral origin of most of this oxysterol in the circulation. *J. Lipid Res.* 1998, **39:** 594–600.

Borchelt, D.R., Scott, M., Taraboulos, A., Stahl, N., and Prusiner, S.B. Scrapie and cellular prion protein differ in their kinetics of synthesis and topology in cultured cells. J. Cell Biol. 1990; *110*, 743–752.

Bretillon, L., A. Siden, L. O. Wahlund, D. Lutjohann, L. Minthon, M. Crisby, J. Hillert, C. G. Groth, U. Diczfalusy, and I. Bjorkhem.. Plasma levels of 24S-hydroxycholesterol in patients with neurological diseases. *Neurosci. Lett.* 2000, **293:** 87–90.

Caughey, B., Race, R.E., Ernst, D., Buchmeier, M.J., and Chesebro, B. (1989).Prion protein biosynthesis in scrapie-infected and uninfected neuroblastoma cells. J. Virol. *63*, 175–181.

Caughey, B., and Raymond, G.J. (1991). The scrapie-associated form of PrP is made from a cell surface precursor that is both protease- and phospholipasesensitive. J. Biol. Chem. *266*, 18217–18223.

Cheng, X., Maher, J., Chen, C. & Klaassen, C. D. Tissue distribution and ontogeny of mouse organic anion transporting polypeptides (Oatps). Drug Metab Dispos 2005, 33, 1062–1073.

Drake M. Amundson, Mingjie Zhou. Fluorometric method for the enzymatic determination of cholesterol J. Biochem. Biophys. Methods 38 (1999) 43–52

Evers, R. & Chu, X. (). Role of the murine organic anion transporting polypeptide 1b2 (Oatp1b2) in drug disposition and hepatotoxicity. Mol Pharmacol 2008, 74, 309–311.

Farkas et al., 2000; Kitajka et al 2002; Sampath and Ntambi, 2005

Farooqui A. A., Liss L., and Horrocks L. A. (1988) Neurochemical aspects of Alzheimer's disease: involvement of membrane phospholipids. *Metab. Brain Dis.* **3,** 19—35

Farooqui AA, Horrocks LA, Farooqui T. Deacylation reacylation of neural membrane glycerophospholipids. J Mol Neurosci 200014:123–135

Flechsig E (2002) Transmission of prions. J Infect Dis 186(Suppl 2):S157–S165; 3.

Folch J., Lees M., Sloane-Stanley G.H., A simple method for the isolation and purification of total lipid from animal tissues, J. Biol.Chem. 226 (1957) 497–509.

Ghaemmaghami S, Phuan PW, Perkins B, *et al*. Cell division modulates prion accumulation in cultured cells. Proc Natl Acad Sci USA 2007; 104: 17971-17976

Gilch, S., Kehler, C. & Schatzl, H. M.. Prion protein requires cholesterol for cell surface localization. Mol Cell Neurosci 2006, 31, 346–353

Haviv, Y., Avrahami, D., Ovadia, H., Ben-Hur, T., Gabizon, R. & Sharon, R. Induced neuroprotection independently from PrPSc accumulation in a mouse model for prion disease treated with simvastatin. Arch Neurol 200865, 762–775.

Huaqi Xiong, Debbie Callaghan, Aimee Jones, Douglas G. Walker, Lih-Fen Lue, Thomas G. Beach, Lucia I. Sue, John Woulfe, Huaxi Xu, Danica B. Stanimirovic, and Wandong Zhang. Cholesterol retention in Alzheimer's brain is responsible for high β- and γ-secretase activities and Aβ production. Neurobiology of Disease 29 (2008) 422–437

Hwang D, Lee IY, Yoo H, *et al*. A systems approach to prion disease. Mol Syst Biol 2009; 5:252. Doi:10.1038/msb.2009.10

Kempster S, Bate C, Williams A. Simvastatin treatment prolongs the survival of scrapie-infected mice. Neuroreport 2006; 18: 479-482

Kikuchi, R., Kusuhara, H., Abe, T., Endou, H. & Sugiyama, Y. Involvement of multiple transporters in the efflux of 3-hydroxy-3-methylglutaryl–CoA reductase inhibitors across the blood–brain barrier. J Pharmacol Exp Ther 2004, 311, 1147–1153.

Kirsch, C., Eckert, G. P. & Mueller, W. E. (2003). Statin effects on cholesterol micro-domains in brain plasma membranes. Biochem Pharmacol 65, 843–856

Koudinov AL, Koudinova NV. Cholesterol homeostasis failure as a unifying cause of synaptic degeneration. J Neurol Sci 2005; 229: 233-240.

Liscum L., Dahal NK. Intracellular cholesterol transport. *J.Lipid Res,* 1992. 33**:** 1239–1254.

Ma DWL, Seo J, Switzer KC, Fan YY, McMurray DN, Lupton JR, Chapkin RS .n-3 PUFA and membrane microdomains: a new frontier in bioactive lipid research. J Nutri Biochem 2004; 15:700–706

Mason R. P., Shoemaker W. J., Shajenko L., Chambers T. E., and Herbette L. G. Evidence for changes in the Alzheimer's disease brain cortical membrane structure mediated by cholesterol. *Neurobiol. Aging* 1992, 13, 413—419.

Mattson MP. Impairment of membrane transport and signal transduction systems by amyloidogenic proteins. Methods Enzymol 1999; 309: 733-768.

Michael C. Irizarry The American Society for Experimental NeuroTherapeutics, Inc Vol. 1, 226–234, April 2004 ©.
Mok SW, Thelen KM, Riemer C, *et al*. Simvastatin prolongs survival times in prion infections of the central nervous system. Biochem Biophys Res Commun 2006; 348: 697–702;.

Naslavsky N, Stein R, Yanai A, Friedlander G, Taraboulos A (1997) Characterization of detergent-insoluble complexes containing the cellular prion protein and its scrapie isoform. J BiolChem 272:6324–6331.

Nezasa, K., Higaki, K., Takeuchi, M., Nakano, M. & Koike, M. Uptake of rosuvastatin by isolated rat hepatocytes: comparison with pravastatin. Xenobiotica 2003; 33, 379–388.

Nyalala John O, Wang Jiang, Dang An,. Faas Fred H, Smith W. Grady. Hypertriglyceridemia and hypercholesterolemia: Effects of drug treatment on fatty acid composition of plasma lipids and membranes. Prostaglandins, Leukotrienes and Essential Fatty Acids April 2008 (Vol. 78, Issue 4, Pages 271-280)

Orrù CD, Cannas MD, Vascellari S, *et al. In vitro* synergistic antiprion effect of cholesterol ester modulators in combination with chlorpromazine and quinacrine. Cent Eur J Biol 2010; 5: 151-165.

R, Lober S, Kujala P, *et al.* Tricyclic antidepressants, quinacrine and a novel, synthetic chimera thereof clear prions by destabilizing detergent-resistant membrane compartments. JNeurochem 2006; 98: 748-759

Pani A, Dessì S. Cell growth and cholesterol esters. New York: Kluwer Academic/Plenum Publisher 2004

Pani A., Norfo C., Abete C., Mulas C., Putzolu M., Laconi S., et al., Accumulation of Cholesterol Esters in ex vivo Lymphocytes from Scrapie-susceptible Sheep and in Scrapie-infected Mouse Neuroblastoma Cell Lines, Am. J. Infec. Dis., 2007, 3, 165-168

Pani A, Norfo C, Abete C, *et al.* Anti-prion activity of cholesterol esterification modulators: a comparative study in ex vivo sheep fibroblasts and lymphocytes and in mouse neuroblastoma cell lines. Antimicrob Agents Chemother 2007; 51: 4141-4147.

Papassotiropoulos A, Lutjohann D, Bagli M, Locatelli S, Jessen F, Buschfort R et al. 24S-hydroxycholesterol in cerebrospinal fluid is elevated in early stages of dementia. *J Psychiatr Res* 36:27–32, 2002;

Prusiner SB. Prions. Proc Natl Acad Sci USA 1998, 95:13363–13383; 2. Weissmann C, Enari M, Klohn PC, Rossi D,

Prusiner, S.B., Scott, M.R., deArmond, S.J., and Cohen, F.E. (1998). Prion protein biology. Cell *93*, 337–348.

Sabine Gilch Æ Christian Bach Æ Gloria Lutzny Æ Ina Vorberg Æ Hermann M. Scha¨tzl;Inhibition of cholesterol recycling impairs cellular PrPSc propagation; Cell. Mol. Life Sci. (2009) 66:3979–3991)

Schonknecht P, Lutjohann D, Pantel J, Bardenheuer H, Hartmann T, von Bergmann K et al. Cerebrospinal fluid 24S-hydroxycholesterol is increased in patients with Alzheimer's disease compared to healthy controls. *Neurosci Lett* 324:83–85, 2002

Sim VL, Caughey B. Recent advances in prion chemotherapeutics.Infect Dis Drug Targets 2009; 9: 81-91. Klingenstein

Simons K., Ikonem E. How cells handle cholesterol Scince 2000; 290:1721-6

Simons K, Ehehalt R. Cholesterol, lipid rafts, and disease. J Clin Invest 2002; 110: 597-603.]

Sjögren M, Mielke M, Gustafson D, Zandi P, Skoog I. Cholesterol and Alzheimer's disease–is there a relation? Mech Ageing Dev 2006;127:138–147.

Soderberg M., Edlund C., Kristensson K., and Dallner G. Fatty acid composition of brain phospholipids in aging and in Alzheimer's disease. *Lipids* 1991, 26, 42 1—425.

Soderberg M., Edlund C., Alafuzoff I., Kristensson K., and Dallner G. Lipid composition in different regions of the brain in Alzheimer's disease/senile dementia of Alzheimer's type. *J. Neurochem.* 1992, **59,** 1646—1653.

Stefani M. Generic cell dysfunction in neurodegenerative disorders: role of surfaces in early protein misfolding, aggregation, and aggregate cytotoxicity. Neuroscientist 2007; 13: 519-531.

Stefani M, Liguri G. Cholesterol in Alzheimer's Disease:Unresolved Questions. Curr Alzh Res 2009; 6: 15-29.

Stillwell W and Wassall SR. Docosahexaenoic Acid: Membrane Properties of a Unique Fatty Acid. Chemistry &Physics &Lipids 2003, 126, 1-27.

Taraboulos, A., Scott, M., Semenov, A., Avrahami, D., Laszlo, L., Prusiner, S.B., Avraham, D.,. Cholesterol depletion and modification of COOH-terminal targeting sequence of the prion protein inhibit formation of the scrapie isoform. J. Cell Biol. 1995, 129, 121– 132.)

Thelen, K. M., Rentsch, K. M., Gutteck, U., Heverin, M., Olin, M., Andersson, U., von Eckardstein, A., Bjo¨ rkhem, I. & Lu¨ tjohann, D. Brain cholesterol synthesis in mice is affected by high dose of simvastatin but not of pravastatin. J Pharmacol Exp Ther 2006; 316, 1146–1152.

Vetrugno V, Cardinale A, Filesi I, Mattei S, Sy MS, Pocchiari M, Biocca S. KDEL-tagged anti-prion intrabodies impair PrP lysosomal degradation and inhibit scrapie infectivityBiochem Biophys Res Commun. 2005 Dec 30;338(4):1791-7.

Vetrugno Vito, Angelo Di Bari Michele, Nonno Romolo, Puopolo Maria, D'Agostino Claudia, Pirisinu Laura, Pocchiari Maurizio and Agrimi Umberto. Oral pravastatin prolongs survival time of scrapie infectedmice. Journal of General Virology (2009), 90, 1775–1780, DOI 10.1099/vir.0.009936-0.

Vey M, Pilkuhn S, Wille H, Nixon R, Dearmond SJ, Smart EJ,Anderson RG, Taraboulos A, Prusiner SB (1996) Subcellular colocalization of the cellular and scrapie prion proteins in caveolae-like membranous domains. Proc Natl Acad Sci USA93:14945–14949; 5

Weissmann C, Enari M, Klohn PC, Rossi D, Flechsig E. Transmission of prions. J Infect Dis, 2002, 186(Suppl 2):S157–S165; 3.

Xie, C., E. G. Lund, S. D. Turley, D. W. Russell, and J. M. Dietschy. Quantitation of two pathways for cholesterol excretion from the brain in normal mice and mice with neurodegeneration. *J.Lipid Res,* 2003. **44:** 1780–1789.

2.1.5 GENERAL CONCLUSIONS OF THE STUDIES ON CHOLESTEROL CHANGES IN PRION INFECTION

In conclusion, our studies on the role of cholesterol in the pathogenesis of prion disorders in different *in vitro*, *ex vivo*, and *in vivo* models, highlighted the presence of metabolic lipid alterations associated with prion infection, involving changes in the content and distribution of the different pools of cellular cholesterol (i.e. free cholesterol and cholesterol esters), as well as of other cellular lipids, including phospholipids and triglycerides. Higher CE pool was observed in brains and skin fibroblasts of healthy sheep with a scrapie susceptible prion genotype compared to sheep carrying a scrapie-resistant prion genotype, opening the possibility of a link between cellular prion polymorphism(s) and cholesterol homeostasis regulation. In addition, we showed increased ACAT1 expression in skin fibroblasts from scrapie-affected and scrapie-susceptible sheep. In prion- infected N2a cells, we found increased content and altered distribution of FC, TG, phospholipids and CE, which were not organized in LDs. In the infected N2a cultures, analysis of the CE-Fatty acid composition showed, with the only exception of Arachidonate, an increase of the amounts of each fatty acid of the CE-FA fraction. In addition, N2a cell treatments with combinations of various cholesterol interfering drugs showed synergic anti-prion effects, apparently by restoring cholesterol homeostasis in the prion- infected cells. In our hands, in agreement with the results in *in vitro* and *ex vivo* prion models, we have shown that also prion-affected mouse brains were characterized by an altered cholesterol metabolic profile associated with increased TC, FC and CE levels, and that pravastatin treatment determined significative reduction of the free cholesterol, an increase of the cholesterol ester, while total cholesterol remained unchanged.

On the basis of these data, we propose a mechanism by which cholesterol may influence protein misfolding and amyloid generation (Figura 11). It is well known that cells are normally protected from the accumulation of potentially toxic FC excess by ACAT-1–mediated esterification and by cholesterol efflux. Stored CE do not usually exceed the nCEH capacity to re-hydrolize CE to FC and to recycle FC back to PM. In the brain, excess FC is then converted to the efflux form of cholesterol (24S-hydroxy-cholesterol) that cross BBB and enter the blood stream. Therefore, failure of one or more of these homeostatic mechanisms, possibly caused by genetic and/or environmental factors, may be responsible for the altered cholesterol distribution found in protein misfolding-affected cells. One consequence of this is a slowing of the transportation of cellular FC to the PM that, over time, may lead to lipid raft disassembly. These events may favour interaction between PrPc and PrPsc, inducing structural conversion of the normal PrPc into amyloidogenic PrPsc, which is widely reported to trigger pathological events.

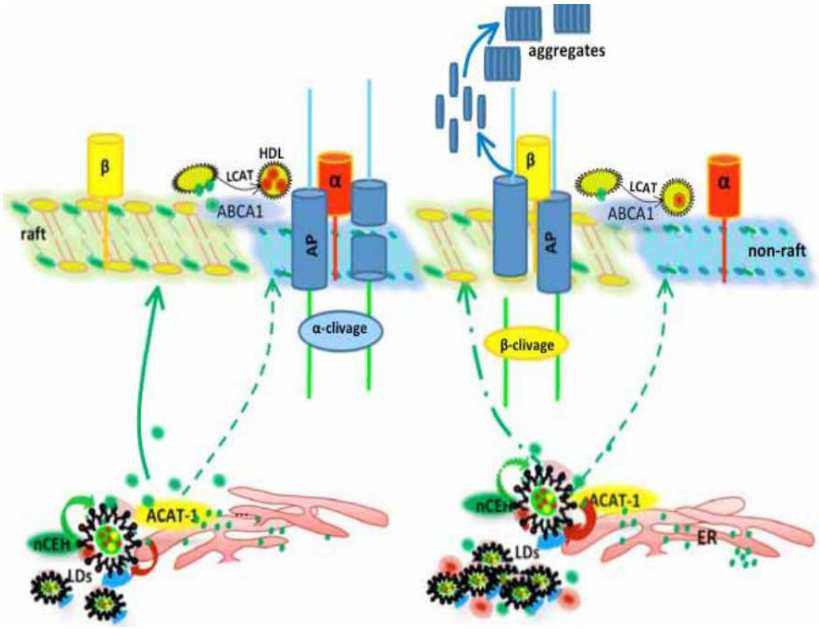

Figure. 11. Proposed cholesterol network modifications influencing protein misfolding and amyloid generation.

According to this model, the use of multitarget therapeutic strategies, aimed at re-establishing right cholesterol amounts and their differential distribution in PM microdomains, could represent a more successful approach than monotherapy-based treatments for the prevention/treatment of misfolding disorders.

2.1.6 FUTURE OBJECTIVES

I will compare the quali-quantitative analysis of intracellular lipids (by HPLC and NMR) in the various models (sheep brains and N2a cells), either untreated and treated with modulators of esterification (i.e. everolimus), both alone and in combination one with another, as well as with chlorpromazine and quinacrine.

In addition to these studies, I will focus on the evaluation and characterization lipid alterations that are related to different polymorphisms of the prion protein and likely associated to progression of infection (pre-clinical, initial and terminal illness stage) by NMR and TLC analysis, both in the CNS and in peripheral cells, in a natural model of prion disease such as scrapie in sheep that is endemic in our Region.

2.2 CHAPTER II

STUDY OF SOLUBLE INFECTIVITY FROM SCRAPIE-INFECTED HAMSTER BRAIN

2.2.1 INTRODUCTION

Despite TSEs (transmissible spongiform encephalopathies), such as CJD (Creutzfeldt–Jakob disease), are relatively rare but have received much attention in recent years because of the potential number of individuals in the U.K. affected following the epidemic of BSE (bovine spongiform encephalopathy). A major issue of current concerns is that blood donors may be subclinically infected with the BSE agent and could potentially transmit variant CJD through blood transfusion to healthy individuals. (Llewelyn *et al*., 2004; Peden *et al*., 2004).

Currently, efforts are directed, on one side, toward the development of tests capable of detecting infectivity in asymptomatic individuals (i.e. PMCA, QUIC), and on the other, toward the development procedures (e.g, leucodepletion; nanofiltration; depth filtrations; chromatography; NaPTA, trichloroacetic acid , polyanions precipitation), able to remove or inactivate prions from blood components or plasmaderived products with brain fractions of transmissible spongiform encephalopathy (TSE)-infected rodents as spiking materials. These spiking materials (e.g.,brain homogenates, microsomal fraction, caveolae-like domains, purified PrPsc), however, are loaded with pathological prion protein (PrP TSE) aggregates that are likely not associated with blood infectivity. The presence of these aggregates may invalidate these studies. In this contest, recently, Pocchiari's research group has developed a simple and fast method to prepare a soluble infectious material, containing small amounts of PrPTSE from hamster brains infected with the scrapie strain 263k (V. Berardi, F Cardone ., Valanzano A., Lu M, Pocchiari M., Transfusion, 2006). This fraction, called SHS (high speed supernatant), is virtually free from PrPTSE in aggregate form and contains only small amounts of PrPTSE in soluble form. In this regard, the SHS fraction can therefore be an excellent material for endogenous spiking of human blood in validation experiments aimed at demonstrating procedures to remove or inactivate TSE infectious agents.

On these premises, the experimental activity during the first year of my PhD, in the Department of Clinica, Diagnostica e Terapia delle Malattie Neurodegenerative del Sistema Nervoso Centrale"(ISS, Rome) directed by Professor Maurizio Pocchiari, was focused on the studies on characterization of the infectivity soluble from scrapie-adapted hamster's brain homogenates.

I compared two different extraction methods to precipitate the PrP pathological: streptomycin extraction method and ultracentrifugation in the presence of denaturing detergent Sarkosyl. Subsequently, to evaluate the presence of PK-sensitive isoform in the SHS fraction, the SHS

fraction was subjected to digestion with thermolysin, a thermostable neutral metalloproteinase enzyme, which preserve both PK-sensitive and PK-resistant isoforms of disease related PrP. In addition, I have also acquired experience in the handlling of highly infectious brain tissue in a containment facility of class III; in the biochemical methods utilised for the purification and characterization of PrPres from affected tissues; and with the histological techniques aimed to verify the amount and distribution of neurological injury in affected individuals. Finally, I have gained experience on procedures relaying: animal restraint; intraperitoneal anesthesia, and intracerebral inoculation with brain homogenates experimentally infected with scrapie; sampling of the major organs within the accumulation of pathogenic prion protein.

2.2.2 MATERIALS AND METHODS

2.2.2.1 Preparation of 263K brain homogenates

Scrapie-adapted (i.e. 263K prion) hamsters brain tissues were homogenized in nine volumes (10% w/v) of lysis buffer (100 mM NaCl, 10 mM EDTA, 0.5%, Nonidet P40, 0.5% w/v sodium deoxycholate, 10 mM Tris HCl, pH 7.4) and then brain homogenates were dispersed by sonication pulses (Vibra Cell, Sonics & Materials Inc., Newtown, CT) while kept on ice. Scrapie-adapted hamster's brain homogenates were clarified at 1000 × *g* for 10 minutes at 4°C ( ). The supernatants were used as PrP^{Sc} stock sample for deposition on SDS-PAGE.

2.2.2.2 Western blot measurement by ECL chemiluminescence detection

The supernatant were thawed and treated for 60 minutes at 37 ° C with proteinase K (PK; Sigma Chemical Co., St. Louis, MO) at a final enzyme concentration of 50 μ g per mL. The digestion was stopped by adding protease inhibitors (Complete, Roche Diagnostics GmbH Roche Applied Science, Mannheim, Germany) in accordance with the manufacturer's instruction. After PK treatment, the samples were serially diluted in half-log steps in NuPAGE gel loading buffer, boiled for 10 minutes in a water bath, and electrophoresed on 12 percent NuPAGE Bis-Tris gels (Invitrogen Corp., Carlsbad, CA) for 60 minutes at 125 V. The nitrocellulose membrane (Hybond ECL, Amersham Biosciences Europe GmbH, Freiburg, Germany) was soaked in Towbin transfer buffer for 5 minutes before "sandwich" assembly and semidry transfer for 60 minutes at 125 mA at 4 ° C. The membrane was blocked for 60 minutes at 37 ° C in 5 percent nonfat dry milk (Bio-Rad, Hercules, CA), dissolved in Tris-buffered saline (pH 8) with 0.05 percent Tween 20 (TBST), and incubated overnight at 4 ° C with 3F4 monoclonal anti-hamster 27- to 30-kDa fragment of protease-resistant prion protein (PrP 27-30) antibody 16 (provided by H. Diringer) diluted 1:1000 in TBST. The membrane was rinsed with TBST (five changes of solution in 25 min), incubated for 120 minutes at 37°C with an HRP antimouse (Amersham) diluted at 1:3000 in TBST, and rinsed again. Bands were revealed by the ECL chemiluminescence detection kit (Santa Cruz) andrecorded onto sensitive films (Hyperfilm ECL, Amersham)

2.2.2.3 Western blot measurement by CDP-star chemiluminescence detection

The supernatant were thawed and treated for 60 minutes at 37 ° C with proteinase K (PK; Sigma Chemical Co., St. Louis, MO) at a final enzyme concentration of 50 μg per mL. The digestion was stopped by adding protease inhibitors (Complete, Roche Diagnostics GmbH Roche Applied Science, Mannheim, Germany) in accordance with the manufacturer's instruction. Sodium dodecyl sulfate–polyacrylamide gel electrophoreses and Western blot assays were performed according to

Lee and coworkers 15 with some modifications. After PK treatment, the samples were serially diluted in half-log steps in NuPAGE gel loading buffer, boiled for 10 minutes in a water bath, and electrophoresed on 12 percent NuPAGE Bis-Tris gels (Invitrogen Corp., Carlsbad, CA) for 60 minutes at 125 V. The nitrocellulose membrane (Hybond ECL, Amersham Biosciences Europe GmbH, Freiburg, Germany) was soaked in Towbin transfer buffer for 5 minutes before "sandwich" assembly and semidry transfer for 60 minutes at 125 mA at 4 ° C. The membrane was blocked for 60 minutes at 37 ° C in 3 percent nonfat dry milk (Bio-Rad, Hercules, CA), dissolved in Tris-buffered saline (pH 8) with 0.05 percent Tween 20 (TBST), and incubated overnight at 4 ° C with 3F4 monoclonal anti-hamster 27- to 30-kDa fragment of protease-resistant prion protein (PrP 27-30) antibody 16 (provided by H. Diringer) diluted 1:2000 in TBST. The membrane was rinsed with TBST (five changes of solution in 25 min), incubated for 90 minutes at room temperature with an alkaline phosphatase–labeled goat antimouse IgG (Perkin-Elmer Sciences, Wellesley, MA) diluted at 1:5000 in TBST, and rinsed again. Bands were revealed by the CDP-star chemiluminescence detection kit (Applied Biosystems, Foster City, CA) andrecorded onto sensitive films (Hyperfilm ECL, Amersham)

2.2.2.4 Extraction of PrPres by Streptomycin precipitation method

Scrapie-adapted hamster's brain homogenates were treated for 60 minutes at 37 ° C with proteinase K (PK; Sigma Chemical Co., St. Louis, MO) at a final enzyme concentration of 80-100 μg/mL. The digestion was stopped by adding protease inhibitors (Complete, Roche Diagnostics GmbH Roche Applied Science, Mannheim, Germany) in accordance with the manufacturer's instruction. The samples were then incubated for 1 h at 37°C in presence of 0.7 M of streptomycin (Sigma) and were centrifuged at 12000 g for five minutes at room temperature. The supernatants were carefully discarded and the pellets were resuspended in 50% v/v 8 M urea and 2X sample loading buffer (SDS 4%, mercaptoethanol 2%, glycine 192 mM Tris 25mM and 5% sucrose denaturing buffer). After vigorously vortex stirring for five minutes the preparations were heated at 100°C for ten minutes. The supernatants that corresponded to re-solubilized materials from pellets were gathered by centrifugation at 10000 g for five minutes and used as PrP^{Sc} stock sample for deposition on SDS-PAGE.

2.2.2.5 Extraction of PrPres by Sarkosyl ultracentrifugation method

Scrapie-adapted hamster's brain homogenates were treated for 60 minutes at 37 ° C with proteinase K (PK; Sigma Chemical Co., St. Louis, MO) at a final enzyme concentration of 80-100 μg/mL. The digestion was stopped by adding protease inhibitors (Complete, Roche Diagnostics GmbH Roche

Applied Science, Mannheim, Germany) in accordance with the manufacturer's instruction. The PK treated samples were incubated with 10% sarkosyl at 30% for 15 minutes at room temperature and ultracentrifugated at 100000 rpm for 2 h at 20°C. The supernatants were carefully discarded and the pellets were resuspended in 2X sample loading buffer (SDS 4%, mercaptoethanol 2%, glycine 192 mM Tris 25mM and 5% sucrose denaturing buffer). After the preparations were heated at 100°C for ten minutes. The supernatants that corresponded to re-solubilized materials from pellets were gathered by centrifugation at 12000 rpm for five minutes at room temperature and used as PrP^{Sc} stock sample for deposition on SDS-PAGE.

2.2.2.6 Extraction of water-soluble scrapie infectivity (SHS)

263K scrapie–infected hamster brains were suspended in 9 vol of sterile phosphate-buffered saline (PBS; pH 7.4) and homogenized by use of a Teflon-glass Potter tissue
grinder. The homogenate was dispersed with 10 sonication pulses (Vibra Cell, Sonics & Materials Inc., Newtown, CT) while kept on ice and then centrifuged at 825 × *g* for 15 minutes at 25 ° C (GS-6R, rotor GH-3.7, Beckman Coulter, Fullerton, CA). Low speed supernatant (S LS) was sonicated as above and ultracentrifuged at 220,000 × *g* for 30 minutes at 25 ° C (Optima TL-100, rotor TLA 100.3, Beckman Coulter, Fullerton, CA). This highspeed supernatant (S HS) was collected and the highspeed pellet (P HS) was sonicated in sterile PBS to obtain a 10 percent suspension (gram-equivalents of brain/PBS). These three fractions (S LS , S HS , and P HS) were stored at− 70° C until assayed.

2.2.2.7 Extraction of PrPres in SHS fraction by Streptomycin precipitation method

This highspeed supernatant (SHS) was collected from 263K scrapie–infected hamster brains as desribed above. Subsequently, SHS fraction was treated for 60 minutes at 37 ° C with proteinase K (PK; Sigma Chemical Co., St. Louis, MO) at a final enzyme concentration of 50 μg/mL. The digestion was stopped by adding protease inhibitors (Complete, Roche Diagnostics GmbH Roche Applied Science, Mannheim, Germany) in accordance with the manufacturer's instruction. The samples were then incubated for 1 h at 37°C in presence of 0.7 M of streptomycin (Sigma) and were centrifuged at 12000 g for five minutes at room temperature. The supernatants were carefully discarded and the pellets were resuspended in 50% v/v 8 M urea and 2X sample loading buffer (SDS 4%, mercaptoethanol 2%, glycine 192 mM Tris 25mM and 5% sucrose denaturing buffer). After vigorously vortex stirring for five minutes the preparations were heated at 100°C for ten minutes.

The supernatants that corresponded to re-solubilized materials from pellets were gathered by centrifugation at 10000 g for five minutes and used as PrP^{Sc} stock sample for deposition on SDS-PAGE.

2.2.2.8 Detection of PK-sensitive disease-related prion protein with Thermolysin

SLS and SHS fraction from 263K scrapie–infected hamster brains were treated for 30 minutes at 70 ° C with Thermolysin at a final enzyme concentration of 20 and 10 μg/mL respectively. The digestion was stopped by adding EDTA 2 mM. After Thermolysin treatment, the samples were serially diluted in half-log steps in NuPAGE gel loading buffer, boiled for 10 minutes in a water bath. PK-resistant and PK-sensitive disease-related prion protein isoforms were detected by Western blot procedure with CDP-star chemiluminescence detection as previously described.

2.2.3 RESULTS AND DISCUSSION

At present it is not possible to have a definite *ante-mortem* diagnosis for prion encephalopathies, nor there are therapies that can cure or halt the progression of these disorders. In this respect prion disorders are not dissimilar from other neurodegenerative disease, yet the possibility to study highly reliable, non enginereed, animal models confers to prion disorders a primary role in the fight against the growing threat posed by neurodegenerative diseases. In the prion field, the possibility to formulate an early diagnosis before the appearance of clinical symptoms is essential in order to identify infectious carriers and also to start a therapeutic treatment before the appearance of clinical symptoms and permanent neuronal damage. Currently protease-resistant disease-associated prion protein is the best-known biological marker for TSEs, and the demonstration of PrPsc in human or animal tissues is essential to formulate a definite diagnosis of TSE. One important limitation to this approach is the sensitivity of the detection system: amounts of PrPsc high enough to be revealed by conventional methods are only present in the brain at the relatively late stage of the disease, whereas, animal transmission studies clearly demonstrated that infectivity replication starts during the early stage of the incubation period and gradually increases as the disease progresses.

During my internship at the Istituto Superiore di Sanità, I learned all the operative procedures recommended by the World Health Organization to work with the infectious agents responsible for Transmissible Spongiform Encephalopathies (World Health Organization Infection control guidelines for transmissible spongiform encephalopathies, Report of a WHO consultation, Geneva Switzerland, 23-26 March 1999; WHO/CDs/CSR/APH/2000.3), and the detailed procedures of the WHO laboratory manual (WHO laboratory biosafety manual, Third edition, WHO press, Geneva, Switzerland, 2004) to work with class III pathogens in a BSL III facility.

The acquisition of this know-how was the basis for the realization of the experiments described in the rest of this paragraph. Recently, Moussa et al. (2006) published that streptomycin sulphate is able to combine and selectively precipitate PrPsc from brain homogenates. It is likely that electrostatic interaction occurs between guanidine and/or ammonium groups of streptomycin sulphate and amino acids residues selectively exposed by pathological PrP. When PrP molecules are cross-linked by streptomycin, reticulation develops, leading to the formation of flocculated aggregates in liquid solutions. These authors claim that this new and selective extraction procedure may help to produce fast and reliable diagnosis from infected tissues. Based on these results, I decided to evaluate the reliability and the sensitivity of this precipitation method in brain homogenates from hamsters infected with scrapie strain 263K.

I also compared the yield of PrPsc recovery by the streptomycin extraction method to that of an alternative protocol based on ultracentrifugation steps in the presence of the non-denaturing detergent sarkosyl (Figure 12).

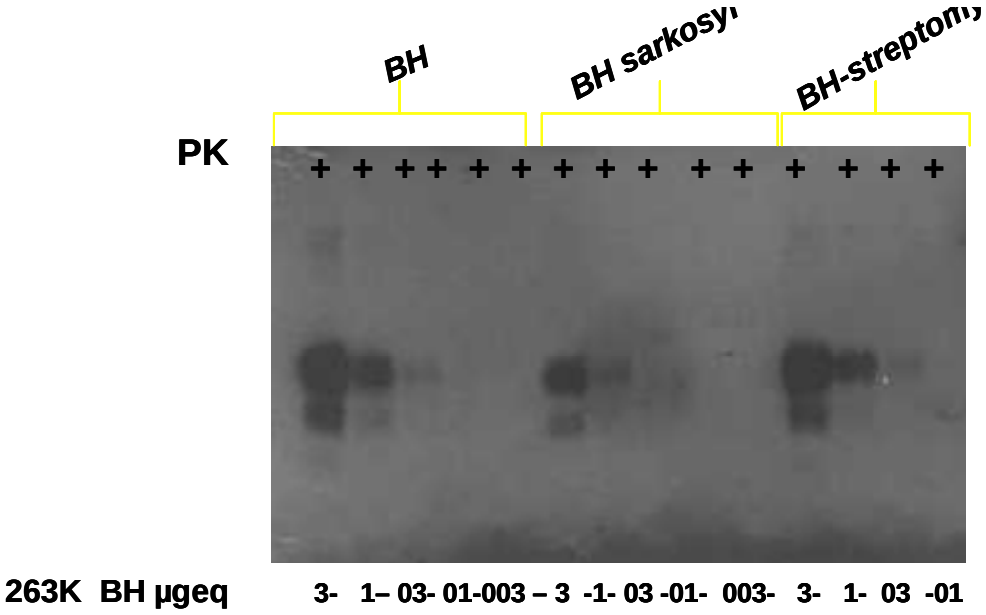

Figure 12: Comparisons of PrPres detection by streptomycin extraction method and sarkosyl ultracentrifugation method.

I found that starting from identical amounts of brain tissue, the streptomycin extraction mehod yield a western blot signal that is three times higher than the sarkosyl-based extraction method (Figure. 12). However, the latter protocol allows to obtain a final fraction that contains a lower amount of contaminants which translate into the possibility to load a higher amount of sample in each well, thus giving a higher sensitivity than the streptomycin extraction mehod.

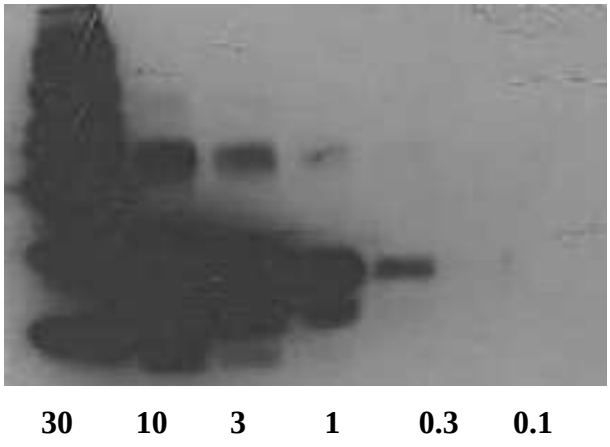

Figure 13: PrPres (263K) by immunoblotting ECL chemioluminascence detection system (esposition over night).

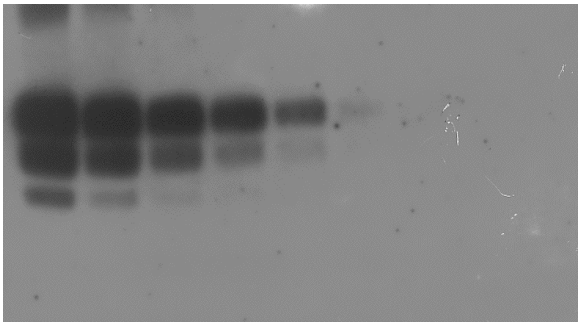

263K BH µgeq **5 2.5 1 0.5 0.25 0.1 0.05 0.025**

Figure 14: PrPres (263K) by immunoblotting CDP-star chemioluminascence detection system (esposition over night).

In the second part of my work on the development of an optimized method for the identification of PrPsc, I set up and compared two different systems to detect the prion protein by immunoblotting: ECL chemiluminescence detection system (Figure. 13) and CDP-star chemiluminescence detection system (Figure. 14) in brain homogenates from scrapie-infected (strain 263K) hamsters. I found that the CDP-star chemiluminescence detection system allows to demonstrate the presence of PrPsc in 0.1 micrograms of brain tissue whereas the ECL system can only identify the presence of PrPsc in 1 microgram of tissue. This translates into a difference of about one order of magnitude.With the aim to assess the sensitivity and specificity of the secondary antibody, I have also executed a screening of different anti-mouse IgG Alkaline Phosphatase antibodies produced in goat (data no snown).

The optimized procedures described above are been then applied to studies on the characterization of infectivity soluble from scrapie-adapted hamster's brain homogenates.

Recently the Pocchiari's research group has developed a simple and fast method to prepare a soluble infectious material (called SHS), containing small amounts of PrPTSE from hamster brains infected with scrapie strain 263k. (Berardi *et al*., 2006). This fraction, called SHS (high speed supernatant), is virtually free from PrPTSE in aggregate form and contains only small amounts of PrPTSE in soluble form and can therefore be an excellent material for studies on the characterization of the infecting agent and for experiments aimed at removing and inactivation of the infectious agent of TSEs. My research goal was to characterize the infectivity soluble from scrapie-adapted hamster's brain homogenates. This procedure involves homogenization of hamster brains in 9 volumes of phosphate buffer, followed by centrifugation at low speed, and by ultracentrifugation at high speed. In order to measure the PrPTSE in SHS fraction, I treated the SHS fraction with streptomycin, a molecule capable of binding and selectively precipitate PrP pathological, creating an electrostatic interaction between the guanidine and/or group of

streptomycin sulfate ammonium itself and amino acids residues, selectively exposed by the pathological PrP (Moussa *et al.*, 2006; Leclere *et al.*, 2008).

The SHS analysis by Western blot shown that the streptomycin is unable to precipitate the infectivity in the SHS fraction. Subsequently, to characterize SHS fraction, I submitted the SHS to digestion with proteinase K, assaying the enzyme at different concentrations, to detect the presence of pathological PrP isoforms sensitive to digestion with this enzyme (Owen *et al*., 2007), which commonly used in both diagnostic and research to remove PrP cell and identify the pathological PrP. PK-treatment shown that, at low concentrations of PK tested, the electrophoretic pattern of PrPTSE was slightly different respect to uninfected controls (Figure15).

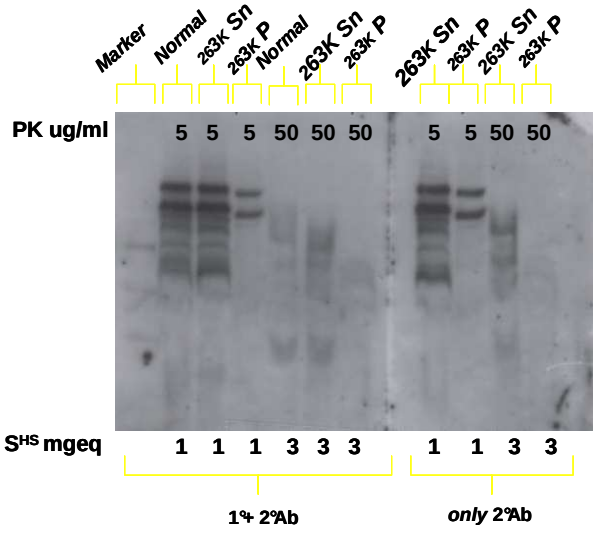

Figure 15: Detection of proteinase K-sensitive desease –related prion protein in SHS after streptomycin precipitation.

The result therefore not excluded the presence of pathological PrP isoforms sensitive to digestion with proteinase K. In a subsequent experiment, I submitted the SHS digestion with thermolysin, a proteolytic enzyme that degrades efficiently PrPc, preserving both the pathological isoform of PrP resistant to digestion with proteinase K, and those susceptible (Cronier *et al*., 2008). Digestion was performed varying some experimental parameters (temperature, pH and incubation time) to identify the optimum conditions for efficiently removes the PrPc, leaving PrPTSE in its entire length. I founded that the PrPTSE produced under these experimental conditions shown a modest reduction in signal intensity compared to that obtained with the standard protocol of digestion with proteinase K (Figure 16), this suggested that PrP pathological in the SHS fraction is formed by isoforms resistant to digestion with proteinase K.

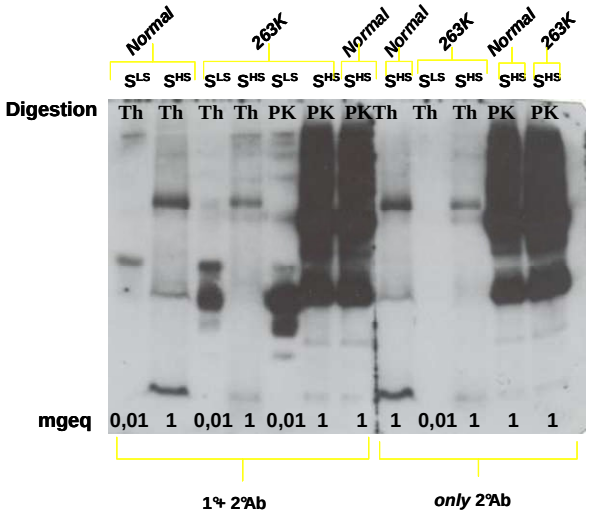

Figure 16: Detection of proteinase K-sensitive desease –related prion protein with Thermolysin.

2.2.4 CONCLUSIONS

Overall, our data suggested that the streptomycin extraction method yield a higher western blot signal that the sarkosyl-based extraction method in 263k scrapie-infected hamster brain homogenates. However, this antibiotic is unable to precipitate the infectivity in SHS fraction. Probably the infectivity in the SHS fraction is associated with dimmers or small aggregates of PrPTSE. In addition the SHS digestion with thermolysin, that preserving both PK-sensitive and PK-resistant isoforms of disease related PrP, showed a modest reduction in signal intensity compared to that obtained with the standard protocol of digestion with proteinase K. This result seems to exclude the presence of PK-sensitive isoform in the SHS fraction and suggests that PrP pathological contained within the SHS fraction is formed by isoforms resistant to digestion with proteinase K.

2.3 CHAPTER III

NEUROINFLAMMATION IN ALZHEIMER DISEASE: ALZHEIMER'S PEPTIDES BEHAVE AS SUPERANTIGENS?

2.3.1 INTRODUCTION

2.3.1.a Neuroinflammation in Alzheimer's Disease

In many chronic neurodegenerative diseases, including disease Alzheimer's and prion disorders, the role of neuroinflammation correlated with the presence of misfolded proteins in the System Central nervous (CNS) has been analyzed. In these conditions, glial cells (astrocytes, microglia and oligodendrocytes) are described as "activated", a term used to indicate their morphological change relative to their resting state, which is accompanied by a number of over-expression of antigens on their cell surface or in cytoplasm. The activation of glia, although by mechanisms not fully clarified yet, is the first defense mechanism against the pathological abnormalities that occurs in neurodegenerative diseases (Farfara *et al*., 2008). The most characteristic inflammation associated with chronic disease and neurodegenerative disorder is well documented in Alzheimer's disease (McGeer *et al*., 2002). Recent studies have shown that close association between deposits of amyloidogenic Aβ peptide and microglial cells, can have a role in the development of Alzheimer's disease, by activating immune response and inflammatory cytokines and chemokines production (Hashioka *et al*., 2009). Activated microglia are associated with Aβ fibrils in AD brain samples, and may interact with infiltrated T cells to induce inflammation. (Akiyama *et al*., 2000).

To limit undesiderable and dangerous auto-immune effects, the brain evolved to limit access of the immune system. This limitation is mediated by mechanisms such as the physical blood-brain barrier and a molecular milieu that suppresses immune function (Moalem *et al*., 1999; Aloisi *et al*., 2001). The CNS is thus often described as "immune privileged." However, a body of evidence suggests that T cells normally, although to a limited extent, survey the CNS (Hickey *et al*., 1991; Aloisi *et al*., 1993). This ability of T cells to cross the blood-brain barrier has primarily been described for activated cells that survey the organs of the body during an immune response. To elicit T cell activation in the CNS, an Ag must be phagocytized and processed by local APCs. The professional APCs of the CNS are the parenchymal microglia and the perivascular cell**s.** The parenchymal microglia have recently been characterized as myeloid progenitors cells that can differentiate into macrophage-like or dendritic-like cells (Fischer *et al*., 2001; Santambrogio *et al*., 2001). Differentiation of microglia and its effect on T cell activation may relate to brain pathology, such as that induced by amyloid β-peptide in Alzheimer's disease.

Aβ peptides induce in fact microglia and astrocytes activation, and are actually recognized as Ag that must be removed. If microglia and astrocyte activities are not able to eliminate the Ag-Aβ complexes, this response may become chronic and neurotoxic (Monsonego *et al*., 2003).

2.3.1.b Studies on Alzheimer's peptides as potential superantigens

In the last two decades it has become apparent that Aβ plaques are associated with inflammatory mediators and adhesion molecules, and that neurons re-express cell cycle proteins during AD pathogenesis. The presence in neocortical areas of clusters of activated microglia in classic plaques is consistent with a neurological form of low grade chronic inflammation (Akiyama *et al*., 2000).

Moreover, studies on the alteration systemic of cholesterol homeostasis in peripheral cells of AD patients by some collegues that collaborate with my group, had revealed increased proliferation in PBMCs from AD patients compared to those from healthy donors. Based on these observations, we investigated whether the AD peptides, sAPPα, Aβ40 and Aβ42 act as superantigens being able to activate a non-specific response of all T cell. The antigenic molecules with superantigen activity are able to induce an abnormal non-specific activation of T-cells resulting in polyclonal T cell activation leading to massive cytokines release. Examples of superantigens are exotoxins SEB and SPE-C produced by Gram-positive bacteria Staphylococcus aureus and Streptococcus pyogenes, respectively (Fraser & Proft, 2008).

Superantigens bind to the variable portions of MHC-II of the APC and the T-cell Receptor (TCR) of helper T-cell (Th), but in a way different from the physiologic antigen-receptor binding. The interaction with MHC-II usually occurs in the variable region of α chain (Alouf *et al*., 2003) and more rarely in the β-chain variable region (Mehindate *et al*., 1995); this link makes the correct placement of the molecule for interaction with the variable β chain of TCR. A common antigen is able to activate approximately 0.001-0.0001% of total T cells in the body, while superantigens are able to activate up to 20% of the total (Li *et al*., 1998). The polyclonal activation is due to the extreme affinity of superantigens for TCR. This non-specific response leads to release of massive amounts of cytokines involved in inflammation, including IL-1, IL-2, IL-6, TNF-α, IFN-γ, MIP-1α and β (macrophage inflammatory protein 1α and 1β) and MCP-1 (monocyte chemoattractant protein 1) (Stiles *et al*., 2005). The massive systemic release of cytokine, that normally are produced and acted locally, especially TNF-α, may lead to SIRS (systemic inflammatory response syndrome), or toxic shock, a condition of very severe systemic inflammation that can rapidly lead to coma and death. Therefore, a better understanding of the interactions between T cells and amyloidogenic peptides could help to identify mechanisms underlying a atypical inflammatory response, and reveal new targets to modulate inflammation in the brain of AD patients.

2.3.2 MATERIALS AND METHODS

2.3.2.1 Isolation of human lymphocytes from peripheral blood

Blood samples were centrifuged at 2200 rpm for 15 minutes, the buffy coat was collected and PBMCs were isolated by density gradient centrifugation (lymphoprep, density 1.077 g / L; Nycomed Pharma) at 1200 rpm for 10 minutes at 20 ° C. and washed twice with Hanks balanced salt solution (HBSS). The PBMCs purified, were seeded onto 24-well plates at a density of 1 x 104 cells / mL in RPMI 1640 medium with the standard supplements: (10% fetal calf serum (FCS), 200 mM L-glutamine, and 100 U/mL penicillin-streptomycin) and growth-stimulated with 10 μg/ml phytohemagglutinin (PHA; Sigma) for 24, 48 and 72 hours. The trypan blue exclusion test was used to assess cell viability. These freshly isolated (*ex vivo*) PBMCs were utilized for the experiments: proliferation assays with labeled thymidine, MTT , Oil red O staining of neutral lipids and aggregation assay.

2.3.2.2 Proliferation Assay of PBMCs treated with AD-peptides by [3H]-TdR incorporation

For [3H]-Thymidine-incorporation studies, the cells were seeded onto 24-well plates at a density of 2 x 106 cells/mL, in RPMI supplemented with 10% FBS, 1% antibiotic and 1% glutamine. All proteins PHA, sAPPα, Aβ40 and Aβ42 were added to cultures at a final concentration of 1 mg/well. An equal volume of PBS without Ca2 + and Mg2 + was added to controls. At 24 and 48 hours after seeding, cells were incubated in duplicate for 24 h with [3H]-thymidine (3 μCi/well). After incubation, the cells were rinsed twice with phosphate buffered saline (PBS), and DNA was precipitated by adding 10% trichloroacetic acid at 4°C for 30 minutes. Cells were digested with 0,1 M NaOH at room temperature. Aliquots were harvesting and counting to determinate the [3H]-thymidine radioactivity content on a β-scintillation counter.

2.3.2.3 Proliferation Assay of PBMCs treated with AD-peptides by MTT method

The cells were seeded onto 96-well plates, at the density of 2 x 106 cells/mL, in RPMI supplemented with 10% FBS, 1% antibiotic and 1% glutamine. All proteins, PHA, sAPPα, Aβ40 and Aβ42 were added to cultures at a final concentration of 1 mg/well. An equal volume of PBS without $Ca2^{+}$ and $Mg2^{+}$ was added to controls. After 48 and 72 hours incubations, cell proliferation was determined, by the 3-(4,5 dimethylthiazol-2-yl)-2,5-diphenyl-tetrazolium bromide (MTT) (Sigma,Italy) method.

Yellow MTT was reduced to purple formazan in the mitochondria of living cells. The absorbance of this colored solution was quantified after 4 days by measuring at a wavelength 570 nm by a spectrophotometer.

2.3.2.4 Staining of neutral lipids of lymphocytes treated with AD-peptides

The cells were seeded onto 12-well plates at the density of 2 x 106 cells/, in RPMI supplemented with 10% FBS, 1% antibiotic and 1% glutamine. All proteins, PHA, sAPPα, Aβ40 and Aβ42 were added to cultures at a final concentration of 1 mg/well. An equal volume of PBS without $Ca2^{+}$ and $Mg2^{+}$ was added to controls. After 48 hours incubation, cells were centrifuged twice at 1600 rpm for 3 minutes to remove any medium residual. Pellet was suspended in 50 µL of PBS and the cell suspension was seeded onto 12-well plates for Oil red O staining. The cells were fixed by soaking in 10% formalin and then treated with isopropyl alcohol (60%), washed, and stained with oil red O (ORO) (a lipid-soluble dye which stains NL, including CE, but not FC). They appear as bright red spots in the cytoplasm, and are then counterstained with Mayer's hematoxylin. After staining, cells were imaged using a Leitz inverted-phase microscope fitted with a digital camera. At least two different fields per sample were imaged and analyzed.

2.3.2.5 Aggregation Assay of LG-2 Cells

Healthy Lymphoblastoid cells LG-2 (a kind gift of John D. Fraser, University of Auckland, New Zealand) were seeded onto two 96-well plates respectively at the density of 5 x 105 cells/mL and 1 x 105 cells/mL in RPMI supplemented with 10% FBS, 1% antibiotic and 1% glutamine. Cells in duplicate wells were stimulated by the addition of peptide, sAPPα Aβ40 and Aβ42. All proteins were added at two different concentrations 0.1g/well and 1g/well. An equal volume of PBS without $Ca2^{+}$ and $Mg2^{+}$ was added to controls. Cells were incubated at 37° C for 24 hours and cell clusters were counted and photographed under by light microscopy every hour.

2.3.3 RESULTS

2.3.3.1 Effect of AD-peptides on clusters formation of B lymphocytes

To assess the ability of sAPPα, Aβ40 and Aβ42 peptides to activate B-cells, which express MHC-II molecules, we used the LG-2 cell aggregation assay. These cells when exposed to the presence of superantigen toxins, have the tendency to aggregate, forming typical clusters. To assess the experimental conditions suitable for the aggregation assay, cells were seeded at two different density and treated with two different concentrations of peptides. Respect to control, as shown in Figure 17, cells seeded at the density of 1 x 10^4 cells/mL and treated with the proteins at the concentration of 0.1 g /well, showed no significant differences in the clusters formation at 90 minutes after addition of peptides. While after 24 hours incubation, cells treated with both sAPPα and Aβ40, at the concentration of 1 g/well, showed some clusters. Cells incubated with both concentrations of Aβ42 used, showed typical aggregates which, although consisting of few cells, appeared more regular and more compact.

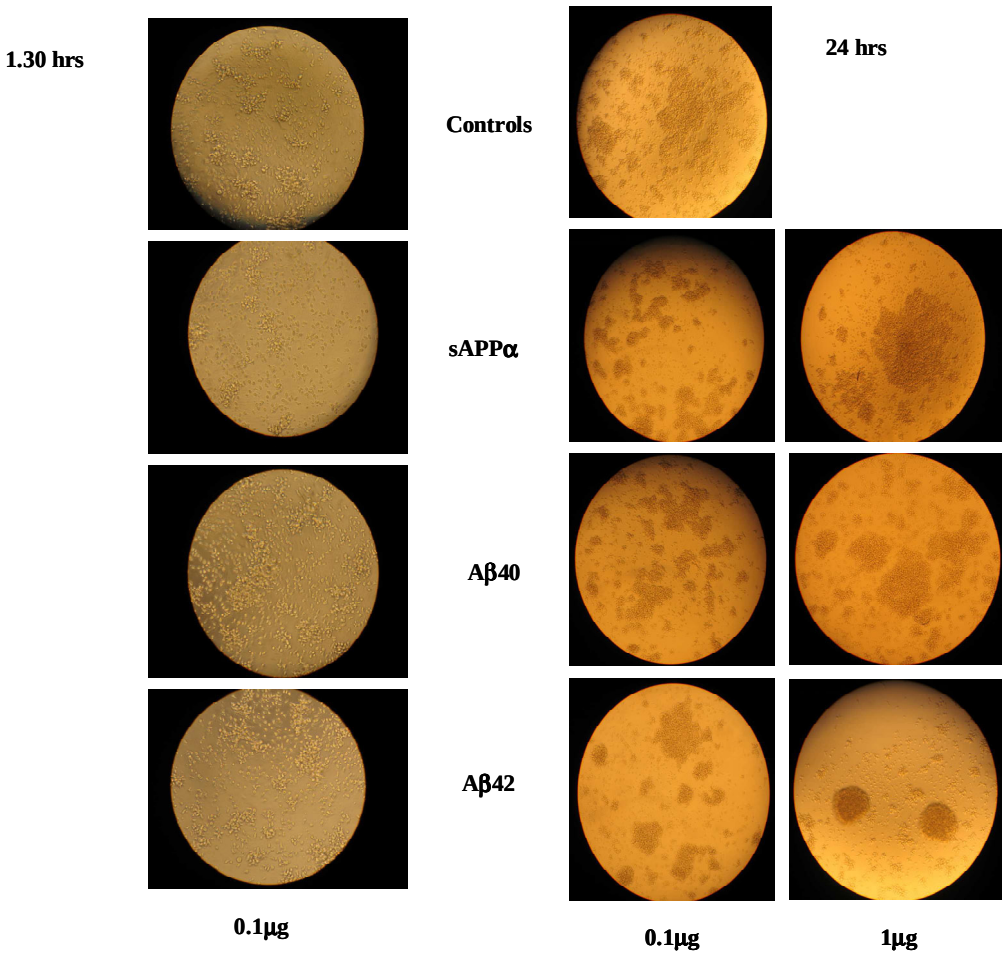

Figure 17. Aggregation assay of B lymphocytes (1 x 10^4 LG-2 cells/mL) untreated versus treated with AD-peptides.

The cells seeded at higher density and treated with sAPPα and Aβ40 peptides, at the concentration of 0.1 and 1 µg/well after 30 minutes of incubation, showed no visible differences compared to untreated controls. Peptide Aβ42-treatment, after 30 and 90 minutes, induced the formation of more aggregates at both concentrations tested (Figure. 18).

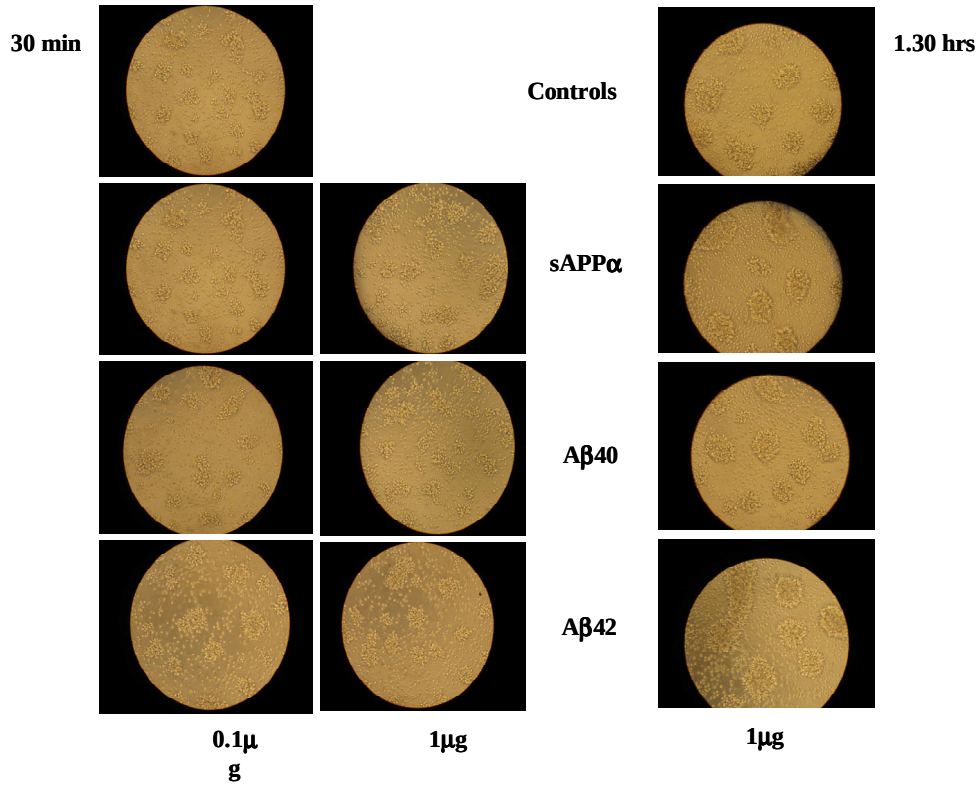

Figure 18. Aggregation assay of B lymphocytes (5 x 10^4 LG-2 cells/mL) untreated versus treated with AD-peptides.

2.3.3.2 Effect of AD-peptides on clusters formation of T lymphocytes

To assess the ability of proteins to act as superantigens and bind directly to TCR of T lymphocytes, without being processed by the cells expressing MHC-II molecules, we used the T lymphocytes cell aggregation assay. Cells were photographed after 72 hours the addition of peptides, sAPPα, Aβ40 and Aβ42 at a concentration of 0.2 µg/well. The mitogen PHA was used as positive control. Cells treated with sAPPα appeared slightly aggregated, respect to lymphocytes treated with PHA, which showed several clusters, index cellular activation (Figure. 19). Cells treated with peptides Aβ40 and Aβ42, showed abnormal distribution similar to monolayer accompanied by the presence of cells similar to blasts.

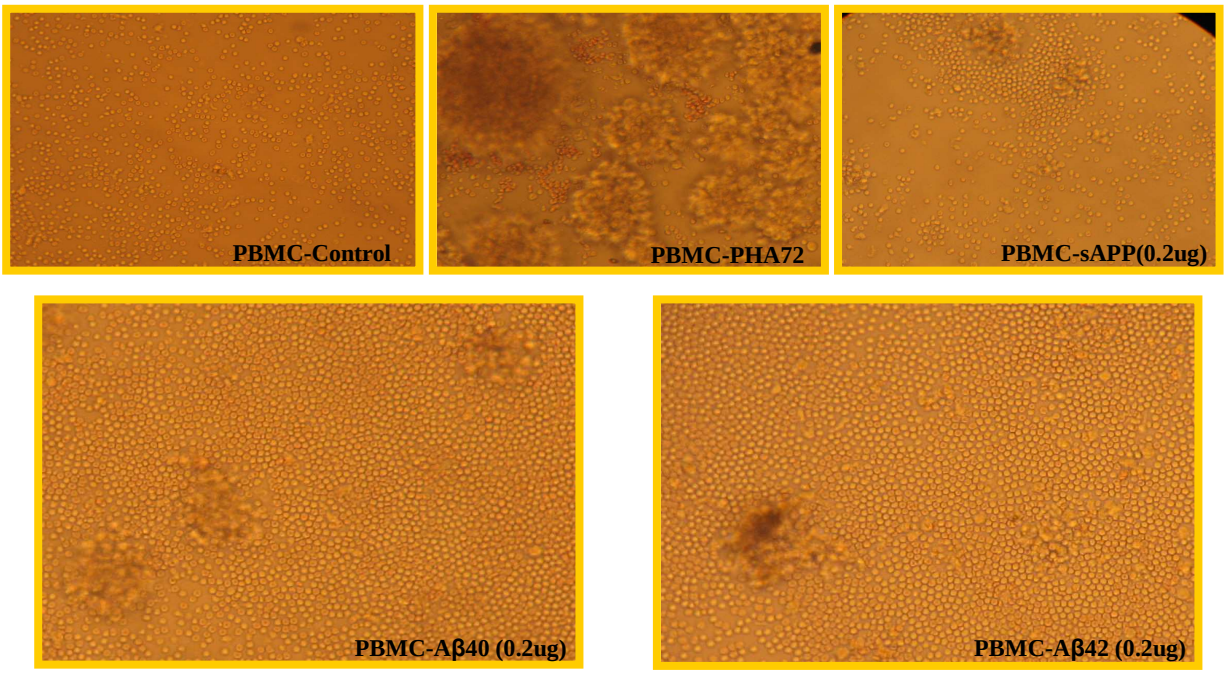

Figure 19. Aggregation assay of T lymphocytes untreated versus treated with AD-peptides.

2.3.3.3 Content of neutral lipids in normal human lymphocytes treated with AD-peptides

To verify the activation status of lymphocytes treated with the protein in study, we stained the cells with Oil red O. Figure 20 shows neutral lipid staining of healthy lymphocytes treated with PHA, sAPPα, Aβ40 and Aβ42. As expected lymphocytes stimulated with PHA seemed all colored red, indicating their activation status. While cells treated with sAPPα showed no significant differences to untreated control. Lymphocytes incubated with Aβ40 and Aβ42 seemed red, dead and atrophic; this result was more evident in cells treated with Aβ42.

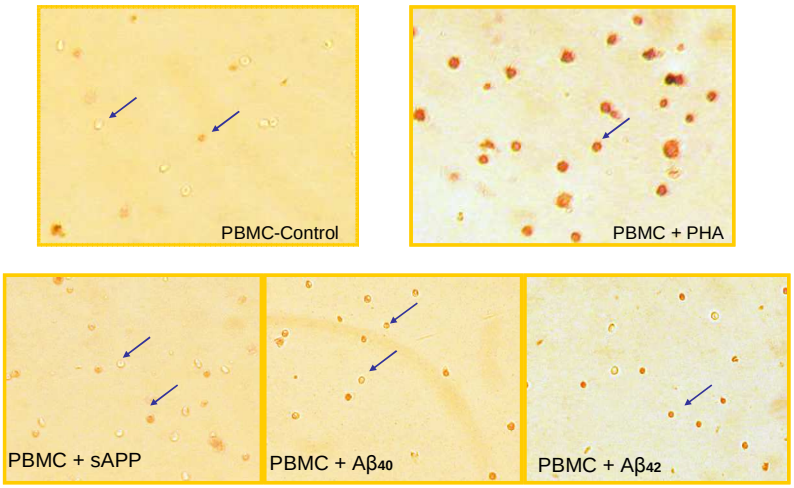

Figure 20. Oil Red O stained of T lymphocytes untreated versus treated with AD-peptides.

2.3.3.4 Proliferation assay in normal human lymphocytes treated with AD-peptides

To assess the ability of proteins, sAPPα, Aβ40 and Aβ42, to stimulate the T lymphocytes proliferation , two assays were performed in parallel, [3H]-thymidine proliferation assay and the MTT assay. Through the incorporation assay with [3H]-thymidine was quantified the DNA synthesis of normal lymphocytes stimulated both with PHA, the non- amyloidogenic peptide sAPPα and amyloidogenic peptides Aβ40 and Aβ42. DNA synthesis was measured 48 and 72 hours after the addition of proteins. With respect to controls, as shown in Figure 21, cells treated with PHA showed an increase of DNA synthesis after 48 hours by adding of mitogen, with a further increase to 72 hours. While the cells treated both with sAPPα, Aβ40 and Aβ42 showed no significantly differences in DNA synthesis, compared to control.

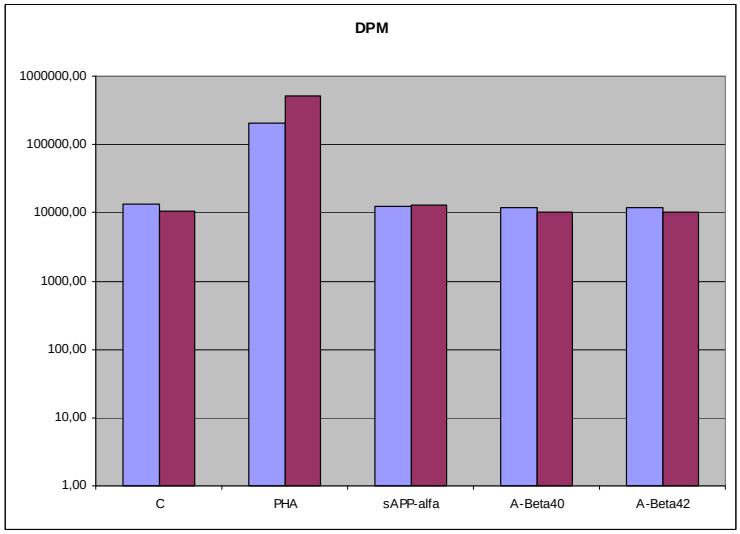

Figure 21. DNA synthesis of lymphocytes treated with AD-peptides by [3H]-thymidine incorporation assay.

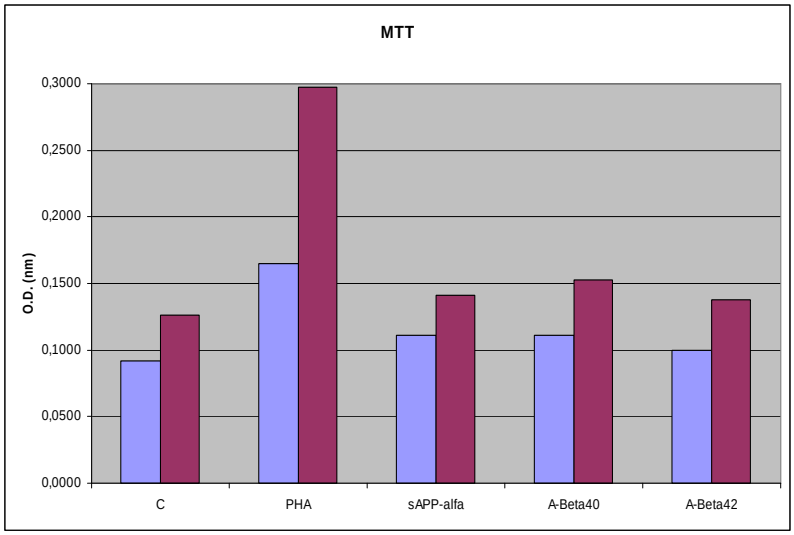

Figure 22. Cells viability of lymphocytes treated with AD-peptides by MTT assay **.**

Although assays performed with nucleotides labeled with radioactive isotopes are considered among the most sensitive for measuring DNA synthesis, we used also another method, the MTT assay, which is widely used to assess cell viability and activity screening, especially for its easy implementation and speed of response. As shown in Figure 22, cell viability in lymphocytes treated with PHA, sAPPα Aβ40 and Aβ42 peptides by MTT methods confirming the results obtained by [3H]-thymidine incorporation assay. In conclusion, these results showed no significantly increase in the cell proliferation induced by the AD peptides, with both assays used. These results indicated that at the times considered, both the non-amyloidogenic fragment sAPPα and amyloidogenic peptides Aβ40 and Aβ42 do not act as superantigens.

3.3.4 DISCUSSION

In the studies carried out to evaluate the ability of AD peptides to act as superantigens, LG-2 cell aggregation assay showed a slight difference in cells incubated with the amyloidogenic Aβ42 peptide, while showed no significant differences was seen in cells incubated with sAPPα and Aβ42 peptides. Although proliferation assays in human lymphocytes showed no significantly differences in the proliferation of cells exposed to AD peptides, the aggregation assay showed abnormal, epitelial-like morphology, accompanied by blast-like enlargment of cell size of T lymphocytes. More information were obtained by Oil red O staining of T lymphocytes. Noteworthy is the fact that cells incubated with Aβ40 and Aβ42 peptides, especially those treated with Aβ42, showed more intensive stain, although apparently atrophic cells, confirming the data in the literature of a higher toxicity of the Aβ42 than Aβ40 peptide (Bitan *et a*l., 2003; Chen *et a*l., 2006). The most immediate interpretation of these results is that the exposure of cells to Aβ40 and Aβ42 peptides probably cause activation of T cells in a relatively short period of time, with consequent cell death, likely by apoptosis. These data are in line with the results of previous co-culture studies carried out to characterize the interaction between Aβ-presenting cells and some T cells-subpopulations, which showed that exposure of Th1 cells to Aβ40 and Aβ42 peptides cause cell death by apoptosis. It is no accident that stress conditions, e.g. due to the presence of toxic molecules, can induce a cell to initiate apoptosis. Often, cells in the diseased brain are more susceptible to enter apoptosis due to overexpression of cellular death receptors and sub-decoy-receptor expression, by binding with TRAIL (TNF-related apoptosis-inducing ligand). It has been demonstrated that together with other cytokines, the TRAIL is involved in some neurodegenerative diseases, including Alzheimer's disease **(**Hoffmann *et a*l., 2009).

By contrast, the effect of Aβ40 and Aβ42 peptides on the proliferation of T lymphocytes it is not yet clear. Previous studies on the reactivity of human T cells following exposure with Aβ peptide, showed a high proliferative index of T cells after treatment with the Aβ42 peptide, rather than with Aβ40 (Monsonego *et al.*, 2003). This result is in conflict with our results and those of Trieb et al. and Ethell et al. Possibly, these discrepancies could be ascribed to the use of peptides with different purities, as well as to other differences in experimental models used (Miscia et al., 2009). Another possible interpretation is that other cofactors, closely associated with fibrils in vivo and perhaps lost during the purification procedures, may play a key role in activating T lymphocytes. Moreover, the mode of temporal activation of T cells could be related to the number of fibrils, and/or to the concentration of peptides.

Further experiments should be carried out to assess whether and how these peptides are able to activate a non-specific inflammatory response, and if this is followed by apoptosis. Indeed, recent

studies have shown that use of drugs that interfere with the inflammatory response may represent a therapeutic approach to prevent and possibly slow down some forms of neurodegenerative disorders whose pathogenesis involves chronic inflammation. Therefore, a better understanding of factor(s) driving the neuroinflammation could help to develop novel strategies for treatment of these diseases.

3.3.5 CONCLUSIONS

Our preliminary studies carried out to evaluate the ability of AD peptides to act as superantigens have not given clear and unambiguous results. This could be dependent on several factors such as peptides concentrations, incubation times, cells used, co-factors absent in purified peptides. Further studies to specifically address these aspects are presently in progress in our laboratories.

3. ACKNOWLEDGEMENTS

I wish to thank in particular my Supervisor at the Department of Biomedical Science and Technology, Prof. Alessandra Pani, for her indispensable scientific support and precious suggestions that made possible to obtain the results reported herein. I wish to express my gratitude also to all senior and junior researchers at the Istituto Superiore di Sanita', in Rome, for their support and affection during my stay in the Institute.

4. REFERENCES

Akiyama H, Barger S, Barnum S, Bradt B, Bauer J,Cole GM, Cooper NR, Eikelenboom P. *et al*. Inflammation and Alzheimer's disease. Neurobiol Aging. 2000; 21: 383–421.

Albrecht C, Viturro EP. The ABCA subfamily-gene and protein structures, functions and associated hereditary diseases. Pflugers Arch 2007; 453: 581-589.

Allinson TMJ, Parkin ET, Turner AJ, Hooper NMJ. ADAMs family members as amyloid precursor protein alpha-secretases. J Neurosci Res 2003; 74: 342-352.

Aloisi, F., E. Ambrosini, S. Columba-Cabezas, R. Magliozzi, and B. Serafini. 2001. Intracerebral regulation of immune responses. *Ann. Med. 33:510*.

Alouf JE, Müller-Alouf H (Feb.2003). "Staphylococcal and streptococcal superantigens: molecular, biological and clinical aspects". Int. J. Med. Microbiol. 292 (7-8): 429–40

Bach, C.; Gilch S.; Rost R, *et al*. Prion-induced activation of cholesterogenic gene expression by SREBP2 in neuronal cells. J Biol Chem 2009; 284: 31260-31269.

Bate C, Salmona M, Diomede L, Williams A. Squalestatin cures prion-infected neurons and protects against prion neurotoxicity. J Biol Chem 2004; 279: 14983–14990.

Bate C, Rumbold L, Williams A. Cholesterol synthesis inhibitors protect against platelet-activating factor-induced neuronal damage. J Neuroinflam 2007, 4:5. Doi:10.1186/1742-2094-4-5.

Berardi VA, Cardone F, Valanzano A, Lu M, Pocchiari M.Preparation of soluble infectious samples from scrapie-infected brain: a new tool to study the clearance of transmissible spongiform encephalopathy agents during plasma fractionation. Transfusion. 2006 Apr;46(4):652-8.

Bitan, G., Kirkitadze, M. D., Lomakin, A., Vollers, S. S., Benedek,G. B., and Teplow, D. B. [2003] Amyloid β-protein [Aβ] assembly:Aβ40 and Aβ42 oligomerize through distinct pathways. Proc. Natl. Acad. Sci. U.S.A. 100, 330–335.

Bjorkhem, I., U. Andersson, E. Ellis, G. Alvelius, L. Ellegard, U. Diczfalusy, J. Sjovall, and C. Einarsson. 2001. From brain to bile. Evidence that conjugation and omegahydroxylation are important for elimination of 24S-hydroxycholesterol (cerebrosterol) in humans. *J Biol Chem* 276: 37004-37010.

Bjorkhem, I., and S. Meaney. 2004. Brain cholesterol: long secret life behind a barrier. Arterioscler Thromb Vasc Biol 24: 806-815.

Campana V, Sarnataro D, Zurzolo C. The highways and byways of prion protein trafficking. Trends Cell Biol 2005; 15: 102-111.

Caughey B, Raymond GJ. The scrapie-associated form of PrP is made from a cell surface precursor that is both protease- and phospholipase-sensitive. J Biol Chem 1991; 266: 18217-18223.

Chen, Y.-R., and Glabe, C. G. [2006] Distinct early folding and aggregation properties of Alzheimer amyloid-β peptides Aβ40 and Aβ42: Stable trimer or tetramer formation by Aβ42. J. Biol. Chem. 281, 24414–24422.

Chiesa R, Harris DA. Prion diseases: what is the neurotoxicmolecule? Neurobiol Dis 2001; 8: 743-763.

Clejan S. In: *Methods in Molecular Biology, Phospholipid Signaling Protocols;* Bird and Clejan, Eds. New Jersey: HumanaPress 1998, Vol. 105: pp. 275-285.

Cossec JC, Marquer C, Panchal M, Lazar AN., Duyckaerts C, Potier MC. Cholesterol changes in Alzheimer's disease: methods of analysis and impact on the formation of enlarged endosomes Biochimica et Biophysica Acta 1801 (2010) 839–845.

Cronier S., Gros N., Tattum MH., Jackson GS., Clarke AR., Collinge J, Wadsworth JDF. Detection and characterization of proteinase K-sensitive disease-related prion protein with thermolysin. Biochemical Journal 2008.

Dessi S, Batetta B. In: Cell Growth and Cholesterol Esters; Pani and Dessì Eds. New York, NY, USA: Kluwer Academic/Plenum Publisher 2004; pp 1-10.

De Strooper B, Annaert W. Proteolytic processing and cell biological functions of the amyloid precursor protein. J Cell Sci 2000; 113: 1857-1870.

Dietschy, J. M., and S. D. Turley. 2004. Thematic review series: brain Lipids. Cholesterol metabolism in the central nervous system during early development and in the mature animal. J Lipid Res **45**: 1375-1397.

Donne DG, Viles JH, Groth DF. Structure of the recombinant fulllength hamster prion protein PrP (29-231): the N terminus is highly flexible. Proc Natl Acad Sci USA 1997; 94: 13452-13457.

Downing, D. T. 1968. Photodensitometry in the thinlayer chromatographic analysis of neutral lipids. J. Chromatogr.38: 91-99.

Drake M. Amundson, Mingjie Zhou. Fluorometric method for the enzymatic determination of cholesterol J. Biochem. Biophys. Methods 38, 1999, 43–52
Esler WP, Wolfe MS. A portrait of Alzheimer secretases—new features and familiar faces. Science 2001; 293: 1449-1454.

Ehehalt R, Keller P, Haass C, Thiele C, Simons K. Amyloidogenic processing of the Alzheimer beta-amyloid precursor protein depends on lipid rafts. J Cell Biol 2003; 160: 113-123.

Farfara D., Lifshitz V., Frenkel D.. Neuroprotective and neurotoxic properties of glial cells in the pathogenesis of Alzheimer’s disease. J. Cell. Mol. Med. Vol12, No 3, 2008 pp. 762-780.

Fischer, H. G., and G. Reichmann. 2001. Brain dendritic cells and macrophages/microglia in central nervous system inflammation. *J. Immunol. 166:2717*.

Fraser JD., Proft T. The bacterial superantigens and superantigenlike proteins. Immunological Reviews 2008. Vol. 225: 226–243.

Forman M.S., Trojanowski J.Q., Lee V.M.Y., (2004), Neurodegenerative diseases: a decade of discoveries paves the way for therapeutic breakthroughs. Nature medicine 10: 1038-1113.

Gabizon R, Rosenmann H, Meiner Z, Kahana I, Kahana E, Shugart Y, Ott J, Prusiner SB. Mutation and polymorphism of the prion protein gene in Libyan Jews with Creutzfeldt-Jakob disease (CJD). Am J Hum Genet. 1993 Oct;53(4):828-35.

Goldmann W., Hunter, Smith, G., Foster, J., Hope J. PrP genotype and agent effects in scrapie: change in allelic interaction with different isolates of agent in sheep, a natural host of scrapie Journal of General Virology (1994) 75, 989-995.

Govaerts L, Schoenen J, Bouhy D: Pathogenesis of Alzheimer's disease: molecular and cellular mechanisms. Rev Med Liege 2007, 62:209-216.

Giannakopoulos P, Kövari E, Gold G, von Gunten A, Hof PR, Bouras C: Pathological substrates of cognitive decline in Alzheimer's disease. Front Neurol Neurosci 2009, 24:20-29.

Harris DA. Cellular biology of prion diseases. Clin Microbiol Rev 1999; 12: 429-444.

Hashioka S, McGeer PL, Monji A, Kanba S. Anti-inflammatory effects of antidepressants: possibilities for preventives against Alzheimer's disease. Cent Nerv Syst Agents Med Chem. 2009 Mar;9[1]:12-9.

Haviv Y, Avrahami D, Ovadia H, *et al*. Induced neuroprotection independently from PrPSc accumulation in a mouse model for prion disease treated with simvastatin. Arch Neurol 2008; 65: 762-773.

Hickey, W. F., B. L. Hsu, and H. Kimura. 1991. T-lymphocyte entry into the central nervous system. *J. Neurosci. Res. 28:254*.

Hsiao, K., Baker, H.F., Crow, T.J., Poulter, M., Owen, F., Terwilliger, J.D., Westaway, D., Ott, J. & Hoffmann O, Zipp F, Weber JRJ. Tumour necrosis factor-related apoptosisinducing ligand (TRAIL) in central nervous system inflammation. Mol Med. 2009 Aug;87[8]:753-63.

Hwang D, Lee IY, Yoo H, *et al*. A systems approach to prion disease. Mol Syst Biol 2009; 5:252. Doi:10.1038/msb.2009.10.

Klunk WE; Pettegrew JW, Abraham D.J. Quantitative evaluation of congo red binding to amyloid-like proteins with a beta-pleated sheet conformation. J Histochem Cytochem 1989; 37: 1273-1281.

Koster T., Singh K., Zimmermann M., Gruys E., (2003) Emerging therapeutic agents for transmissible spongiform encefalopathies: a review. Journal of vet. Pharmacol. Therap. 26: 315-326.

Lebouvier T, Perruchini C., Panchal M., Potier M.C., Duyckaerts C., Cholesterol in the senile plaque: often mentioned, never seen, Acta Neuropathol. 117 (1) (2009) 31–34.

Leclere E., Moussa A., Chouaf-Lakhdar L.,. Coleman AW., Seigneurina JM., Perron H., Bencsik A., Prion early kinetics revisited using a streptomycin-based PrPres extraction method, Biochem. Biophys.Res. Commun. (2008), doi:10.1016/j.bbrc.2008.05.040.

Legname G, DeArmond SJ, Cohen FE; Prusiner SB. (2007) Coll. Biomed. Life Sci. Springer Link, 6, 125-146.

Li H, Llera A, Tsuchiya D, et al. "Three-dimensional structure of the complex between a T cell receptor beta chain and the superantigen staphylococcal enterotoxin B". Immunity 9 [6]: 1998 807–16.

Llewelyn CA, Hewitt PE, Knight RS, et al. Possible transmission of variant Creutzfeldt-Jakob disease by blood transfusion. Lancet 2004;363:417-21.

London E. Insights into lipid raft structure and formation from experiments in model membranes. Curr Opin Struc Biol 2002; 12: 480-486.

Lucero HA, Robbins PW. Lipid rafts-protein association and the regulation of protein activity. Arch Biochem Biophys 2004; 426: 208-224.

Mehindate K, Thibodeau J, Dohlsten M, Kalland T, Sékaly RP, Mourad W (Nov.1995). "Cross-linking of major histocompatibility complex class II molecules by staphylococcal enterotoxin A superantigen is a requirement for inflammatory cytokine gene expression". J. Exp. Med. 182 [5]: 1573–7.

Miscia S., Ciccocioppo F., Lanuti P., Velluto L., Bascelli A., Laura Pierdomenico, Genovesi D., Di Siena A., Eugenio S., Gambi F., Ausili-C`efaro G.,. Grimley PM., Marchisio M., Gambi D. Aβ1–42 stimulated T cells express P-PKC-δ and P-PKC-ζ in Alzheimer disease. Neurobiology of Aging 30 (2009) 394–406.

Moalem, G., A. Monsonego, Y. Shani, I. R. Cohen, and M. Schwartz. 1999. Differential T cell response in central and peripheral nerve injury: connection with immune privilege. *FASEB J. 13:1207*

Monsonego A., Imitola J., Zota V., Oida T., and Weiner HL. Microglia-Mediated Nitric Oxide Cytotoxicity of T Cells Following Amyloid β-Peptide Presentation to Th1 Cells1. *J. Immunol.* 2003;171;2216-2224.

Maxfield FR, Tabas I. Role of cholesterol and lipid organization in disease. Nature 2005; 438: 36-45.

Mattson MP. Impairment of membrane transport and signal transduction systems by amyloidogenic proteins. Methods Enzymol 1999; 309: 733-768.

Mok SW, Thelen KM, Riemer C, *et al*. Simvastatin prolongs survival times in prion infections of the central nervous system. Biochem Biophys Res Commun 2006; 348: 697–702.

Moussa A., Coleman AW, Bencsik A, Leclere E, Perret F., A. Martin, H. Perron, Use of streptomycin for precipitation and detection of proteinase K resistant prion protein (PrPsc) in biological samples, Chem. Comm, 2006; DOI: 10.1039/b516965h.

Naslavsky N, Stein R, Yanai A, Friedlander G, Taraboulos A (1997) Characterization of detergent-insoluble complexes containing the cellular prion protein and its scrapie isoform. J BiolChem 272:6324–6331.

Novakofski J., Brewer M. S., Mateus-Pinilla N., Killefer J., McCusker R.H., (2005), Prion biology relevant to bovine spongiform encephalopathy. J.Anim. Sci. 83: 1455-1476.

Nunan J, Small DH. Regulation of APP cleavage by α-, β- and γ-secretases. *FEBS Lett* 2000; 483: 6-10.

Ohvo-Rekila H, Ramstedt B, Leppimaki P, Slotte JP. Cholesterol interactions with phospholipids in membranes. Prog Lipid Res 2002; 41: 66-97.

Owen JP., Maddison BC., Whitelam GC., and Gough KC. Use of Thermolysin in the Diagnosis of Prion Diseases. Molecular Biotechnology 2007:2/161–170.

Pani A., Abete C., Norfo C., Mulas C., Laconi S., Cannas M.D., et al., Cholesterol Metabolism in Brain and Skin Fibroblasts from Sarda Breed Sheep With Scrapie-resistant and Scrapie-susceptible Genotypes, Am. J. Infec. Dis., 2007, 3, 143-150.

Pani A., Norfo C., Abete C., Mulas C., Putzolu M., Laconi S., et al., Accumulation of Cholesterol Esters in ex vivo Lymphocytes from Scrapie-susceptible Sheep and in Scrapie-infected Mouse Neuroblastoma Cell Lines, Am. J. Infec. Dis., 2007, 3, 165-168.

Peden AH, Head MW, Ritchie DL, Bell JE, Ironside JW. Preclinical vCJD after blood transfusion in a PRNP codon 129 heterozygous patient. Lancet 2004;364:527-9.

Pernes, J. F. 1980. Lipids: thin-layer chromatographic separation in twelve fractions by three successive unidirectional developments on the same plate. J. Chromatogr. 181: 254-258.

Pitas, R. E., J. K. Boyles, S. H. Lee, D. Foss, and R. W. Mahley. 1987. Astrocytes synthesize apolipoprotein E and metabolize apolipoprotein E-containing lipoproteins. *Biochim Biophys Acta* 917: 148-161.

Pocchiari M. Prions and related neurological diseases. Mol Aspects Med. 1994;15(3):195-291.
Prinz W. Cholesterol trafficking in the secretory and endocytic systems. Sem Cell Dev Biol 2002; 13: 197-203.

Privett, 0. S., K. A. Dougherty, and J. D. Castell. 1971.Quantitative analysis of lipid classes. Am. J. Clin. Nutr. 2 4 1265-1 275.

Prusiner, S.B. (1989) Nature (London) 338, 342-345.

Prusiner SB. Prions. Proc Natl Acad Sci USA 1998; 95: 13363-13383.

Ridgway ND, Byers DM, Cook HW, Storey MK. Sphingomyelin and related lipids: structure, occurrence, biosynthesis and analysis. Prog Lipid Res 1999; 38: 337-360.

Rouvinski A, Gahali-Sassa I, Stavb I, *et al.* Both raft- and non-raft proteins associate with CHAPS-insoluble complexes: some APP in large complexes. Biochem Biophys Res Com 2003; 308: 750-758.

Rudolf M., Curcio C.A., Esterified cholesterol is highly localized to Bruch's membrane, as revealed by lipid histochemistry in wholemounts of human choroid, J. Histochem. Cytochem. 57 (8) (2009) 731–739.

Russell, D. W., R. W. Halford, D. M. Ramirez, R. Shah, and T. Kotti. 2009. Cholesterol 24 hydroxylase: an enzyme of cholesterol turnover in the brain. *Annu Rev Biochem* **78**: 1017-1040.

Santambrogio, L., S. L. Belyanskaya, F. R. Fischer, B. Cipriani, C. F. Brosnan, P. Ricciardi Castagnoli, L. J. Stern, J. L. Strominger, and R. Riese. 2001. Developmental plasticity of CNS microglia. *Proc. Natl. Acad. Sci. USA 98:6295*.

Sarnataro D, Caputo A, Casanova P, *et al.* Lipid rafts and clathrin cooperate in the internalization of PrPc in epithelial FRT cells. PLoS ONE 2009; 4(6), e5829.
Selkoe DJ. Presenilin, Notch, and the genesis and treatment of Alzheimer's disease. Proc Natl Acad Sci USA 2001; 98: 11039-11041.

Schmitz G, Beuck M, Fischer H, Nowicka G, Robenek H. Regulation of phospholipid biosynthesis during cholesterol influx and high density lipoprotein-mediated cholesterol efflux in macrophages. J Lipid Res 1990; 31: 1741-1752.

Simons K, Ehehalt R. Cholesterol, lipid rafts, and disease. J Clin Invest 2002; 110: 597-603
Snipe, G., and U. Suter. 1997. Cholesterol and myelin.

Sorensen G, Medina S, Parchaliuk D, *et al*. Comprehensive transcriptional profiling of prion infection in mouse models reveals networks of responsive genes. BMC Genom 2008; 9:114. Doi:10.1186/1471-2164-9-114.

Soto C. Unfolding the role of protein misfolding inneurodegenerative diseases. Nature Rev Neurosci 2003; 4: 49-60.

Stefani M. Generic cell dysfunction in neurodegenerative disorders: role of surfaces in early protein misfolding, aggregation, and aggregate cytotoxicity. Neuroscientist 2007; 13: 519-531.

Stefani M, Liguri G. Cholesterol in Alzheimer's Disease:Unresolved Questions. Curr Alzh Res 2009; 6: 15-29.

Sjögren M, Mielke M, Gustafson D, Zandi P, Skoog I. Cholesterol and Alzheimer's disease–is there a relation? Mech Ageing Dev 2006;127:138–147.

Stiles BG, Krakauer. "Staphylococcal Enterotoxins: a Purging Experience in Review, Part I". Clinical Microbiology Newsletter. 2005, 27: 23McGeer PL, McGeer EG. Local neuroinflammation and the progression of Alzheimer disease. J.Neurovil 8, 2002, 529-538.

Vetrugno Vito, Angelo Di Bari Michele, Nonno Romolo, Puopolo Maria, D'Agostino Claudia, Pirisinu Laura, Pocchiari Maurizio and Agrimi Umberto. Oral pravastatin prolongs survival time of scrapie infectedmice. Journal of General Virology (2009), 90, 1775–1780, DOI 10.1099/vir.0.009936-0.

Vey M, Pilkuhn S, Wille H, Nixon R, Dearmond SJ, Smart EJ,Anderson RG, Taraboulos A, Prusiner SB (1996) Subcellular colocalization of the cellular and scrapie prion proteins in caveolae-like membranous domains. Proc Natl Acad Sci USA93:14945–14949; 5.

Taraboulos, A., Scott, M., Semenov, A., Avrahami, D., Laszlo, L., Prusiner, S.B., Avraham, D., 1995. Cholesterol depletion and modification of COOH-terminal targeting sequence of the prion protein inhibit formation of the scrapie isoform. Cell Biol. 129, 121– 132.

Wekerle, H. 1993. T-cell autoimmunity in the central nervous system. *Intervirology 35:95*.